Molecular Dissection and Functional Definition of Estrogen-Related Receptor Alpha Signaling Pathway

by

Junfei Liu

Department of Biochemistry
Duke University

Date:_____

Approved:

_____
Donald P. McDonnell, Supervisor

_____
Arno L. Greenleaf, Co-supervisor

_____
Christopher B. Newgard

_____
Dewey G. McCafferty

Dissertation submitted in partial fulfillment of the requirements for the degree of Doctor of Philosophy in the Department of Biochemistry in the Graduate School of Duke University

2013

ABSTRACT

Molecular Dissection and Functional Definition of Estrogen-Related Receptor Alpha Signaling Pathway

by

Junfei Liu

Department of Biochemistry
Duke University

Date:_____
Approved:

_____
Donald P. McDonnell, Supervisor

_____
Arno L. Greenleaf, Co-supervisor

_____
Christopher B. Newgard

_____
Dewey G. McCafferty

An abstract of a dissertation submitted in partial fulfillment of the requirements for the degree of Doctor of Philosophy in the Department of Biochemistry in the Graduate School of Duke University

2013

Abstract

The estrogen-related receptor alpha (ERRα) is an orphan nuclear receptor (NR) with no natural ligand identified. Recent studies report that ERRα expression and activity correlate with poor prognosis in breast cancer. It is also suggested that ERRα is involved in tumor growth and progression, thus this receptor may be a therapeutic target in the treatment of breast cancer. However, the specific role of ERRα in breast cancer is not fully understood. Similar to other nuclear receptors, ERR has been suggested to regulate target gene transcription through both classical (direct DNA binding) and non-canonical (tethering to other transcription factors) to effect various aspects of tumor pathogenesis, such as angiogenesis, regulation of hypoxic response, tumor growth, and migration. Thus, the objective of this dissertation research is to explore the roles of ERRα in breast cancer by (a) identifying novel ERRα target genes important for tumor pathogenesis, (b) characterizing the molecular mechanism of non-canonical actions of ERRα-mediated gene transcription, and (c) examining the structure basis of ERRα antagonism for future pharmaceutical exploitation. First, we identified an ERRα target gene, ECM1, which is relevant to breast cancer angiogenesis. The role of ECM1 in angiogenesis was confirmed by endothelial tube formation assay. We further showed that knocking down ECM1 has a dramatic inhibitory effect on tumor xenograft growth. This result, for the first time, directly demonstrates the role of ECM1 in tumor

environment and further sheds light on the significance of ERRα-regulated genes in tumors angiogenesis. Next, we explored the non-canonical pathways regulated by ERRα with a focus on the gene targets of ERRα and hypoxia inducible factor (HIF-1) pathways. It's been demonstrated previously that ERRα affect some HIF-1 target gene through a tethering mechanism. Using a candidate gene approach, we discovered that the expression of carbonic anhydrase 9 (CA9), an important regulator of pH balance in tumor microenvironment is a target gene co-regulated by ERRα and HIF-1. However, it remains to be determined whether ERRα regulates CA9 through canonical, non-canonical, indirect mechanisms, or some combinations of these. To further dissect the mechanism by which ERRα and HIF-1 cross talk, we used simply reporter gene assay and determined that even in the absence of a discernible ERR responsive element (ERRE) an intact ERR DNA binding domain is indispensible. Finally, to determine the molecular mechanisms underlying ERRα antagonism, we probed the conformations of ERRα upon antagonist treatments. M13 phage display was used to screen for ERRα-interacting peptides. We identified peptides that interact with ERRα in the activation function 2 (AF2) domain, some of which are able to distinguish the binding of different classes of ERRα antagonists. Cumulatively, these studies have explored the biological functions of ERRα and the molecular basis ERRα-mediated signaling pathways.

Contents

List of Tables

List of Figures

Abbreviations

AD	Activation Domain
AF-1	Activation Function 1
AF-2	Activation Function 2
β-cat	β-catenin
β-gal	β-galactosidase
cDNA	Complementary Deoxyribonucleic Acid
ChIP	Chromatin Immunoprecipitation
DBD	DNA-Binding Domain
DNA	Deoxyribonucleaic Acid
E. coli	*Esherichia coli*
ECM1	Extracellular Matrix protein 1
ELISA	Enzyme-Linked Immunosorbent Assay
ER	Estrogen Receptor
ERE	Estrogen Response Element
ERRα	Estrogen-related Receptor alpha
ERRE	Estrogen-related Receptor Response Element
FBS	Fetal Bovine Serum
GAPDH	Glyceraldehyde-3-Phosphate Dehydrogenase

HIF-1	Hypoxia-Inducible Factor-1
L2L3M	PGC-1α LxxLL Motif 2 and 3 Mutant
LBD	Ligand-Binding Domain
LEF	Lymphoid enhancer-binding factor
Luc	Luciferase
M2H	Mammalian-two-Hybrid assay
mRNA	Messenger Ribonucleic Acid
NaPyr	Sodium Pyruvate
NEAA	Non-Essential Amino Acids
NR	Nuclear Receptor
OD	Optical Density
Oligo	Oligonucleotide
PBS	Phosphate Buffered Saline
PCR	Polymerase Chain Reaction
PGC-1α	PPAR-gamma Coactivator 1 alpha
PPAR	Peroxisome Proliferator-Activated Receptor
qPCR	Quantitative PCR
RT-qPCR	Reverse Transcriptase Quantitative PCR
SDS-PAGE	Sodium Dodecyl Sulfate Polyacrylamide Gel Electrophoresis
SERM	Selective Estrogen Receptor Modulator

SF9	*Spodoptera frugiperda*
siRNA	Small Interfering Ribonucleic Acid
TCA	Tricarboxylic Acid Cycle
TCF	T-cell factor
TOPFlash	TCF-LEF luc-reporter
VEGF	Vascular Endothelial Growth Factor

Acknowledgements

I am grateful to all the members of the McDonnell lab, past and present, for creating a productive and enjoyable scientific environment. Thank you for generous sharing of your time, advise, expertise, and friendship. I appreciate immensely the contribution from each of you to my scientific training. I especially want to thank Dr Ching-yi Chang, Dr Tricia Wright, Dr Sunghee Park, Dr Erik Nelson, Dr Scott Lawrence and Dr Stephanie Ellison-Zelski for all your advice and help in the preparation of this manuscript. A special thanks to Trena Martelon for all your assistance and ready smiles.

I cannot thank enough to my mentor Dr. Donald McDonnell. Thank you for bringing together such a remarkable team and also for your great mentorship over the past several years. Your guidance and support have been absolutely critical to my graduate school education. I would also like to acknowledge the encouragement and scientific insight of my thesis committee, comprised of Dr. McDonnell, Dr. Greenleaf, Dr. Newgard and Dr.McCafferty. I appreciate the time and effort you have invested in this project.

I am fortunate to meet so many friends at Duke. Being surrounded by people with high intelligence, warm hearts and caring characters, I gained strength as well as inspiration for time to time. Your cheerful companionship made me less anxious and more confident.

I am deeply indebted to my family back in China. Though I visited only a few times in the past five years, their support and encouragement are accompanying me through each stage of my education and life.

Lastly, I would like to thank my husband Yuanjie Jin for his patience, integrity, intelligence, and companionship. The five years we spent in graduate school is my most valuable experience. I look forward to the next adventure with you in our lives.

Chapter 1 Estrogen-related receptor

1.1 Nuclear receptor superfamily

Nuclear receptors comprise a superfamily of transcription factors that are responsible for a variety of physiological processes such as growth, development, homeostasis and reproductive function. The importance of nuclear receptors is underscored by their dysfunction in many diseases, including diabetes and various cancers. Out of the 49 human nuclear receptors identified, most members (except for the orphan nuclear receptors) can be regulated in terms of their transcriptional activities by small lipophilic molecules, such as steroid hormones, thyroid hormones, vitamin D, rexinoids, and fatty acids. Thus, these nuclear receptors serve as important regulators of gene transcription in response to extracellular signals.

In the classic model of nuclear receptor action, the binding of ligands enables the receptors to undergo conformational changes that allow the receptors to form either homodimers or heterodimers. The dimeric receptor binds specific DNA response elements on target gene promoters and recruits cofactors. Different cofactors regulate diverse aspects of transcriptional initiation, from chromatin remodeling to recruitment of the basal transcription machinery. A key defining feature of this family, however, is that they do not possess DNA-binding activity and must be recruited by DNA-bound transcription factors. The recruitment of cofactors and the general transcription

machinery results in increased transcription of target genes that mediate biological responses.

While the first few nuclear receptors were identified by their ability to bind known ligands, more nuclear receptors were subsequently discovered based on sequence and structure similarities. However, not all of the newly discovered receptors have had their respective ligands identified. Nuclear receptors with no known ligands are considered orphan nuclear receptors until their endogenous ligands are identified. However, it is also possible that some orphan nuclear receptors may be constitutively active and thus do not require ligands.

1.2 Nuclear receptor structure and function

Despite the diverse functions of nuclear receptors, their structures are highly conserved. As shown in Figure 1.1, nuclear receptors consist of five or six functional domains. The DNA binding domain (DBD) and ligand/hormone binding domain (LBD), labeled as domains C and E respectively, are the most conserved motifs for almost all nuclear receptors.

Region A/B located at the N-terminus of the nuclear receptor is the least evolutionarily conserved domain. In this domain, many nuclear receptors contain an activation function 1 region (AF-1), which acts in a ligand-independent manner.

Region C, a highly conserved region that harbors the DNA-binding domain (DBD), is responsible for the recognition of hormone responsive elements on the

promoters of target genes. The DBDs of most NRs are well-characterized and the functional regions within DBDs have also been identified. The DBD of a NR binds to the major groves of the DNA helix through two zinc-finger motifs, which contains eight cysteines that interact with two zinc atoms (Glass 1994, Laudet 1997). As shown in Figure 1.2, in between the two zinc-finger motifs, the DBD domain also contains two other key regions, the Proximal-box (P-box) region and the Dimerization-box (D-Box) region. The P-Box determines the DNA binding specificity, while the D-Box is involved in nuclear receptor dimerization.

Region D, a highly variable region between NRs, is less structured and can thus be considered as a flexible "hinge" between region C and region E. Region D has important roles in nuclear localization, heterodimerization and DNA binding.

Region E, a strongly conserved domain consisting of 11-12 helices, is responsible for ligand binding and transactivation. Unlike AF-1, the AF-2 region in LBD recruits coactivators and transcriptional machinery in a ligand-dependent manner. Upon ligand binding, the LBD undergoes conformational changes that expose the hydrophobic AF-2 pocket, which is the binding site for most of the coregulator proteins for transcriptional regulation. Usually, AF-2 pocket can interact with the LXXLL motif (where L is leucine and X any amino acid) of the coactivators. On many known coactivators, the Leucine residues form a hydrophobic surface on their α-helices, which can bind within the hydrophobic groove formed by helices three, four, five, and twelve of a nuclear receptor.

Without ligand binding, helix twelve is positioned away from the hydrophobic groove, thus the coactivator is unable to bind the receptor. Upon ligand binding, helix twelve changes its position, forming the completed hydrophobic groove for coactivator binding.

Region F is only found in a few receptors and its function is largely unknown.

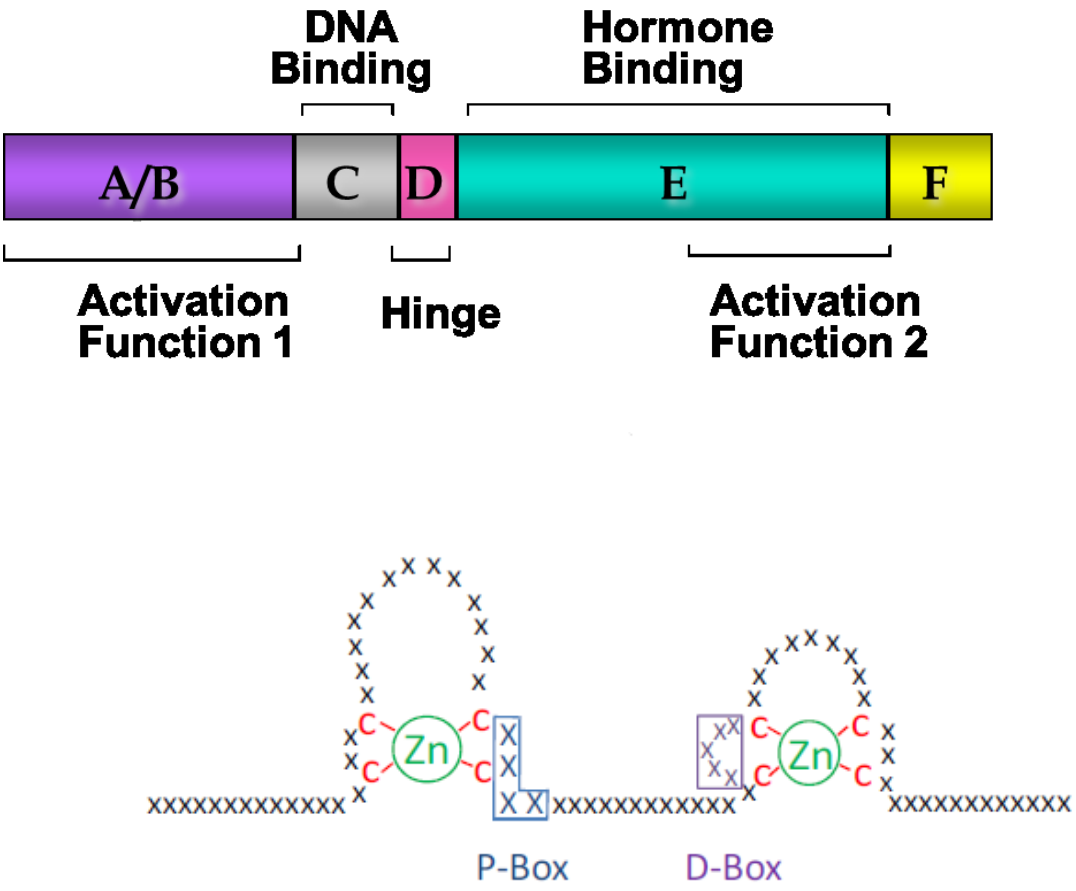

Figure 1.1: Diagram of nuclear receptor structure and function.

A. Schematic of domains A-F of nuclear receptors. The modular structure of NRs consists of seven (A-F) domains. The DNA-binding domain (DBD) in Region C and ligand-binding domain (LBD) in Region E are highly conserved. Region A/B contains the activation function 1 (AF-1), Region D has a flexible "hinge" between region C and region E, and Region F is of unknown function and is not well-conserved.

B. The functional regions of the nuclear receptor DBD domain. Between the two zinc finger motifs for DNA binding, this domain contains a Proximal-box (P-box), which determines DNA sequence specificity, and a Dimerization-box (D-box), which forms part of the dimerization interface.

1.3 The orphan nuclear receptor subfamily of estrogen-related receptors (ERR)

The estrogen-related receptors (ERR) are an orphan nuclear receptor subfamily consisting of three members: ERRα, ERRβ and ERRγ. Compared with the restricted expression pattern of ERRβ, the subtypes of ERRα and ERRγ have wider distribution in both developing and adult tissues. ERRα is expressed in almost all adult tissues, with higher expression levels in tissues with higher energy demands, such as the kidney, heart and brown adipocytes, suggesting its potential role in the regulation of energy balance (Sladek, Bader et al. 1997). Similar to the distribution pattern of ERRα, ERRγ is also widely expressed in adult tissues such as skeletal muscle, brain, kidney, and retina, with lower expression levels detected in adrenal, heart, pancreas, and thyroid tissues (Eudy, Yao et al. 1998, Chen, Zhang et al. 1999, Heard, Norby et al. 2000). The wide distribution pattern of the ERRs, especially ERRα and ERRγ, indicates that they are important for the development and maintenance of a variety of physiological processes.

The estrogen receptor-related receptors were discovered using the DNA-binding domain of estrogen receptor alpha (ERα) as a probe to screen recombinant DNA libraries (Giguere, Yang et al. 1988). Sequence comparisons show that ERRs and ERα share 66-70% sequence identity in the DBD and 34-37% in the LBD. Consistent with their high similarity in DBD sequences, ERRs and ERs also recognize similar DNA response elements containing the core motif 5′-AGGTCA-3′. While the classic Estrogen Response Element (ERE) is a palindromic sequence of 5′-AGGTCAnnnTGACCT-3′ with two core

motifs and three random nucleotides in between, the consensus Estrogen-related Receptor Response Element (ERRE) consists of an extended single motif: 5'-TnAAGGTCA-3'. Both ERR and ER subfamilies can interact with the ERE and all members except ERβ can also recognize ERRE. Although ER and ERR can compete for the same DNA binding elements, ERα binds more efficiently to an ERE, while ERRs prefer an ERRE (Vanacker, Bonnelye et al. 1999).

Unlike their high sequence similarity in DBD domain, ERRs and ERα exhibit more sequence divergence in the LBD. Moreover, the ERRs were the first orphan nuclear receptors discovered and have not been shown to interact with any natural ligand, suggesting that these receptors may function without the need for ligands. Indeed, crystallographic studies of ERRα and ERRγ have revealed that the structure of the ERR LBD in the apo form is similar to those of agonist-bound NRs, suggesting that the LBD domain is already in a constitutively active conformation for coregulator binding (Greschik, Wurtz et al. 2002, Greschik, Flaig et al. 2004, Kallen, Schlaeppi et al. 2004).

1.4 Transcriptional regulation by ERRα

Although ERRα has no natural ligand identified so far, it appears that ERRα utilizes a mechanism very similar to those previously described for other nuclear receptors to regulate gene transcription. ERRα recognizes a specific ERR response element (ERRE) within target gene promoters and initiates the assembly of a large

complex of proteins, known as coregulatory proteins, which either positively or negatively regulate target gene transcription. Thus, these transcriptional coregulators are thought of as "protein ligands" of ERRα. It appears that ERRα activity can be regulated by alterations of the expression level and activity of its coregulators.

The best-characterized coactivators for ERRα are members of the peroxisome proliferator-activated receptor-γ coactivator-1 (PGC-1) family of coregulators (Schreiber, Knutti et al. 2003). ERRα and its coactivator PGC-1 are known to regulate energy metabolism in tissues with high metabolic demands such as cardiac and skeletal muscles. Many of their target genes encode enzymes responsible for tricarboxylic acid (TCA) cycle, oxidative phosphorylation (OXPHOS) and lipid metabolism (Schreiber, Emter et al. 2004). Classical mapping studies, together with a recently completed ChIP-chip analysis, have revealed that most of the metabolic gene targets of PGC-1/ERRα, such as rate-limiting enzymes in β-oxidation of fatty acids, the tricarboxylic acid (TCA) cycle and oxidative phosphorylation (OXPHOS), contain a canonical ERRE (Deblois, Hall et al. 2009). The requirement for this element has been established in a significant number of the direct targets of ERRα (Schreiber, Knutti et al. 2003, Huss, Torra et al. 2004, Mootha, Handschin et al. 2004, Huss, Imahashi et al. 2007).

In addition to the model of direct ERRE recognition stated above, ERRα may function together with other transcriptional factors and cofactors. Our laboratory has recently shown that ERRα can interact with β-catenin (β-cat) and enhance the

transcription of a reporter gene (TOP-flash) of β-cat (Dwyer, Joseph et al. 2010). It has been established in a definitive manner that β-cat interacts with members of the T-cell factor (TCF) family of factors, an interaction that is required for the activation of target gene transcription. We have also shown that endogenous β-cat and ERR*α* can physically interact when assayed by coimmunoprecipitation. The significance of this interaction was demonstrated by showing that both ERR*α* and β-cat were required for the positive regulation of a number of endogenously expressed genes that had previously been defined as β-cat target genes, some of which are important for cell migration. Thus, in the context of β-cat target gene transcription, it appears that ERR*α* fulfills the role of a transcriptional coactivator.

Besides β-cat, ERR*α* has also been shown to physically interact with hypoxia-inducible factor-1 (HIF-1) and stimulate its transcriptional activity (Ao, Wang et al. 2008). HIF-1 is a transcription factor composed of two subunits: oxygen-regulated HIF-1*α* and constitutively expressed HIF-1β. Under hypoxic conditions, the HIF-1 dimer binds to specific hypoxia responsive elements (HREs) contained within the regulatory regions of hypoxia-induced genes (Wenger, Stiehl et al. 2005). The finding that ERR*α* can interact with HIF-1 suggests that ERR*α* may be recruited to the promoter of HIF-1 regulated genes and serve as a transcriptional cofactor of HIF-1 in response to hypoxia.

1.5 Synthetic ERRα antagonists

Although no endogenous ligands have been discovered for ERRs, several synthetic compounds have been shown to interact with ERRs. Some potent modulators of ERα have been shown to be relatively weak antagonists of ERRs. For example, diethylstilbestrol (DES), a potent synthetic estrogen that acts as an agonist on ER at nM concentrations, has been shown to act as an inverse agonist on ERRs at μM concentrations (Tremblay, Kunath et al. 2001). Similarly, 4-hydroxytamoxifen (4OH-Tamoxifen), a synthetic selective estrogen receptor modulator (SERM), functions as an inverse agonist for ERRβ and ERRγ (Coward, Lee et al. 2001, Tremblay, Bergeron et al. 2001).

Progress has also been made in developing selective ERRα modulators, as shown in Fig 1.2. The first reported high throughput screening identified an ERRα-selective antagonist, XCT790 (Busch, Stevens et al. 2004), which inhibits ERRα transcriptional activity. This compound was used to define the specific role of ERRα in the regulation of metabolic signaling pathways (Mootha, Handschin et al. 2004, Willy, Murray et al. 2004). Mechanistically, XCT790 has been shown to cause ERRα degradation *in vitro* (Lanvin, Bianco et al. 2007). Compound A is a more recently discovered ERRα selective antagonist. Compound A is an effective inhibitor of ERRα activity when measured on endogenously expressed metabolic gene targets with minimal impact on ERRα stability. Thus, the activities of these two compounds on ERRα are not equivalent with respect to

gene transcription and receptor stability. They are reminiscent of the two classes of ERα antagonists, ICI182,780 (a selective estrogen receptor degrader, or SERD) and tamoxifen (a selective estrogen receptor modulator, or SERM), which have distinct biological activities.

1.6 ERRα and breast cancer

High ERRα level is associated with estrogen receptor (ER)-negative tumor status. ERRα is also correlated with the expression of ErbB2, an indicator of tumor aggressiveness (Ariazi, Clark et al. 2002). High expression and activity of ERRα has been shown to correlate with unfavorable clinical outcomes in breast cancer (Suzuki, Miki et al. 2004, Chang, Kazmin et al. 2011). These clinical outcomes are further supported by *in vitro* data where shRNA-mediated knock down of ERRα decreased tumor growth of MDA-MB-231 xenografts (Stein, Chang et al. 2008). Additionally, using synthetic ERRα antagonists, several groups have shown that inhibition of ERRα significantly reduces the growth of both ER-positive and ER-negative breast tumors (Bianco, Lanvin et al. 2009, Chisamore, Wilkinson et al. 2009). Although the precise function of ERRα remains unclear, these findings establish a causal role for ERRα in the pathogenesis of breast cancer.

Different mechanisms have been proposed to describe how ERRα activity impacts tumor. PGC-1α/ERRα as metabolic regulators not only meet the high energy demand of rapidly growing tumors *in vivo* (Stein, Chang et al. 2008) but also cause

metabolic alterations that are associated with breast cancer brain metastasis (Chen, Hewel et al. 2007). Indeed, ERRα has been shown to be required for breast cancer cells to migrate *in vitro* (Stein, Chang et al. 2008).

Besides the PGC-1α /ERRα signaling axes, ERRα has been found to collaborate with other transcription factors highlighting additional mechanisms by which ERRα can impact tumor growth and progression. It has been shown that dedifferentiated epithelial tumor cells positioned at the invasion front exhibit a strong nuclear localization of β-cat, indicating that the nuclear function of β-cat may contribute to growth and metastasis of tumors (Hlubek, Brabletz et al. 2007). Importantly, knockdown of ERRα and β-cat synergistically reduced the migration of breast cancer cells (Dwyer, Joseph et al. 2010). ERRα has also been reported to interact with HIF-1 and stimulate its transcriptional activity, suggesting that ERRα may be involved in initiating transcriptional responses that enable tumor cell adaptation to hypoxia, a response critical for tumor cell survival and growth (Harris 2002). Recently, VEGF, a well-known pro-angiogenesis factor in cancer, was identified as a target gene of ERRα, regulated either in a PGC-1α dependent (Arany, Foo et al. 2008, Stein, Gaillard et al. 2009, Klimcakova, Chenard et al. 2012) or a HIF-1 dependent manner (Ao, Wang et al. 2008). These studies suggest that ERRα may play a role in tumor angiogenesis through the transcriptional regulation of pro-angiogenic factors. Altogether, these data suggest that

ERRα is a key regulator of several important processes in breast cancer proliferation and progression.

The limited treatment options for ER-negative and triple negative breast cancer necessitate the development of novel therapeutics for the treatment of this devastating disease. The association of ERRα with poor prognosis in breast cancer patients, combined with the demonstrated efficacy of ERRα inhibition in models of triple negative breast tumors, suggests that ERRα may be a novel target in the treatment of breast cancer. The development of small molecule antagonists targeting this receptor and/or the signaling pathways associated with ERRα is impeded by the lack of understanding of the mechanism(s) by which ERRα activity impacts tumor biology and the structural basis of compounds that inhibit the activity of this receptor. Answers to these compelling questions will both inform and motivate future exploitation of ERRα as a therapeutic target within the settings of breast cancer. My thesis research focuses on three specific areas: (1) identification of ERRα target genes important for breast tumor pathogenesis, (2) characterization of the molecular basis of ERRα crosstalk with other transcriptional regulation pathways, and (3) characterization of the structural basis of ERRα antagonism, the completion of which we believe will aid the development of therapeutic strategies targeting ERRα.

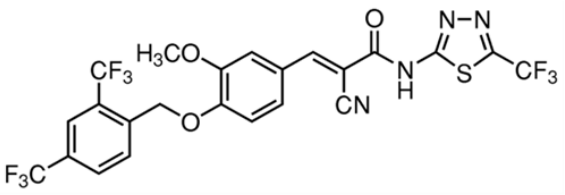

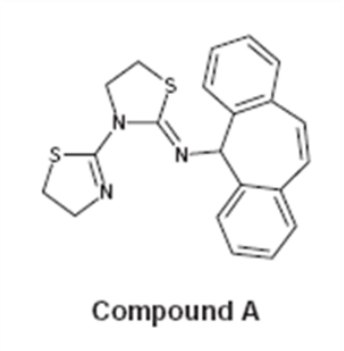

Figure 1.2: Structures of ERRα selective antagonists.

Depiction of compounds with selective activity on ERRα. A. A thiadiazolopyrimidinone derivative (XCT790) selectively inhibits ERRα activity and degrades the receptor. B. Compound A: N-[(2Z)-3-(4,5-dihydro-1,3-thiazol-2-yl)-1,3-thiazolidin-2-yl idene]-5H dibenzo[a,-d][7]annulen-5-amine.

Chapter 2 ECM1, a novel target gene of ERRα

Although the mechanism remains unclear, estrogen-related receptor alpha (ERRα) expression has been shown to correlate with unfavorable clinical outcomes and to play a causal role in the pathogenesis of breast cancer. It was of particular significance, therefore, that we and others demonstrated that VEGF mRNA expression was positively regulated by ERRα, implicating angiogenesis as one mechanism by which this receptor impacts tumor biology. Motivated by this observation we undertook a more extensive analysis of the target gene repertoire of ERRα in breast cancer cells with the goal of identifying additional proteins that may be involved in breast tumor angiogenesis. The details of this study have been published previously (Stein, Chang et al. 2008). In brief, cells were infected with an adenovirus expressing PGC-1α, an obligate cofactor for ERRα, or with an adenovirus expressing a variant of PGC-1α that is unable to interact with the receptor. This approach was used since no agonists of ERRα have been identified thus far. Bioinformatics analysis of the mRNA expression data confirmed that VEGF was upregulated upon ERRα activation. In addition, this analysis indicated that the expression of the mRNA encoding ECM1, a protein that has been shown to have angiogenic activities in other model systems, was upregulated under the same conditions. Thus, analysis of the role of the ERRα/ECM1 axis in validated models of breast cancer became the focus of our efforts in this area. The results of this analysis confirmed that ECM1 was a direct target of ERRα in cellular models of breast cancer.

Further, the angiogenic activity of ECM1 was confirmed in an *in vitro* tube formation assay. Finally, we demonstrated for the first time that disruption of ECM1 expression dramatically reduced the growth of breast cancer xenografts.

2.1 Introduction

The estrogen-related receptor alpha (ERRα) is an orphan nuclear receptor (NR) that is widely expressed in all tissues of the body. High expression and activity of ERRα has been shown to correlate with unfavorable clinical outcomes in breast cancer (Suzuki, Miki et al. 2004, Chang, Kazmin et al. 2011). Importantly, shRNA-mediated knockdown of ERRα expression resulted in decreased growth of MDA-MB-231 breast cancer cells when propagated as xenografts (Stein, Chang et al. 2008). Additionally, using synthetic ERRα antagonists, several groups have now shown that inhibition of ERRα significantly reduces the growth of both estrogen receptor (ER)-positive and ER-negative breast tumors (Bianco, Lanvin et al. 2009, Chisamore, Wilkinson et al. 2009). These findings establish a causal role for ERRα in the pathogenesis of breast cancer, although the precise mechanisms by which ERRα impacts tumor biology remain unclear.

A natural ligand for ERRα has not yet been identified, and it now appears likely that, unlike other members of the nuclear receptor superfamily, the activity of ERRα is regulated by the expression level and/or activity of the PGC-1 (peroxisome proliferator-activated receptor-γ coactivator-1) family of coactivators (Schreiber, Knutti et al. 2003). ERRα and its coactivator PGC-1 have been shown to regulate energy metabolism in

tissues with high metabolic demands such as cardiac and skeletal muscles. Many of their target genes encode enzymes responsible for the tricarboxylic acid (TCA) cycle, oxidative phosphorylation (OXPHOS) and lipid metabolism (Schreiber, Emter et al. 2004). Several non-exclusive hypotheses have been put forward to explain how ERRα impacts tumor biology. There is considerable data to suggest that the PGC-1α/ERRα complex helps in satisfying the high energy demand of rapidly growing tumors (Stein, Chang et al. 2008) and also facilitates the metabolic alterations that favor breast cancer brain metastasis (Chen, Hewel et al. 2007). There is also substantial data indicating that ERRα is also required for breast cancer cells to migrate *in vitro* (Stein, Chang et al. 2008). Taken together, these data suggest that ERRα is a key regulator of several important processes in breast cancer. The observation that VEGF, a well-known pro-angiogenic factor in cancer, can be regulated by ERRα and PGC-1α (Ao, Wang et al. 2008, Arany, Foo et al. 2008, Stein, Gaillard et al. 2009, Klimcakova, Chenard et al. 2012), suggests that PGC-1α/ERRα may play a role in tumor angiogenesis through the transcriptional regulation of pro-angiogenic factors. Interestingly, in our microarray analysis of PGC-1α/ERRα-induced gene transcription (Stein, Chang et al. 2008, Chang, Kazmin et al. 2011) we noticed a dramatic induction of the mRNA encoding ECM, a protein which has previously been shown to be overexpressed in human breast tumors and for which an angiogenic role has been demonstrated.

Extracellular matrix protein 1 (ECM1) is a secreted glycoprotein. A loss-of-function mutation in ECM1 has been shown to cause genodermatosis lipoid proteinosis (Hamada, McLean et al. 2002), suggesting that ECM1 plays an important role in maintaining the structural and functional integrity of the skin. In this regard, it has been shown that ECM1 can interact with various extracellular matrix proteins in skin, such as perlecan, fibulin-1C/D, MMP-9, collagen type IV and laminin 332 (Mongiat, Fu et al. 2003, Fujimoto, Terlizzi et al. 2005, Fujimoto, Terlizzi et al. 2006, Sercu, Zhang et al. 2008, Sercu, Lambeir et al. 2009). Interestingly, ECM1 is overexpressed in a significant number of primary and/or metastatic tumors: invasive breast ductal carcinoma (83%), esophageal squamous carcinoma (73%), gastric cancer (88%) and colorectal cancer (78%) (Wang, Yu et al. 2003). Furthermore, ECM1 expression has been identified as a novel prognostic marker for poor long-term survival in breast carcinoma (Lal, Hashimi et al. 2009) and a predictor of the chemo-resistance in ovarian cancer patients (Pan, Cheng et al. 2009). ECM1 expression also correlates with the metastatic properties of epithelial-derived tumors and has been established as a novel prognostic factor for the metastatic potential of hepatocellular carcinoma (Chen, Jia et al. 2011). The highest expression of ECM1 in tumors is found around blood vessels, and a potential role for ECM1 in angiogenesis has been proposed due to its ability to stimulate endothelial cell growth *in vitro* and blood vessel formation in chicken embryos *in vivo* (Han, Ni et al. 2001).

Together, these data highlight the potential importance of our observation that ECM1 is a mediator of the pathogenic activities of ERRα in breast tumors.

In the present study, we undertook studies to (1) define the molecular mechanism(s) by which PGC-1α/ERRα impact ECM1 expression (2) establish the importance of ECM1 in angiogenesis and (3) evaluate the impact of ECM1 knockdown on the growth of breast tumor xenografts *in vivo*. The results of these studies demonstrate a significant role for ECM1 in the establishment of the tumor environment and provide a mechanism to explain the negative impact of ERRα expression on breast tumor pathology.

2.2 Materials and Methods

2.2.1 Cell culture.

All cell lines, unless otherwise noted, were obtained from ATCC (Manassas, VA), expanded for two passages, and cryopreserved. All experiments were performed with cells of passage less than 25. MDA-MB-231 cells and the 4175 metastatic subline of this cell line (Minn, Gupta et al. 2005) (gift from Joan Massague, Memorial Sloan-Kettering Cancer Center, New York, NY, USA) were cultured in DMEM. MDA-MB-436, SKBR3 and HCT-116 cells were cultured in RPMI. MCF-7 cells were cultured in DMEM/F12. The stable MDA-MB-231-4175-derived cells were grown in DMEM supplemented with puromycin. All media above were purchased from Invitrogen and supplemented with 8% fetal bovine serum, 0.1 mM non-essential amino acids and 1 mM sodium pyruvate. HMEC-1 (gift from Gerard Blobe, Duke University, Durham, NC, USA) were cultured on 0.02% gelatin-coated plate in MCDB-131 (Invitrogen) supplemented with 10% FBS, 1 ug/ml hydrocortisone, 10 ng/ml EGF and 2 mM L-glutamine (Tian, Mythreye et al. 2012). IHMVEC cells (gift from Xiaofan Wang, Duke University, Durham, NC, USA) were cultured in EGM-2MV (Lonza) (Curtis, Wang et al. 2013). All cell lines were grown at 37°C in a humidified 5% CO_2 atmosphere.

2.2.2 Transduction of adenoviruses.

The generation of adenoviruses has been previously described (Gaillard, Dwyer et al. 2007). Cells were infected with adenoviruses expressing β-galactosidase (Bgal) or

PGC-1α (WT, 2X9, and L2L3M) at MOI of 100 and harvested after 48 hours. For siRNA experiments, cells were pre-transfected with indicated siRNA 48 hours prior to adenovirus infection, and harvested 24 hours after adenovirus infection.

2.2.3 RNA preparation and analysis.

Total RNA was extracted from cultured cells using the Bio-Rad Aurum RNA purification kit. Total RNA was extracted from tumor samples using a modified TRIzol (Invitrogen) RNA Purification protocol. 0.5 μg of isolated total RNA was used to synthesize cDNA using the iScript cDNA synthesis kit (BioRad). Real-time PCR was performed using the CFX384 Real-Time System (BioRad) with 0.06 μl cDNA, 0.3 μM primers and iQ SYBRGreen supermix (BioRad). cDNA was quantified using the 2-ΔΔCt method (Livak and Schmittgen 2001). Data were normalized to the expression of either 36B4 or RSP18. Cell culture data is representative of three independent experiments, while tumor data is the mean ± SEM.

2.2.4 Immunoblotting.

Whole-cell extracts were obtained by lysing cells in RIPA buffer (50 mM Tris-HCl (pH 7.4), 150 mM NaCl, 1 mM EDTA, 1% Triton X-100, 1% Na-deoxycholate, 0.1% SDS and protease inhibitors (5 μg/ml aprotinin, 5 μg/ml leupeptin,1 mM PMSF)). Secreted proteins were collected for analysis following the culture of cells in serum-free media for 24 hours. StrataClean Resins (Agilent Technologies, 400714-61) were used to precipitate proteins in the media. Proteins were separated by 8% SDS-PAGE and transferred onto

Hybond-C Extra nitrocellulose membrane (Amersham Biosciences) or Odyssey nitrocellulose membrane (LI-COR). Rabbit anti-PGC-1α antibody (Santa Cruz sc-13067, 1:1000 dilution), rabbit anti-ERRα antibody (Epitomics 2131-1, 1:1000 dilution), rabbit anti-ECM1 antibody (Epitomics 5447-1, 1:1000 dilution) and goat anti-GAPDH (V-18) antibody (Santa Cruz sc-20357, 1:1000 dilution) were used for protein detection. Secondary antibodies: Goat Anti-Rabbit IgG (H+L)-HRP (BIO-RAD 170-6515) and Donkey anti-Goat IgG-HRP (Santa Cruz SC-2033) were used for signal detection using autoradiography; CF770 Goat Anti-Mouse IgG (H+L) (Biotium 20077), CF770 Goat Anti-Rabbit IgG (H+L) (Biotium 20078) and CF770 Donkey Anti-Goat IgG (H+L) (Biotium 20277) were used for signal detection by Odyssey Infrared Imager (LI-COR).

2.2.5 Generation of inducible ECM1 knock-down stable cells.

ECM1 siRNA and control siRNA oligonucleotides were ligated into Tet-pLKO-puro vector (Addgene plasmid 21915). 7.5 μg of these constructs were mixed with 3.75 μg pVSVG and 3.75 μg pCMVdR8.2.dvpr and cotransfected (FuGene 6, Roche Applied Science) into the HEK293FT packaging cell line. Viral supernatant was filtered and supplemented with 8μg/ml polybrene. MDA-MB-231-4175 cells were infected by viral supernatants, and the derivative stable cells were selected under 1 μg/ml puromycin. The knock-down of ECM1 expression was induced by 200 ng/ml doxycycline and verified by RT-qPCR and Western blot analysis.

2.2.6 Endothelial tube formation assay.

HMEC-1 cells were plated at a density of 60,000 cells per well in 24-well plates coated with Growth Factor Reduced Basement Membrane Matrix (BD Matrigel 356231, BD Biosciences). Endothelial cells were cultured for 24 hours in serum-free basal media supplemented with 100-200ng/ml recombinant human ECM1 (R&D systems 3937-EC-050) to stimulate tube formation. 20-50ng/ml recombinant VEGF (Pepro Tech 100-20) was used as positive controls for tube formation. Each test concentration was assayed in duplicate wells and two independent biological replicates of each assay were performed. Representative field images were collected by an AMG EVOS XL microscope and tube formation was quantified using Angiogenesis Analyzer for ImageJ (Carpentier 2012).

2.2.7 Tumor xenograft study.

Animal handling and procedures were approved by the Duke University Medical Center Institutional Animal Care and Use Committee. For these studies $1x10^6$ MDA-MB-231-4175 shCON, shECM1(a) or shECM1(b) cells were suspended with 50% Basement Membrane Matrix (BD Matrigel 354234, BD Biosciences) in DMEM and were orthotopically grafted into the inguinal mammary fat pad of 8 week-old female NSG (NOD Scid Gamma) mice (10 mice per group). Water, provided ad libitum, was supplemented with 2mg/ml doxycycline starting three days prior to the cell graft and maintained throughout the experiment. To control for the potential off-target effects of doxycycline, one extra group of mice (n=8) were injected with shControl cells and

provided with normal water (no doxycycline). 23 days after cell graftment, half of the mice in each of the groups that were on doxycycline were switched to normal water. Tumor measurements were taken every 2 days. The volume of the primary tumors was quantified by direct caliper measurements (volume = $width^2$ x length/2). Tumors were removed when they reached a maximum of 2000 mm^3 and frozen in liquid nitrogen.

Statistical analyses. Tumor growth was analyzed by two-way ANOVA followed by Bonferroni posttests, where significance was set at $P<0.05$.Tumor mRNA was analyzed by students T test comparing each shECM1 to shControl.

2.3 Results

2.3.1 ECM1 is a target gene of the PGC-1α/ERRα signaling axis.

There is abundant evidence implicating ERRα in the pathogenesis of breast cancer, although the mechanism(s) by which the receptor impacts processes of pathological importance remains unclear. As a first step in defining the targets of ERRα action in breast cancer, we performed a bioinformatics analysis of the mRNA expression data that were collected following the activation of ERRα by expressing its cofactor PGC-1α. In this manner, it was determined that the mRNA encoding ECM1 was one of the most strongly upregulated genes in breast cancer cells (Stein, Chang et al. 2008). In addition to ERRα, PGC-1α can transcriptionally activate several other nuclear receptors. To specifically implicate ERRα in the induction of ECM1 expression, we confirmed that the induction was maintained when a specificity mutant of PGC-1α, PGC-1α 2x9, developed previously by our laboratory to selectively activate ERRα, was introduced into cells (Gaillard, Grasfeder et al. 2006, Gaillard, Dwyer et al. 2007). Further, as a negative control, we used a PGC-1α variant, PGC-1α L2L3M, in which the nuclear receptor interacting domain in this coregulator was mutated. A β-galactosidase (βgal) expressing adenovirus also served as a negative control for these studies. Using these tools, we confirmed in four different breast cancer cell lines that ERRα activation by PGC-1α wild type or the ERRα-specific PGC-1α 2x9 mutant resulted in an upregulation ECM1 mRNA. We confirmed in MCF-7 cells that ECM1 protein was likewise induced

(Figure 2.1). To verify that the induction of ECM1 by PGC-1α was mediated by ERRα, we evaluated its expression in cells with siRNA-mediated knockdown of ERRα expression. As expected, in the absence of ERRα, neither PGC-1α nor PGC-1-2X9 was able to induce the expression of either ECM1 mRNA or protein (Figure 2.2). It was concluded, therefore, that ECM1 is a *bona fide* target of the PGC-1α/ERRα complex. This finding, coupled with the fact that ECM1 overexpression had been found to be associated with invasive breast carcinoma, motivated our continued investigation into the biological implications of ECM1 upregulation in breast cancer.

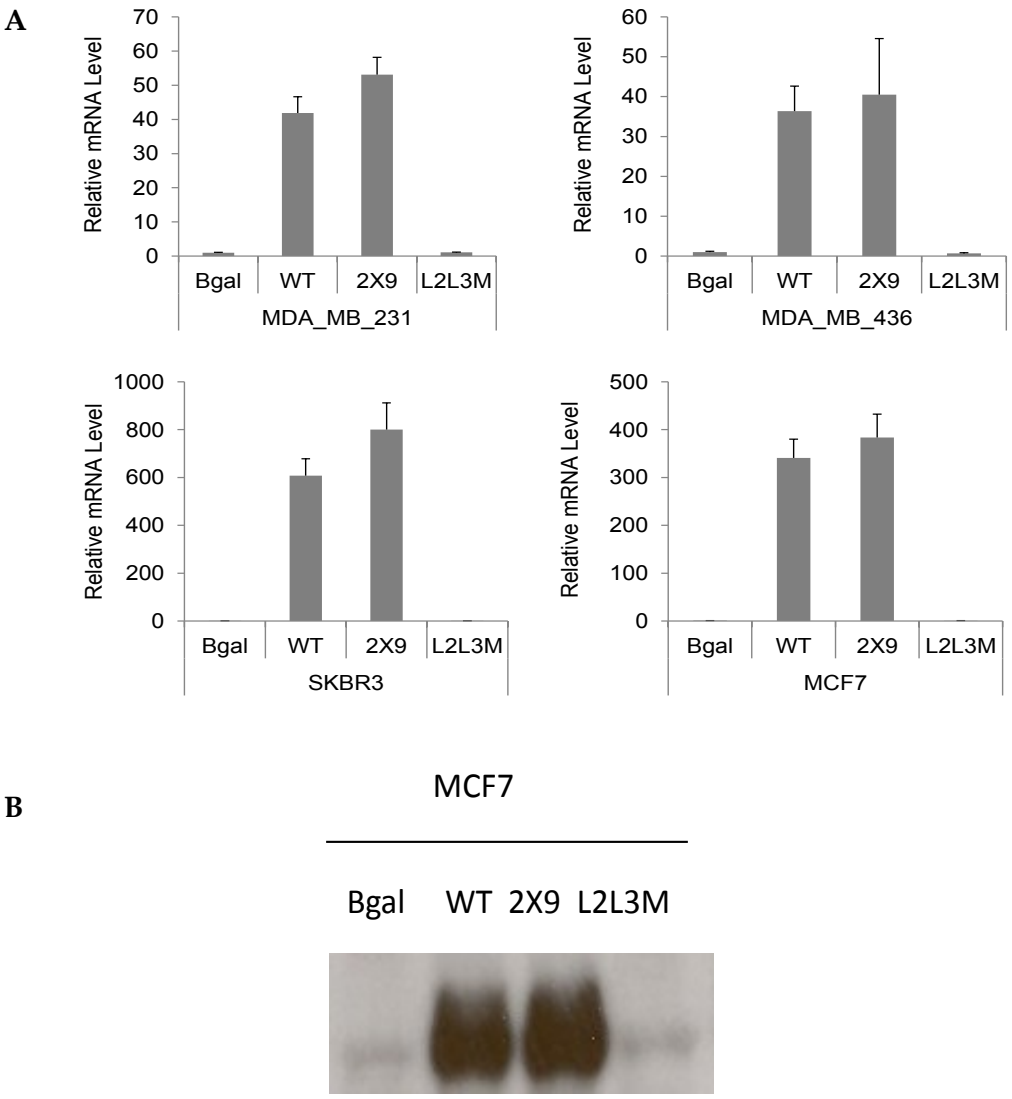

Figure 2.1 Upregulation of ECM1 by ERRα/PGC-1α in breast cancer cells.

A, PGC-1α induces ECM1 mRNA expression. Cells were infected with adenoviruses β-galactosidase (Bgal), wild-type PGC-1α (WT), PGC-1α 2X9 mutant (2X9) or PGC-1α L2L3M mutant (L2L3M) as indicated, followed by qPCR analysis of ECM1 mRNA levels normalized to 36B4 and relative to Bgal, and represented as mean ± SEM of triplicate wells in a representative assay.

B, Western blot analysis of secreted ECM1. Cells were changed to serum-free media 24 hours before media collection and proteins precipitated from culture media were analyzed by western blot.

A

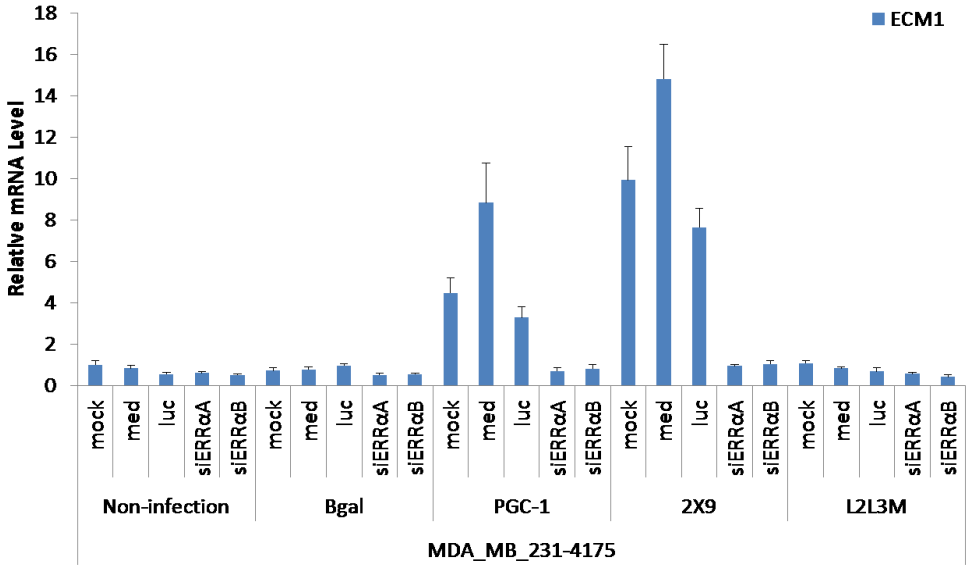
ECM1
Relative mRNA Level
18
16
14
12
10
8
6
4
2
0
mock
med
luc
siERRαA
siERRαB
Non-infection
Bgal
PGC-1
2X9
L2L3M
MDA_MB_231-4175

B

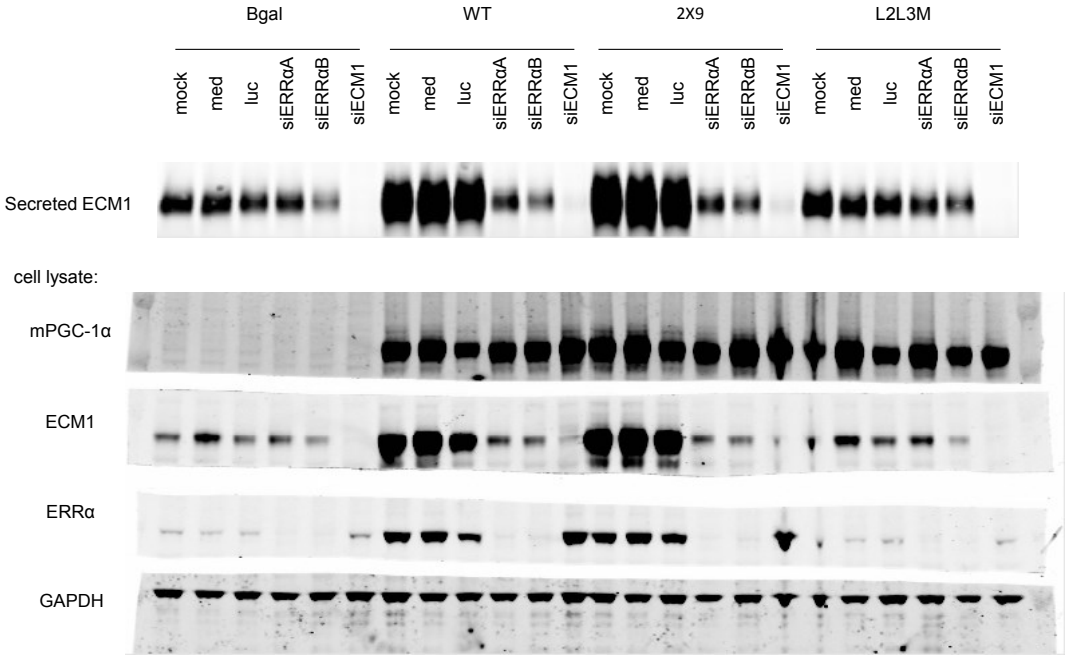
Bgal
WT
2X9
L2L3M
mock
med
luc
siERRαA
siERRαB
siECM1
Secreted ECM1
cell lysate:
mPGC-1α
ECM1
ERRα
GAPDH

Figure 2.2 The upregulation of ECM1 by PGC -1α is ERRα-dependent.

A, PGC-1α mediated induction of ECM1 mRNA expression is dependent on ERRα expression. Cells were subjected to mock transfection or transfected with control siRNAs (luc, med), or siRNAs directed against ERRα (siERRαA, siERRαB) or ECM1 (siECM1) for 48 hours and subsequently infected with adenoviruses as indicated. ECM1 mRNA levels were assessed by RT-qPCR, normalized to 36B4 and relative to mock-Bgal, and represented as mean ± SEM of triplicate wells in representative assay.

B, PGC-1α mediated-induction of ECM1 protein expression is dependent on ERRα expression. siRNA transfection and adenovirus infection were as described in (A). Cells were changed to serum-free media 24 hours before media collection. Whole-cell extracts and proteins precipitated from culture media were analyzed by western immunoblot.

2.3.2 The role of ECM1 on breast cancer proliferation *in vitro*.

As a first step in defining the functional role of ECM1 and how this may relate to breast cancer pathogenesis, we generated a series of derivatives of the MDA-MB-231-4175 cell line, a well-validated model of breast cancer that can be propagated as a xenograft in immunocompromised mice (Minn, Gupta et al. 2005). For these studies, several derivatives of this cell line were constructed by lentiviral transduction and puromycin selection to obtain inducible expression of shRNA directed against ECM1 or a scrambled control shRNA. Two independent shRNAs directed against different regions in the ECM1 transcript, shECM1(a) and shECM1(b), were included to control for potential off-target effects. Characterization of the stable inducible shRNA lines (MDA-MB-231-4175 shECM1(a), shECM1(b) and shControl) demonstrated a quantitative inhibition of ECM1 expression in both shECM1 cell lines upon doxycycline induction as compared to what was observed in the control cell line (Figure 2.3).

We next evaluated the effect of ECM1 knockdown on the proliferation of the stable cell line derivatives *in vitro*. Somewhat surprisingly, we determined that altering ECM1 expression level had no effect on the cell growth rate under the conditions studied (Figure 2.4). Similarly, siRNA-mediated ECM1 knockdown was also without effect on MDA-MB-231 and MDA-MB-436 breast cancer cell lines.

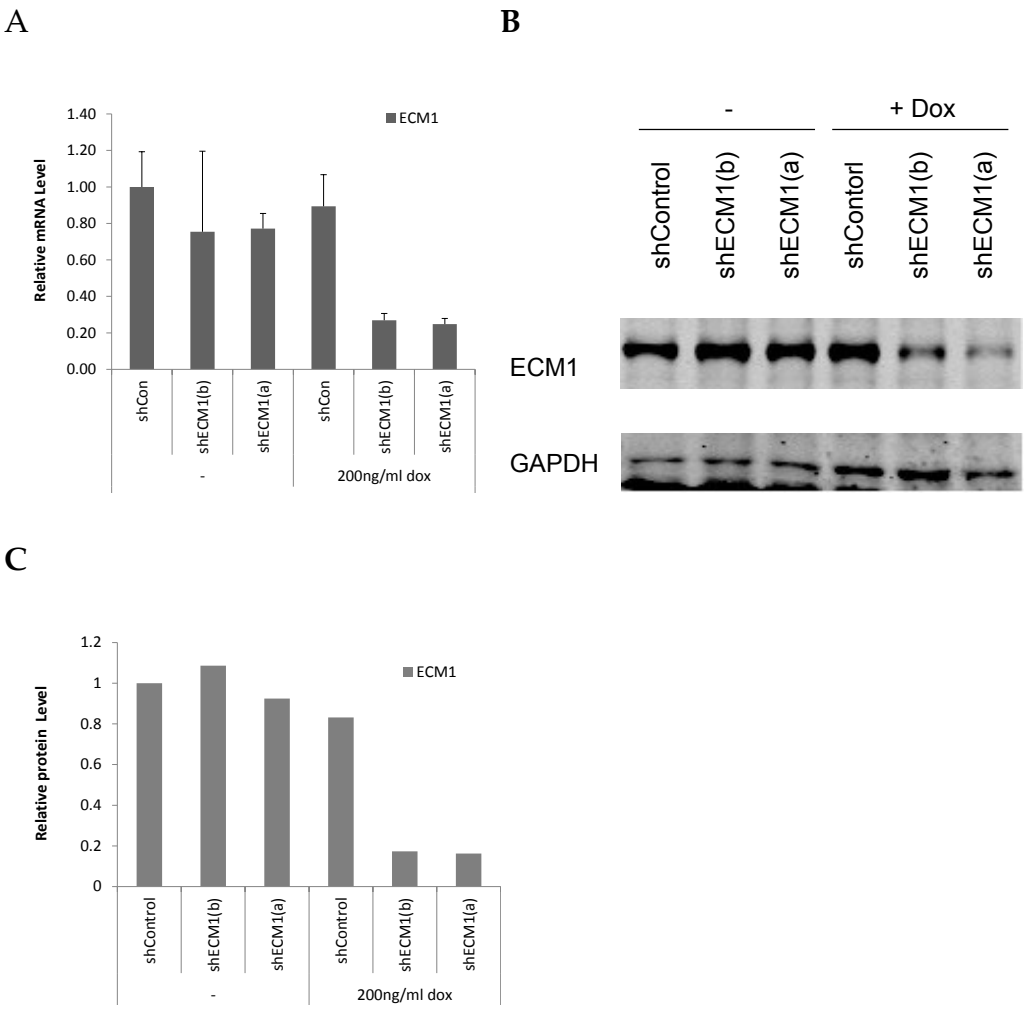

Figure 2.3 Characterization of inducible stable cells expressing ECM1 shRNA

A, Real Time PCR of ECM1 expression in MDA-MB-231-4175 shCON, shECM1-a and shECM1-b cells with or without 200ng/ml doxycycline treatment. Data are normalized to 36B4 and shown as a fraction of shControl mRNA ± SEM of triplicate wells of a representative assay.

B, Western immunoblot analysis of ECM1 protein secreted from MDA-MB-231-4175 shControl, shECM1-a or shECM1-b cells with or without 200ng/ml doxycycline treatment. GAPDH serves as the loading control.

C, Quantification of western immunoblot in B was performed using LiCor densitometry software.

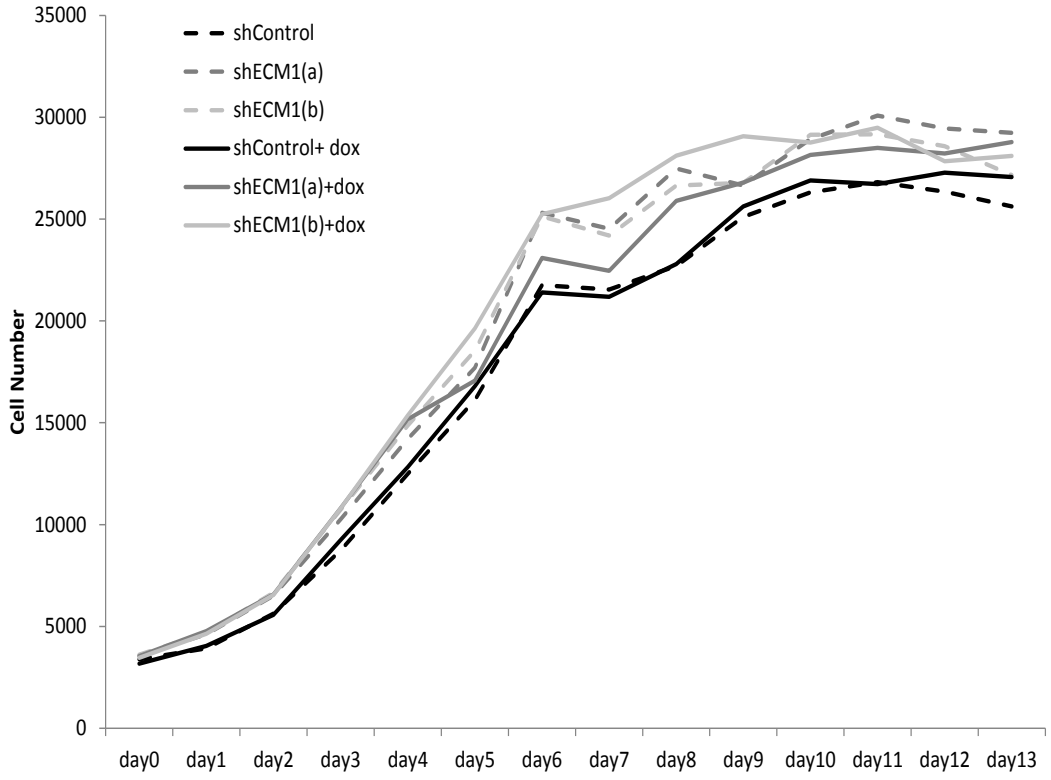

Figure 2.4 ECM1 Silencing does not affect breast cancer cell proliferation *in vitro*.

MDA-MB-231-4175 shControl, shECM1-a and shECM1-b cells were seeded in 96-well plates at a density of 3,000 cells/well with or without 200ng/ml doxycycline. Plates were harvested on the indicated days after seeding. Cell numbers were determined by Fluoreporter assay for DNA content using Hoechst 33258 (Sigma). The fluorescence was read at excitation 346nm and emission 460nm using a Fusion microplate reader (PerkinElmer, Waltham, MA). Data was plotted as cell number ± SEM of triplicate wells in representative assay.

2.3.3 Decreased ECM1 expression impedes breast tumor growth in mice.

We were surprised, given the significant correlation between ECM1 expression and breast tumor aggressiveness, that ECM1 knockdown was without effect on breast cancer cell proliferation *in vitro*. Thus, we next proceeded to evaluate the impact of ECM1 knockdown on the growth of the same cell lines when propagated as xenografts in immunocompromised mice. Specifically, MDA-MB-231-4175 shECM1 (a), shECM1 (b) or shControl cells were orthotopically grafted into the mammary fat pads of female NSG (NOD Scid Gamma) mice. Both real time PCR and immunoblot analyses (Figure 2.5) of the resulting primary tumors revealed that ECM1 levels were decreased in the shECM1 xenografts. Importantly, and in contrast to our findings *in vitro*, shRNA-mediated knockdown of ECM1 significantly impeded the growth of tumors when compared to a control shRNA (Figure 2.6). This important finding suggests that ECM1 is important for tumor growth *in vivo* and that this effect is manifest in the complex tumor microenvironment.

To test whether ECM1 affected tumor angiogenesis, we examined CD31 expression in the xenograft tumors. We found CD31 mRNA was decreased in the MDA-MB-231-4175 shECM1-derived tumors (Figure 2.7A). Furthermore, when the data from all treatment groups were combined, a significant correlation between ECM1 and CD31 expression was observed (slope = 0.1558, R2 =, $P<0.0001$) (Figure 2.7B). Thus, the effects

of ECM1 on tumor growth are likely to be mediated, at least in part, by its ability to promote angiogenesis.

2.3.4 ECM1 protein stimulates angiogenesis of endothelial cells *in vitro*.

Given the dramatic effect of ECM1 knockdown on xenograft growth and the correlation of this activity to decreased CD31 expression, we next evaluated the potential angiogenic activity of purified ECM1 protein when assayed *in vitro*. To this end, we performed an *in vitro* endothelial cell tube formation assay. Specifically, Human Microvascular Endothelial Cells (HMEC-1) were cultured on a reduced growth factor containing basement membrane matrix (Matrigel). Cells initially attached to the matrix, then elongated and migrated toward each other to form capillary-like tubes. As shown in Figure 4.8 A, although elongated processes appeared in the control cells cultured in basal media for 24 hours, only a few short, thin tubes were formed and appeared as disconnected networks. In contrast, in the presence of ECM1 (100-200ng/ml) or VEGF (20-50ng/ml), endothelial cells formed longer, thicker tubes, and the branches were strongly connected as networks. Quantification of the tube formation images shows that ECM1 stimulates the formation of nodes, joints, segments and branches (Figure 2.8 B). Importantly, a similar effect of recombinant ECM1 was observed in the tube formation assay where the transformed IHMVEC endothelial cell line was used (Figure 2.8 C).

The membrane receptor or binding proteins that interact with ECM1 and the signaling events downstream of these activities are not known. As a first step in

defining the ECM1 signaling pathway, we asked whether it acts on endothelial cells in a manner that is similar to VEGF. Notably, VEGF has been shown to stimulate phosphorylation of VEGFR, an activity that initiates a signaling cascade that results in activating phosphorylation of Erk, Akt and p38. However, treatment of (HMEC-1 cells) with ECM1 did not result in the phosphorylation of any of these targets. Surprisingly, we did not observe any synergism between ECM1 and VEGF when added to cells in different ratios. Thus, the mechanism by which ECM1 manifests its angiogenic activity remains elusive and will require further investigation to be elucidated.

A

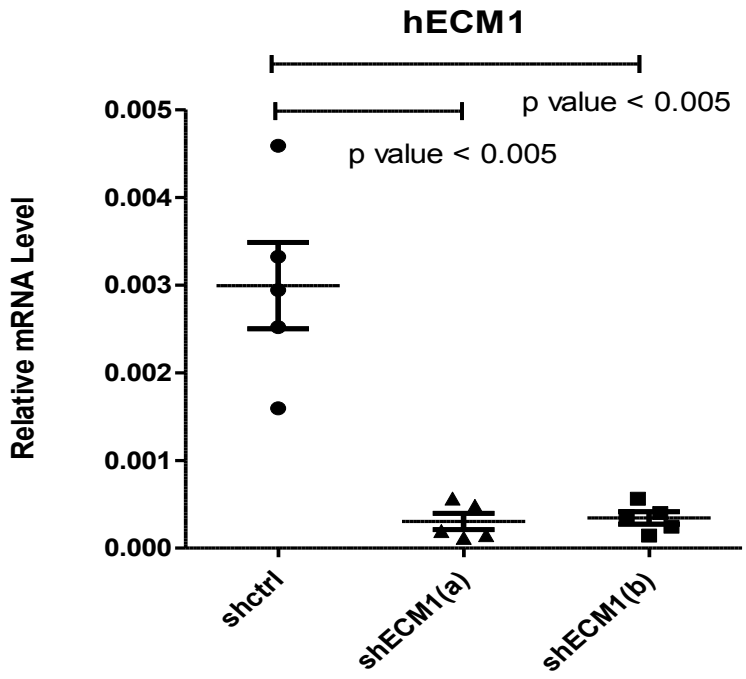

B

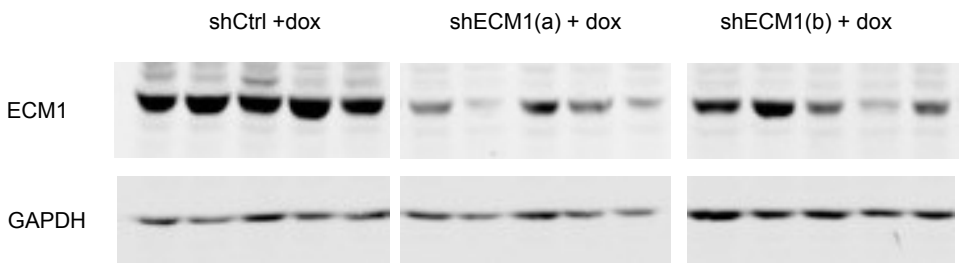

Figure 2.5 Confirmation of conditional knockdown of ECM1 expression in MDA-MB-231-4175 cell - derived xenografts

A, Expression of human ECM1 mRNA was measured by Real-time PCR and normalized to human RSP18 mRNA expression. Three groups of mice were used for data analysis. Group I,II and III: mice injected with shControl cells, shECM1-A cells or shECM1-B cells and treated with doxycycline water (n=5). Differential expression of ECM1 was observed between the shControl and shECM1 groups ($P<0.05$).

B, The impact of ECM1 mRNA knockdown on ECM1 protein expression in tumor xenografts was confirmed by Western immunoblot analysis. GAPDH serves as the loading control.

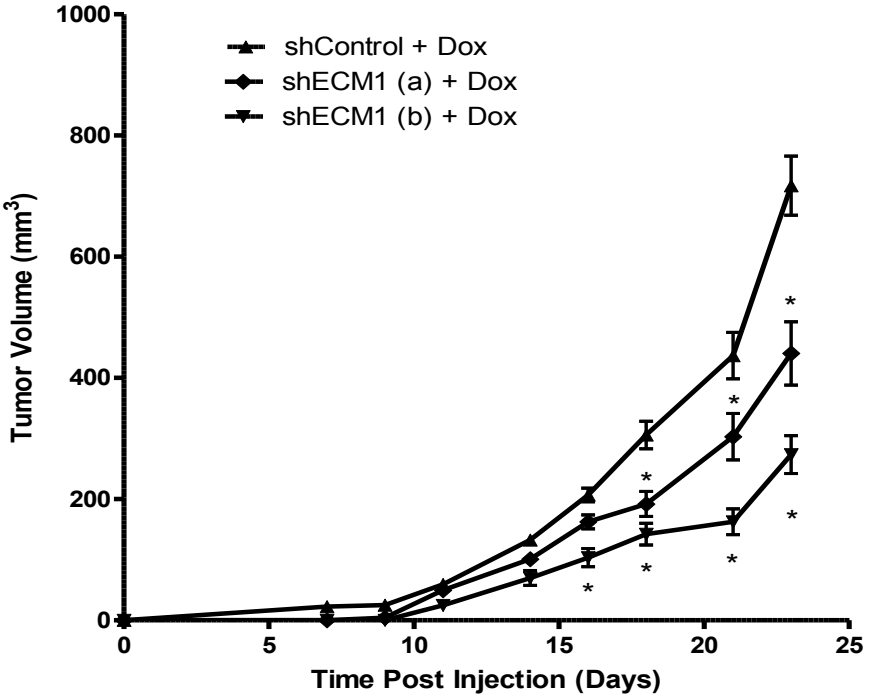

Figure 2.6 Silencing of ECM1 decreases the growth of MDA-MB-231-4175 cell-derived xenografts

Tumor growth rate of the stable cell lines after orthotopic injection. MDA-MB-231-4175 shCON, shECM1(a) and shECM1(b) cells were injected into the mammary fat pad of NSG (NOD Scid Gamma) mice fed with 2mg/ml doxycycline containing water starting three days prior to the cell injection. Tumor measurements were taken every 2 days, while the volume of the primary tumors was quantified by direct caliper measurements (volume = width^2 x length/2). Tumor growth was analyzed by two-way ANOVA followed by Bonferroni posttests. Points: mean volume for 10 mice per cell line. Bars: SEM. Stars: $P < 0.05$.

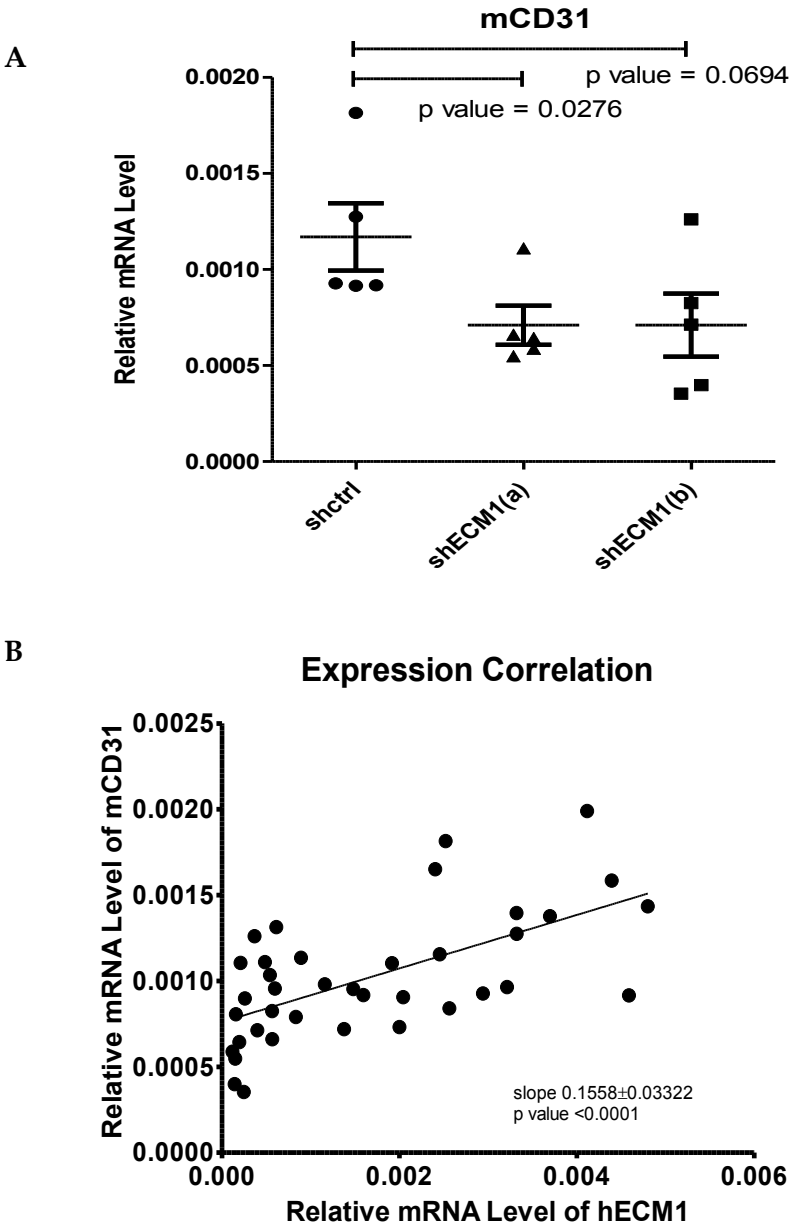

Figure 2.7 The expression of CD31 associates with ECM1 level in tumors

A, Expression of mouse CD31 *in vivo*. CD31 mRNA expression was measured by Real-time PCR and normalized to human RSP18 expression (n=5).

B, Correlation between mouse CD31 and human ECM1 expression in tumor xenografts. For this study, the expression of CD31 and ECM1 was evaluated in all mice (n=38) from all treatment groups and the data were plotted together to show the relationship between ECM1 and CD31 expression in tumors (P<0.0001).

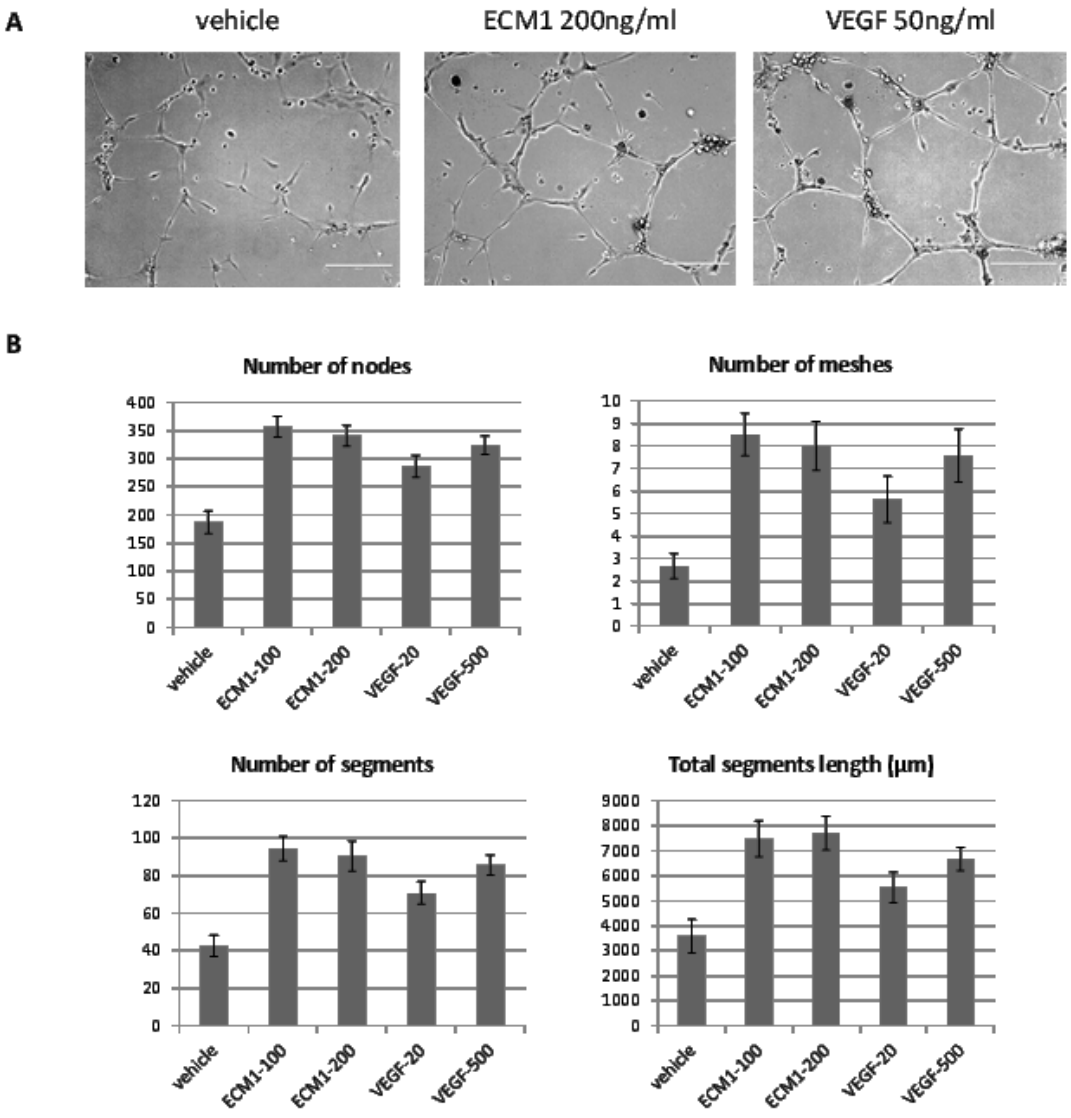
A
vehicle
ECM1 200ng/ml
VEGF 50ng/ml
B
Number of nodes
400
350
300
250
200
150
100
50
0
vehicle
ECM1-100
ECM1-200
VEGF-20
VEGF-500
Number of meshes
10
9
8
7
6
5
4
3
2
1
0
vehicle
ECM1-100
ECM1-200
VEGF-20
VEGF-500
Number of segments
120
100
80
60
40
20
0
vehicle
ECM1-100
ECM1-200
VEGF-20
VEGF-500
Total segments length [µm]
9000
8000
7000
6000
5000
4000
3000
2000
1000
0
vehicle
ECM1-100
ECM1-200
VEGF-20
VEGF-500

C

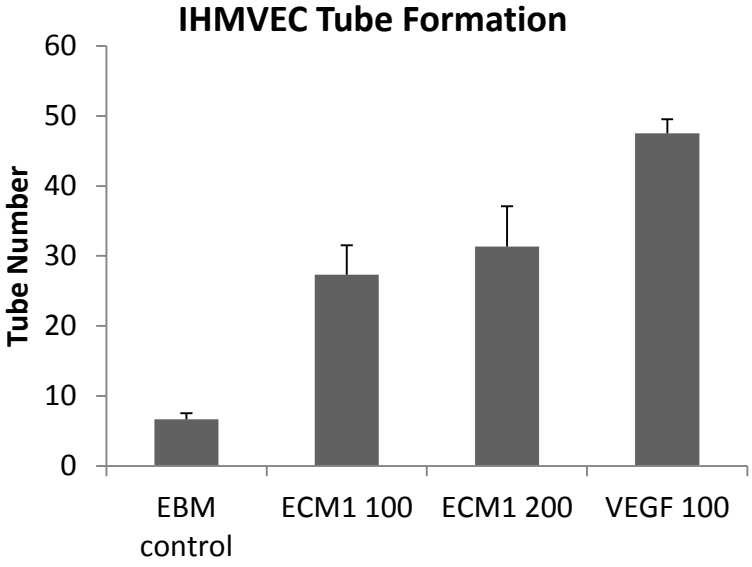

Figure 2.8 ECM1 stimulates tube formation of endothelial cells *in vitro*

A, ECM1 (200ng/ml) stimulates HMEC-1 tube formation. In this study, VEGF (50ng/ml) treatment served as a positive control. Images are representative of duplicate wells and two independent biological replicates. HMEC-1 cells were plated in 24-well plates coated with growth factor reduced Basement Membrane Matrix and cultured in serum-free basal media for between 6-24 hours as indicated.

B, Quantification of HMEC-1 tube formation shows the angiogenic effect of ECM1. Images were processed using "Angiogenesis Analyzer for ImageJ" and data from each treatment were plotted as mean ± SEM of 6-8 pictures from two independent wells.

C. Immortalized Human Microvascular Endothelial cells (IHMVEC) were cultured on Matrigel containing regular basement membrane matrix. IHMVEC cells were plated at a low density of 2,000 cells per well in 96-well plates. Cells were cultured in serum-free basal media for between 6 to 24 hours as indicated. Most of the control cells cultured in basal media were rounded and grew as solitary cells. Only a few tubes were observed arranged as disconnected networks in this control condition. In contrast, in the presence of ECM1 (100-200ng/ml) or VEGF (100ng/ml), a substantial number of endothelial cells formed tubes were organized as connected networks. Tube numbers were manually counted using imageJ software and represented as mean ± SEM of triplicate wells.

2.4 Discussion

Previous studies have demonstrated a relationship between ECM1 expression and poor prognosis in both breast and liver cancers (Lal, Hashimi et al. 2009, Chen, Jia et al. 2011). Nevertheless, a causal relationship between ECM1 and cancer has not been established. It is significant, therefore, that we were able to demonstrate that ECM1 knockdown has a dramatic inhibitory effect on breast tumor growth in mice and that this is likely related to decreased angiogenesis. Additionally, these studies further validate the utility of targeting ERRα and ECM1 expression in breast cancer.

Although ECM1 is overexpressed in breast, esophageal, gastric and colorectal cancers, the mechanisms by which its expression are regulated have not been elucidated. In this study, we demonstrate that ECM1 is a downstream target of the PGC-1α/ERRα signaling complex, and as such, may be a key mediator of the pathogenic activities of ERRα noted in various cancers.

Currently, the role of PGC-1α in cancer remains controversial, and it appears its actions may be highly context- dependent. For example, PGC-1α overexpression has been observed in endometrial cancer (Cormio, Guerra et al. 2009) while several other studies have reported reduced PGC-1α expression in cancers of the breast (Watkins, Douglas-Jones et al. 2003, Watkins, Douglas-Jones et al. 2004) and colon (Feilchenfeldt, Brundler et al. 2004) as well as the surface epithelium of malignant ovarian tumors (Zhang, Ba et al. 2007). Additionally, overexpression of PGC-1α was shown to stimulate

ovarian cancer cell apoptosis though a PPAR gamma-dependent pathway, (Zhang, Gao et al. 2007) and PGC-1α promotes prostate cancer cell growth by activating the androgen receptor (Shiota, Yokomizo et al. 2010). ErbB2/Neu-induced mammary tumors with ectopic PGC-1α overexpression exhibited an increased glucose supply and increased tumor growth (Klimcakova, Chenard et al. 2012). PGC-1α was also shown to coordinately regulate mitochondrial and fatty acid metabolism, and, thus, promote colon tumor growth (Bhalla, Hwang et al. 2011). From these studies, it seems likely that PGC-1α may have multiple roles depending on different biological contexts, potentially due to its interaction with different nuclear receptors. Our study identified ECM1, a novel pro-angiogenic factor, to be a target gene of the PGC-1α/ERRα axis, which suggests that PGC-1α/ERRα may function through the promotion of tumor angiogenesis to adapt to the lack of nutrient sources in rapidly growing tumors

Previously, ECM1 was reported to contribute to the invasion and migration of cholangiocarcinoma cells (CCA) (Xiong, Zhang et al. 2012). However, under the conditions of our assays ECM1 knockdown had no effect on the proliferation or the migratory/invasive properties of several breast cancer cell lines (MDA-MB-231 and MDA-MB-436). Thus, it is tempting to speculate that although breast cancer cells can secrete ECM1, they may not be the primary effector of ECM1. Instead, secreted ECM1 may exert its actions on endothelial cells within the tumor microenvironment and stimulate blood vessel formation. In support of this hypothesis we found that

expression of ECM1 correlates with CD31 in tumors and that recombinant ECM1 can induce endothelial cell tube formation *in vitro*. Identification of the ECM1 receptor/binding protein (if such a protein exists) and subsequent evaluation of its expression will provide clarity as to the validity of this model. However, it has been reported that ECM1 can interact with many extracellular matrix proteins (such as MMP-9) in cultured skin cells. Thus it is possible that ECM1 may have a direct effect on the remodeling of the extracellular matrix, an activity that would not require the involvement of a specific receptor.

In addition to the local effects of ECM1 on tumor vasculature highlighted by our studies, there is considerable data to suggest that it may also have systemic effects. Notably, clinical studies indicate that high ECM1 levels could be detected in serum samples from patients with ovarian carcinoma (Boylan, Andersen et al. 2010). It has been reported that ECM1 can bind to the IL-2 receptor on the surface of Th2 cells to block IL-2 signaling and promote Th2 cell egress from lymph nodes (Sahin, Colla et al. 2011). It is also known that Th2 cells can infiltrate breast cancer tumors and promote tumor growth (Pedroza-Gonzalez, Xu et al. 2011). Thus, it is possible that ECM1 may promote breast tumor development through recruitment of Th2 cells. However, we observed a dramatic effect of ECM1 knockdown on tumor growth in T-cell deficient mice. Thus, any effects of ECM1 on T-cells, and subsequently on tumor biology, are beyond the effects we have noted on angiogenesis.

Although the molecular mechanisms underlying the angiogenic actions of ECM1 remain to be determined, our preliminary study suggests that ECM1 functions in a manner that is distinct from VEGF. We show that unlike VEGF, ECM1 does not trigger phosphorylation of VEGFR, Erk, Akt or p38. Recently, a predicted structural model for ECM1 using the third human serum albumin as template divided ECM1 into four domains: an N-terminal domain of α-helices, followed by three Serum Albumin Subdomain-Like domains (SASDL 2-4). It is proposed that the SASDL domains of ECM1 could form a "finger-like" structure for ECM1 to serve as a scaffolding protein interacting with a variety of extracellular proteins (Sercu, Lambeir et al. 2009). Our *in vivo* study shows that alteration of ECM1 can affect the CD31 levels in tumors without changing VEGF levels. A number of drugs that target VEGF-A or its receptor have been developed to successfully halt tumor angiogenesis and impede tumor growth in animal studies. However, the clinical results in cancer patients have been less impressive. The discovery that ECM1 is a pro-angiogenic factor in tumors may provide an alternative strategy to target tumor angiogenesis.

Chapter 3 Crosstalk of ERRα with other signaling pathways

3.1 Introduction

3.1.1 Canonical pathway of ERRα

ERRα has no known natural ligand identified so far. However, the apo ERRα protein appears to be in the "active" conformation similar to the structures of other agonist-activated nuclear receptors (Greschik, Wurtz et al. 2002, Kallen, Schlaeppi et al. 2004). This finding raises the question as to how the transcriptional activity of ERRα is regulated.

Cofactor availability and activity are likely to be the main mechanism by which ERRα activity is regulated. Indeed, it has been shown that ERRα activity can be dramatically upregulated by increasing the expression of its coactivators PGC-1α and PGC-1β, which in turns is regulated by metabolic stresses, such as fasting, exercise and cold (Kamei, Ohizumi et al. 2003, Schreiber, Knutti et al. 2003, Huss, Torra et al. 2004). Together, this cofactor/receptor pair regulates the transcription of a large number of genes involved in energy metabolism. Chromatin immunoprecipitation (ChIP) analyses have revealed that most of the metabolic gene targets of PGC-1/ERRα contain a canonical ERR response element (ERRE) (Deblois, Hall et al. 2009). The mechanism by which ERRα regulates the transcription of these genes is very similar to that previously described for other nuclear receptors. ERRα recognizes ERRE within target gene

promoters and initiates the assembly of a large complex of cofactors and general transcription machinery that together enable the regulation of target gene transcription.

3.1.2 Non-canonical gene regulation by ERRα

Besides this classical model of direct ERRE binding, emerging evidences also suggest the existence of alternative pathways by which ERRα regulates target gene transcription. Specifically, ERRα can interact or cooperate with other transcriptional factors or cofactors besides PGC-1 to effect target gene transcription. β-catenin (β-cat) and hypoxia-inducible factor-1 (HIF-1) are two of such factors we are particular interested in because of their relevance to cancer.

ERRα/β-cat pathway

Previously, our lab used a chemical biology approach to explore the pathways in which ERRα is engaged (Dwyer, Joseph et al. 2010). Among the compounds identified to modulate the transcriptional activity of ERRα were carbolines, which were known to inhibit the canonical Wnt signaling pathway. In the canonical Wnt pathway, Wnt activation causes GSK-3β inhibition, which leads to an increase in β-cat stability. The stabilized β-cat can translocate to the nucleus, where it regulates target gene expression through its interaction with the T-cell factor (TCF)/ lymphoid enhancer-binding factor (LEF) family of transcription factors. TOPFlash is a TCF-LEF luc-reporter, the activity of which is driven by TCF/LEF and enhanced by the binding of cofactor β-cat. While ERRα expression alone has a minimal effect on TOP-flash, it strongly enhanced the

transcription of this reporter gene in the presence of a constitutively active β-cat mutant. Similarly, expression of β-cat significantly enhanced the activity of ERRα on 3xERE_luc reporter. The crosstalk between ERRα and β-cat was further demonstrated by coimmunoprecipitation studies, which showed that endogenous ERRα physically interacts with β-cat and TCF. That being said, however, it does not rule out the possibility that ERRα and β-cat/TCF complexes bind independently on target genes and cooperate to regulate target gene transcription. One example of this is Wnt 11, a gene involved in cell migration, which was identified to be under the control of this ERRα/ β-cat crosstalk (Dwyer, Joseph et al. 2010). Interestingly, ChIP analysis indicated that both ERRα and β-cat were recruited to the same promoter region of Wnt-11, where several putative ERREs and TCF binding sites were found to be adjacently located. What remains unclear is the mechanism of this crosstalk, as whether ERRα and β-cat bind to adjacent sites or if a tethering mechanism is involved.

ERRα / HIF-1 pathway

The transcription factors hypoxia inducible factor 1 alpha (HIF-1α) and beta (HIF-1β) form a heterodimer to regulate the physiological adaptation to hypoxia. While the protein level of the β-subunit is relatively constant, the α-subunit is highly oxygen sensitive (Wenger, Stiehl et al. 2005). Under normoxia conditions, HIF-1α is hydroxylated on proline 402 and proline 564, which is necessary for binding to von Hippel-Lindau (VHL), a component of an E3 ubiquitin ligase complex, and triggers

ubiquitin-mediated HIF-1α degradation by the proteasome. Prolyl hydroxylases need O_2, ferrous iron and 2-oxoglutarate for their activity. However, under hypoxia conditions, the absence of O_2 inactivates prolyl hydroxylase activity, thus stabilizing the HIF-1α protein. Under normoxic conditions, prolyl hydroxylase inhibitors such as cobalt chloride ($CoCl_2$), desferrioxamine (DFO) and dimethyloxaloylglycine (DMOG) can block HIF-1α degradation. While $CoCl_2$ and DFO are iron chelators, DMOG is a 2-oxoglutarate analogue . Stabilized HIF-1α dimerizes with HIF-1β, recognizes hypoxia response element (HRE) and activates the transcription of genes involved in hypoxia response, angiogenesis, etc. GLUT1 and VEGF are among those identified HIF-1 target genes that are crucially involved in adaption to hypoxia by switching nutrient utilization and turning on angiogenesis.

A potential role for ERRs (including ERRα) in the hypoxic response was recently implicated by the demonstration of a direct interaction between ERR and HIF. Furthermore, overexpression of ERRs enhances HIF-mediated target gene transcription, while ERRs activity appears to be essential for the function of HIF. Both the expression of a dominant negative form of ERR and the treatment of a non-slective ERR inhibitor, diethylstilbestrol (DES) blocked the transcriptional activation of HIF target genes, such as VEGF, PGK1 and GLUT1 (Ao, Wang et al. 2008).

Interestingly, VEGF, a well-characterized HIF-1 target gene, has also been shown to be upregulated by ERRα and its coactivator PGC-1α under normoxia conditions in a

HIF-independent manner (Arany, Foo et al. 2008, Stein, Chang et al. 2008, Klimcakova, Chenard et al. 2012). It is possible that the availability of HIF and/or PGC-1α determines how ERRα mediates the transcription of genes such as VEGF which contain both ERRE and HRE elements on their promoters. However, under hypoxia conditions when HIF is available, it is unknown whether ERRα still needs to be recruited to ERRE sites on the promoter, or it can be recruited by HIF protein via a tethering mechanism.

3.1.3 Dissecting Canonical/Non-Canonical pathway of ERRα

It is clear that ERRα is an important regulator of multiple biological and pathological processes. ERRα manifests these distinct activities by partnering with different cofactors and transcription factors. A better understanding of the transcriptomes regulated by ERRα and its partners, and the mechanisms by these target genes are regulated will inform rationale design of ERRα modulators with favorable biological activities. While the classical pathway of ERRα –mediated gene transcription is well-characterized, the mechanism of non-canonical ERRα pathways is still unclear. A key question is what role the direct DNA binding plays in non-canonical ERRα pathways. As a first step toward dissecting the mechanistic differences between canonical and non-canonical pathways, we performed site-directed mutagenesis in ERRα DBD to abolish its DNA binding ability.

It has been well-characterized that the residues in and around proximal (P-box) of the first zinc finger of the DBD domain are very important for DNA recognition and

binding. Mutations on the DNA recognition helix can cause alteration of DNA binding (Nguyen, Bail et al. 2007). Shown in Figure 3.1 is a model of the amino acid–base interactions underlying ER/ERE binding, where residues of Glu on position 2, Lys on position 5, Lys on position 9 and Arg on position 10 are involved in DNA binding. As shown in Table 3.1 and Figure 3.1, ERRα and ERα have great similarity in their DBD domain and P-Box sequences. The goals of this study were to (1) identify target genes co-regulated by ERRα and HIF-1 that are of pathogenic importance in breast cancer and (2) dissect the mechanisms by which ERRα /HIF-1 co-regulate these genes.

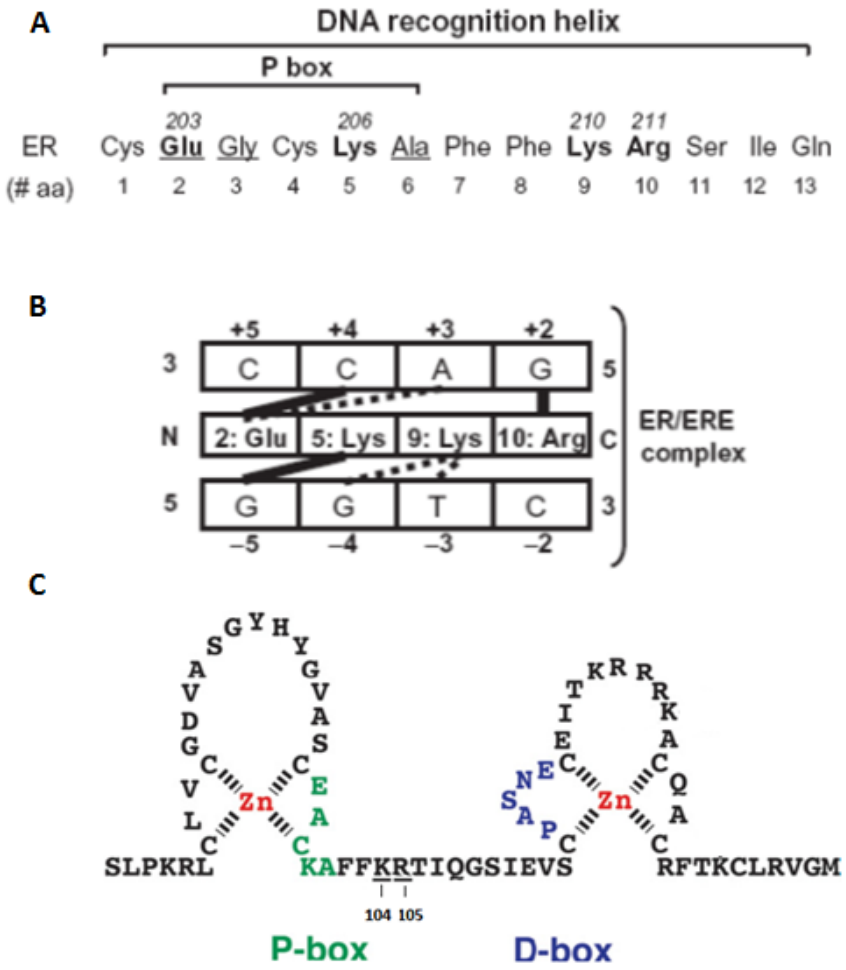

Figure 3.1 DBD domains of ERα and ERRα

A. DNA recognition helix of the estrogen receptor (ER). The position of amino acids in the DNA recognition helix is indicated by numbers from 1 to 13. Base-interacting residues in ERα are indicated in bold, and P box amino acids are underlined.
B. Models of the amino acid–base interactions underlying specific recognition of the estrogen response element by ER. Interactions considered in a proposed model (Suzuki and Yagi 1994) are in bold, while interactions described in the ER-ERE crystal structure (Schwabe, Chapman et al. 1993) but not in the model are in dashed lines.
C. DBD domain of estrogen-related receptor alpha (ERRα) showing the two zinc fingers, proximal box (P-box) and distal box (D-box). Figure was adapted from publication on "Rational design of an estrogen receptor mutant with altered DNA-binding specificity" (Nguyen, Bail et al. 2007).

Table 3.1: P-Box and DNA response element sequences of nuclear receptors.

Receptors	DBD sequence near P-Box	DNA response element
ERR	S**C**EA**C**KAFFKR	ERRE: 5'-TnAAGGTCA-3'
ER	S**C**EG**C**KAFFKR	ERE: 5'-AGGTCAnnnTGACCT-3'
AR/PR/GR	T**C**GS**C**KVFFKR	GRE: 5'-AGAACAnnnTGTTCT-3'
TR	T**C**EG**C**KGFFKR	DR: 5'-AGGTCA-3'
RAR/ RXR	S**C**EG**C**KGFFKR	

3.2 Materials and Methods

3.2.1 Primers

Mutagenesis primers were designed based on an siRNA resistant plasmid pcDNA_ERRαSiR, and the sequences for the forward primers are as follows:

K104A: 5′- CAAAGCCTTCTTCGCGAGGACCATCCAGG -3′

R105A: 5′- CAAAGCCTTCTTCAAGGCGACCATCCAGGGGAG -3′

K104A/R105A:5′-CTGCAAAGCCTTCTTCGCGGCAACCATCCAGGGGAGCATC -3′

3.2.2 Plasmids

Plasmids pcDNA_ERRα_K104A, pcDNA_ERRα_R105A and pcDNA _ ERRα _ K104A/R105A were constructed by site-directed mutagenesis PCR of pcDNA_ERRαsiR. Constructs of VP16_ERRα_K104A, VP16_ERRα_R105A and VP16_ERRα_K104A/R105A were made by cloning their coding sequeces from pcDNA constructs into VP16 vectors.

Transcription reporters of 3xERE-TATA-luciferase, 5xGal4-luciferase and TOPFlash were previously described (Chang, Norris et al. 1999, Dwyer, Joseph et al. 2010). HRE_luc reporter was purchased from Addgene (plasmid 26731).

3.2.3 Cell culture

HepG2 cells and Hela cells were obtained from American Type Culture Collection (Manassas, VA), expanded for two passages, and cryopreserved. Cells were cultured in Minimal Essential Medium (MEM) (Invitrogen) supplemented with 10% fetal bovine serum (HyClone, Logan, UT), 0.1 mM non-essential amino acids and 1 mM

sodium pyruvate (Invitrogen) and maintained in a humidified 37°C incubator with 5% CO_2. All experiments were performed with cells passaged less than 25 times.

For cell transfections and mammalian two-hybrid assays, cells were switched to the less rich medium Basal Medium Eagle (BME) supplemented with 10% fetal bovine serum (HyClone, Logan, UT), 2 mM L-Glutamine, 0.1 mM non-essential amino acids and 1 mM sodium pyruvate (Invitrogen).

3.2.4 Transient transfections

For transient transfections, HepG2 or Hela cells were seeded in wells of 96-well plates 24 hours prior to transfection. On the day of transfection, the media was aspirated and cells were washed once with PBS. Cells were transfect using Lipofectin reagent (Invitrogen, Carlsbad, CA). Briefly, a DNA-Lipofectin mixture containing 600 ng of total plasmids per triplicate samples in 96-well were mixed with Lipofectin® in OptiMEM according to manufacturer's protocol (Invitrogen). Cells in each well were transfected with 10 μl DNA-lipofectin mixture. After indicated hours, transfected cells were harvested, when luciferase and β-galactosidase (β-gal) activities were measured using a Fusion™ Universal Microplate Analyzer (PerkinElmer). Each experiment was repeated at least three times. Representative results are presented as standard luciferase activity normalized with β-Gal for transfection efficiency, ± standard error of the mean (SEM) per triplicate samples.

3.2.5 RNA preparations and analysis

Total RNA of cell culture was isolated using the Bio-Rad Aurum RNA purification kit. 0.5 μg of isolated total RNA was used to synthesize cDNA using iScript cDNA synthesis kit (BioRad). Real-time PCR was performed using CFX384 Real-Time System (BioRad) with 0.06 μl cDNA, 0.3 μM primers and iQ SYBRGreen supermix (BioRad). cDNA was quantified using the 2-ΔΔCt method (Livak and Schmittgen 2001). Data was normalized to either 36B4 or RSP18 internal controls. Cell culture data is representative of three independent experiments, while tumor data is the mean ± SEM.

3.3 Results

3.3.1 Overlap between ERRα and HIF-1 target genes

It was reported in a previous study that ERR*α* and HIF physically interact with each other and coregulate a handful of known HIF target genes. To assess the extent of the crosstalk between these transcription factors, we performed a preliminary examination of available ChIP and microarray datasets to identify genes that can potentially be regulated by both ERR*α* and HIF. HIF target genes were culled from a ChIP-ChIP analysis performed in MCF7 cells using either HIF-1*α* or HIF-2*α* antibodies. (Mole, Blancher et al. 2009). ERR*α* target genes were obtained from a MCF7 microarray analysis previously performed in our lab using PGC-1*α* to activate ERR*α*. Genes that are either up- or down- regulated by PGC-1*α* were included in this analysis (Stein, Chang et

al. 2008). We found a very small overlap of target genes; 62 of the 397 genes bound by HIF-1α and 41 of the 131 genes bound by HIF-2α were found to be ERRα-regulated (Table 3.2).

Unexpectedly, among these selected target genes of HIF, most of them are actually downregulated by the overexpression of the ERRα coactivator, PGC-1α. We have tested a few genes on this list. However, while most of the genes we tested could be induced by hypoxia or hypoxia mimetics in MCF7 and MDA-MB-231 cells, the treatment of siERRα or ERRα antagonists had minor effects on the induction. We were unable to recapitulate the observations made by Ao et al., as we found no repression of PGK-1 induction by siERRα or ERRα antagonists. This could be due to differences in cell line models or treatment conditions. Because we were interested in target genes that are robustly co-regulated by HIF-1 and ERRα in multiple cell lines, as an alternative we turned to the literature to identify well-characterized HIF-1 target genes and tested the effect of ERRα on the regulation of these genes. Using this methodology, we found a well-known HIF-1 target gene, CA9, to be coregulated by ERRα and HIF-1.

.

Table 3.2: Overlap of ERR and HIF target genes.

HIF regulated genes were detected in MCF7 cells treated with 2 mM dimethyloxalylglycine (DMOG) using ChIP-ChIP analysis of HIF-1α and HIF-2α binding (Mole, Blancher et al. 2009). ERRα regulated genes were identified by microarray analysis of MCF7 cells with PGC-1α overexpression (Stein, Chang et al. 2008). PGC-1α upregulated genes are defined as those with more than 2-fold increase, while PGC-1α downregulated genes are those with more than 50% decrease.

	HIF-1/2α	HIF-1α	HIF-2α
PGC1α upregulated	COX7C ID2 KDM3A (JMJD1A) PLEKHA6	FAM162A GLRX IQCG NDUFA5 RAPGEF6 UQCRC2	MFN2
PGC1α downregulated	BAMBI C7orf68 (HIG2) CHD1L GPRC5A HK2 IER3 LOXL2 NFIL3 PAICS RAP2B SAP30 SNAPC1 SPRY1 TMEM97 ZMYND8	ANXA2 ATP9A BBX BRIP1 C15orf39 CARHSP1 CYP24A1 ENO2 HJURP MXI1 MYC NBPF10 RPL10 TGIF1 TRIM33 NBPF10	AGR2 BMP4 CPOX DRAM1 ERO1L IGF1R IL6R KRT18 KRT8 PFN2 PLAC8 S100A4

3.3.2 ERRα is involved in CA9 transcription

Carbonic anhydrases are a family of zinc metalloenzymes that catalyze the reversible hydration of carbon dioxide to bicarbonate and protons:

$$CO_2 + H_2O \leftrightarrow HCO_3^- + H^+$$

They participate in a variety of biological processes, including respiration, calcification, acid-base balance, bone resorption, the formation of aqueous humor, cerebrospinal fluid, saliva, and gastric acid. Members in the family have extensive diversity in tissue distribution and subcellular localization (Chegwidden and Carter 2000, Supuran 2008).

Carbonic anhydrase 9 (CA9) is a membrane-associated member in the family with extracellular carbonic anhydrase activity. It is a clinical indicator of aggressive breast, bone and lung cancer (Chia, Wykoff et al. 2001, Giatromanolaki, Koukourakis et al. 2001, Generali, Fox et al. 2006). CA9 expression is most notably induced by hypoxia conditions under the regulation of hypoxia-inducible factor 1 alpha (HIF-1α), and is an established marker of tumor hypoxia.

To test the influence of modulating ERRα on HIF-1 transcriptional activity, we first performed a combination treatment of ERRα antagonists and hypoxia mimetics that stabilize HIF-1α. As shown in Figure 3.2, the treatment of HIF-1α stabilizers ($CoCl_2$ or DFO) robustly induced the transcription of CA9. However, the addition of ERRα antagonists (XCT790 or Compound A) dampened the induction of CA9 transcription.

Consistently, knocking down ERRα expression by siRNA has similar effect on CA9 induction, as shown in Figure 3.3. Not only does ERRα expression level affect the function of the HIF-1α mimetics, $CoCl_2$, DFO and DMOG, it also affects hypoxia induced CA9 expression. As shown in Figure 3.4, the induction of CA9 by low oxygen conditions (either 5% or 0% oxygen) is reduced by ERRα knockdown. Interestingly, overexpression of the ERRα coactivator PGC-1α has no effect on CA9 induction (Figure 3.5), suggesting a PGC-1α independent function of ERRα in the regulation of CA9. This is clearly different from the transcriptional regulation of VEGF, where both low oxygen and PGC-1α overexpression induced VEGF.

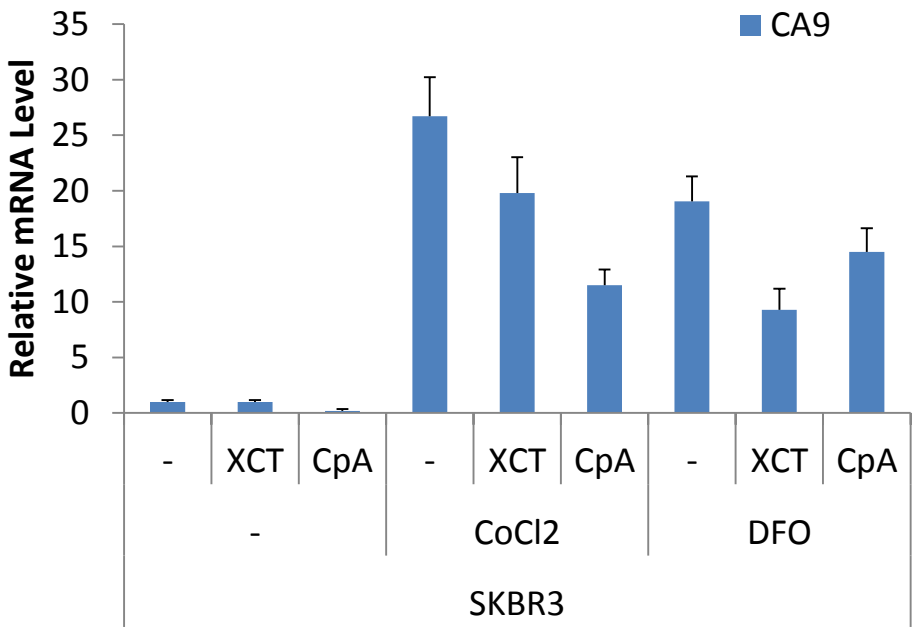

Figure 3.2 ERRα antagonists decrease CA9 induction by HIF-1α stabilizer

SKBR3 cells were seeded in wells of 6-well plates. To manipulate ERRα activity, cells were treated with 10 μM XCT790, 10 μM Compound A, or DMSO vehicle. To stabilize HIF-1α, cells were treated with 100 μM $CoCl_2$ or 100 μM DFO. Cells were treated for 17 hours, and harvested. Representative result shows the qPCR analysis of CA9 mRNA levels normalized to 36B4 and represented as mean ± SEM of triplicate wells.

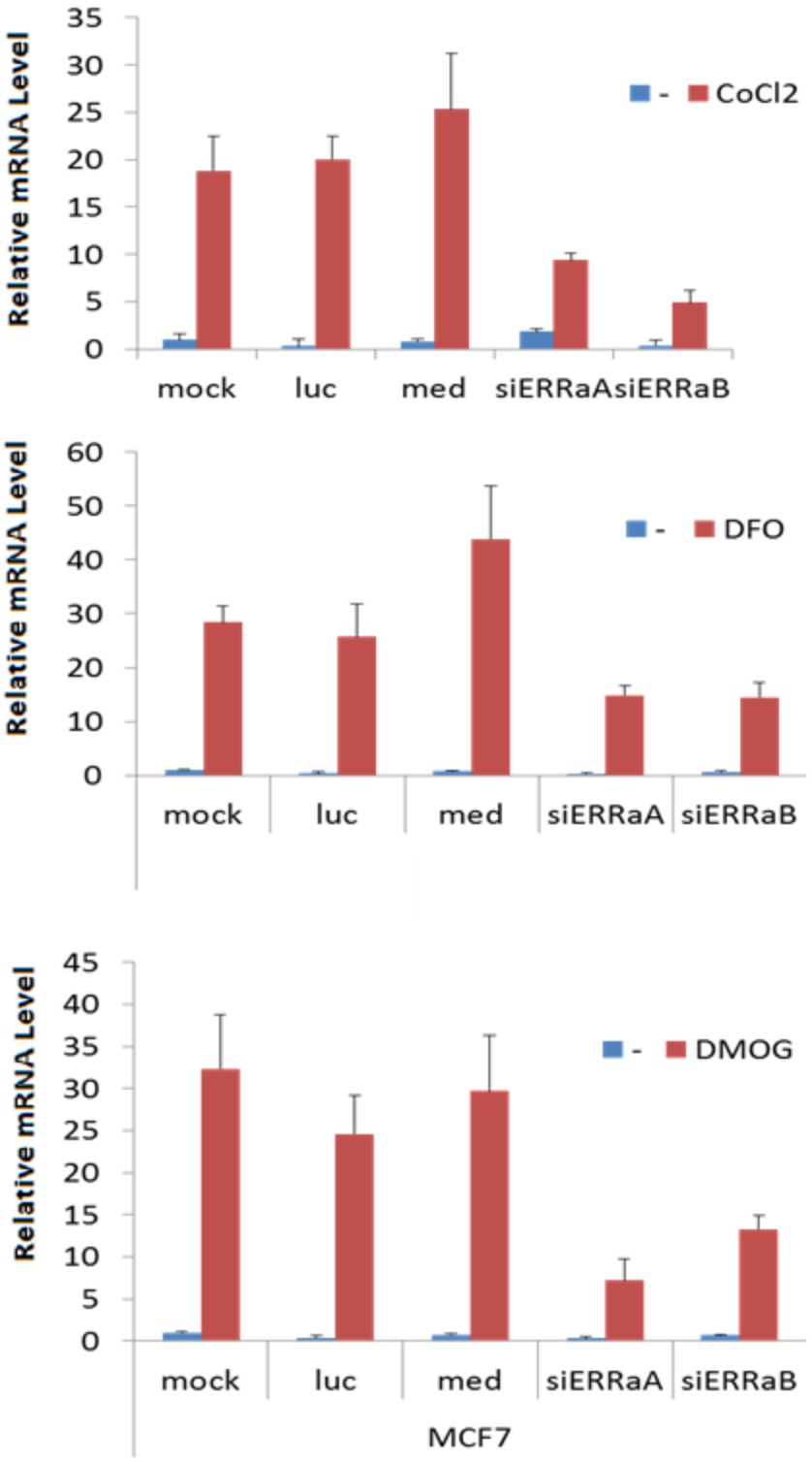
Relative mRNA Level
35
30
25
20
15
10
5
0
- CoCl2
mock
luc
med
siERRaA
siERRaB
Relative mRNA Level
60
50
40
30
20
10
0
- DFO
mock
luc
med
siERRaA
siERRaB
Relative mRNA Level
45
40
35
30
25
20
15
10
5
0
- DMOG
mock
luc
med
siERRaA
siERRaB
MCF7

Figure 3.3 ERRα siRNA decreases CA9 induction by HIF-1α stabilizer

MCF7 cells were seeded in wells of 12-well plates. To knockdown ERRα, cells were transfected with siRNAs targeting ERRα, either siERRαA or siERRαB. Siluc and siMed were two negative controls. A mock transfection was also included as a control. 48 hours after transfection, cells were treated with 100 μM $CoCl_2$, 250 μM DFO or 100 μM DMOG. Cells were harvested 8 hours after treatment. Representative result shows the qPCR analysis of CA9 mRNA levels normalized to 36B4 and represented as mean ± SEM of triplicate wells.

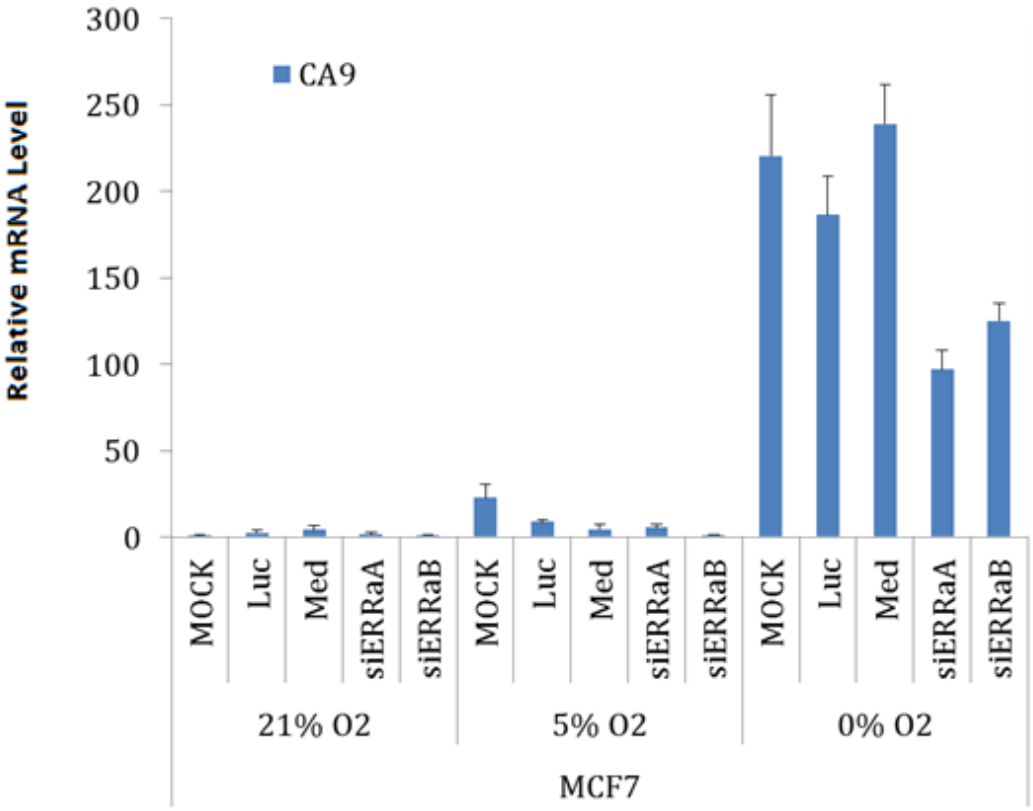

Figure 3.4 ERRα siRNA decreases CA9 induction by hypoxia

MCF7 cells were seeded in wells of 12-well plates. To knockdown ERRα, cells were transfected with siRNAs targeting ERRα, either siERRαA or siERRαB. Siluc and siMed were two negative controls. A mock transfection was also included as a control. 48 hours after transfection, cells were moved to hypoxia chamber with 0% or 5% O_2. Cells were harvested after overnight hypoxia treatment. Representative result shows the qPCR analysis of CA9 mRNA levels normalized to 36B4 and represented as mean ± SEM of triplicate wells.

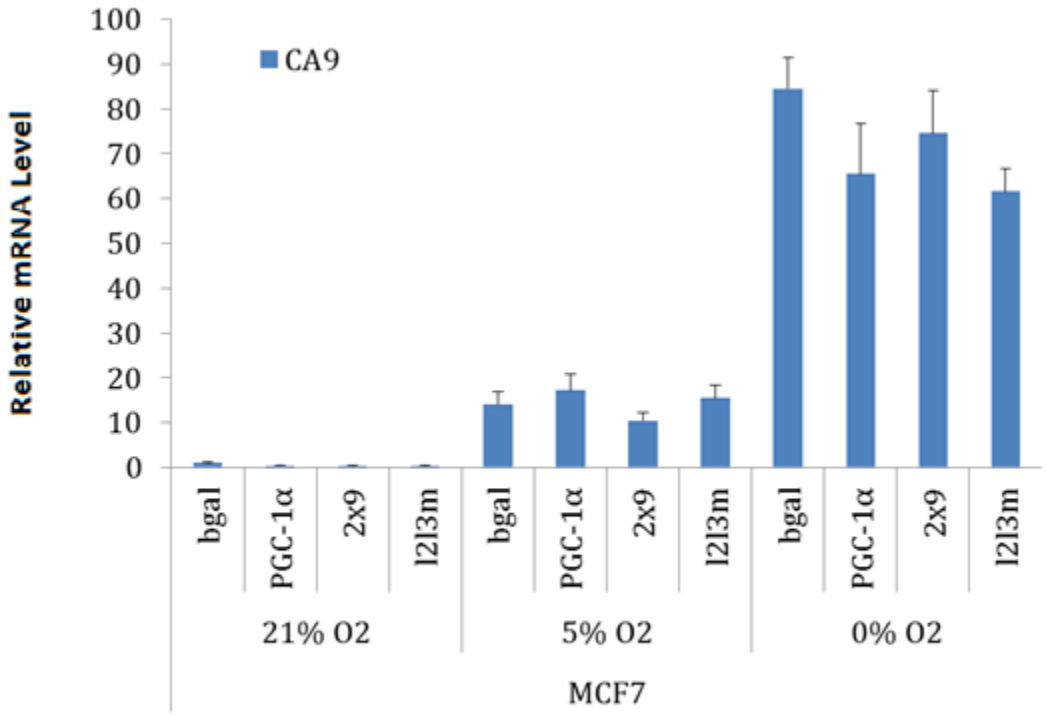

Figure 3.5 PGC-1α overexpression has no effect on CA9 induction by hypoxia

MCF7 cells were seeded in wells of 6-well plates. Cells were infected with adenoviruses β-galactosidase (βgal), wild-type PGC-1α (WT), PGC-1α 2X9 mutant (2X9) or PGC-1α L2L3M mutant (L2L3M) as indicated. 48 hours after infection, cells were moved to hypoxia chamber with 0% or 5% O_2. Cells were harvested after overnight hypoxia treatment. Representative result shows the qPCR analysis of CA9 mRNA levels normalized to 36B4 and represented as mean ± SEM of triplicate wells.

3.3.3 Controversial role of ERRα on HIF-1 transcription

While ERRα is previously reported to stimulate HIF-induced transcription (Ao, Wang et al. 2008) , to our surprise, we found that the expression of ERRα shows a dose-dependent repression of HIF-1 transcriptional activity in Hela cells. Hela cells were transfected with HRE_luc reporter, the transcription of which was activated by the addition of $CoCl_2$, a compound which mimics hypoxic stimulus and stabilizes HIF-1α. Meanwhile, cells were also transfected with various amount of pcDNA_ERRα plasmid. As shown in Figure 3.6, the addition of 50 ng and 100 ng of ERRα expression plasmid clearly reduced the luciferase gene expression of the reporter, while no enhancement of transcription was seen for any dose of ERRα expression. Similar effect was also seen for ERRβ expression.

It is possible that the ERR proteins expressed were not functionally active on the promoter of the HRE_luc reporter, which may need activation by coactivators. Thus, we modified the experimental settings and included the expression of the ERRα coactivator PGC-1α. Again, surprisingly, the addition of the PGC-1α expression plasmid did not promote, but suppressed, the transcription of HIF reporter gene (Figure 3.7).

Because HIF-1α protein level is a key determinant of hypoxia-mediated target gene transcription, we wanted to determine if ERRα and PGC-1α affect HIF-1 mediated gene transcription by indirectly affecting HIF-1α protein level. SKBR3 cells were treated with ERRα antagonists for 8 hours before $CoCl_2$ treatment. We were surprised to find

that XCT790 but not compound A reduced the protein level of HIF-1α (Figure 3.8). It remains to be determined whether XCT790 affects HIF-1α at the level of transcription, translation, or protein stability. . At this point, it is unclear if the dramatic down regulation of HIF-1 reporter gene with PGC-1a overexpression is due to down regulation of the HIF-1 protein, an experiment worth testing in the future.

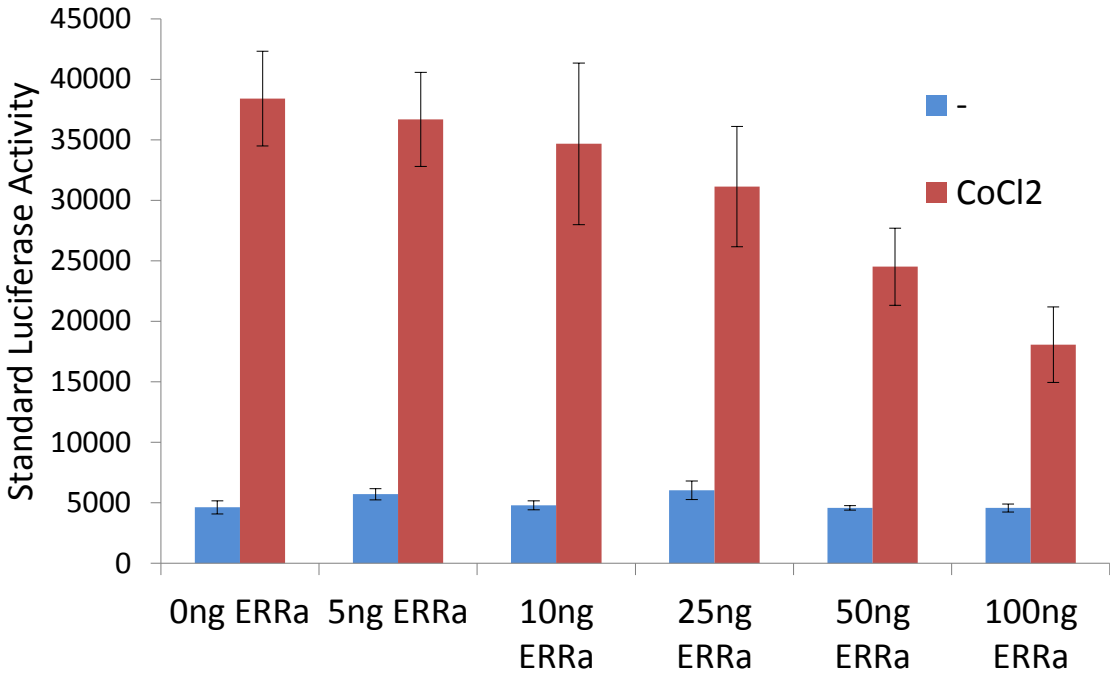
45000
40000
35000
30000
25000
20000
15000
10000
5000
0
Standard Luciferase Activity
-
CoCl2
0ng ERRa
5ng ERRa
10ng ERRa
25ng ERRa
50ng ERRa
100ng ERRa

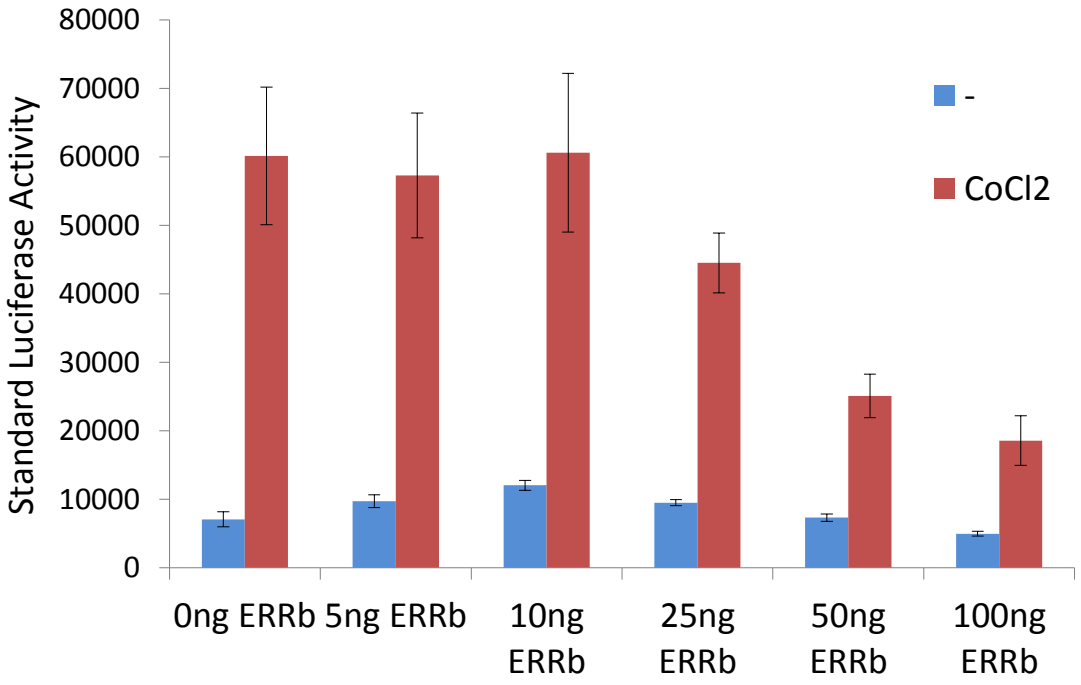
80000
70000
60000
50000
40000
30000
20000
10000
0
Standard Luciferase Activity
-
CoCl2
0ng ERRb
5ng ERRb
10ng ERRb
25ng ERRb
50ng ERRb
100ng ERRb

Figure 3.6 ERRα decreases HIF-1 transcriptional activity on HRE_luc reporter

Hela cells were seeded in wells of 96-well plates 24 hours prior to transfection. For triplicate wells, plasmid DNA containing 300 ng HRE_luc, 20 ng pCMV B-GAL and indicated amount of pcDNA_ERRα or pcDNA_ERRβ was normalized to a total of 600 ng DNA with pBSII. The plasmid DNA was mixed with Lipofectin® in OptiMEM. Cells in each well were transfected with 10 μl DNA-lipofectin mixture. After 2 hours of transfection, cells were treated with 100 μM $CoCl_2$ to stabilize the HIF-1α protein. Non-treated samples were included as negative controls. After 20 hours of treatment, cells were harvested, when luciferase and β-galactosidase (β-gal) activities were measured using a Fusion™ Universal Microplate Analyzer (PerkinElmer). Each experiment was repeated at least three times. Representative results are presented as standard luciferase activity normalized with β-Gal for transfection efficiency, ± standard error of the mean (SEM) per triplicate samples.

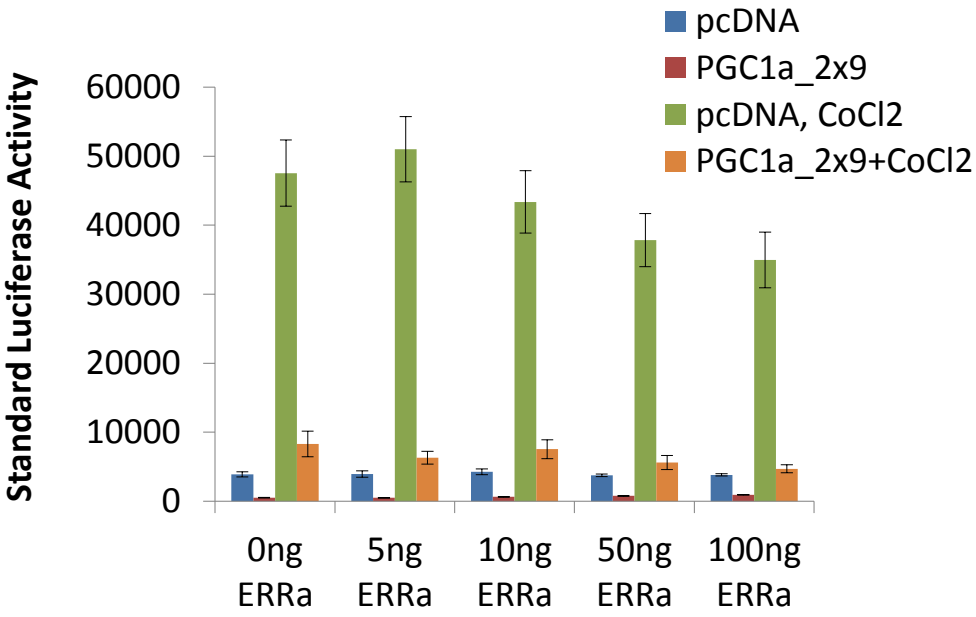
pcDNA
PGC1a_2x9
pcDNA, CoCl2
PGC1a_2x9+CoCl2
Standard Luciferase Activity
60000
50000
40000
30000
20000
10000
0
0ng ERRa
5ng ERRa
10ng ERRa
50ng ERRa
100ng ERRa

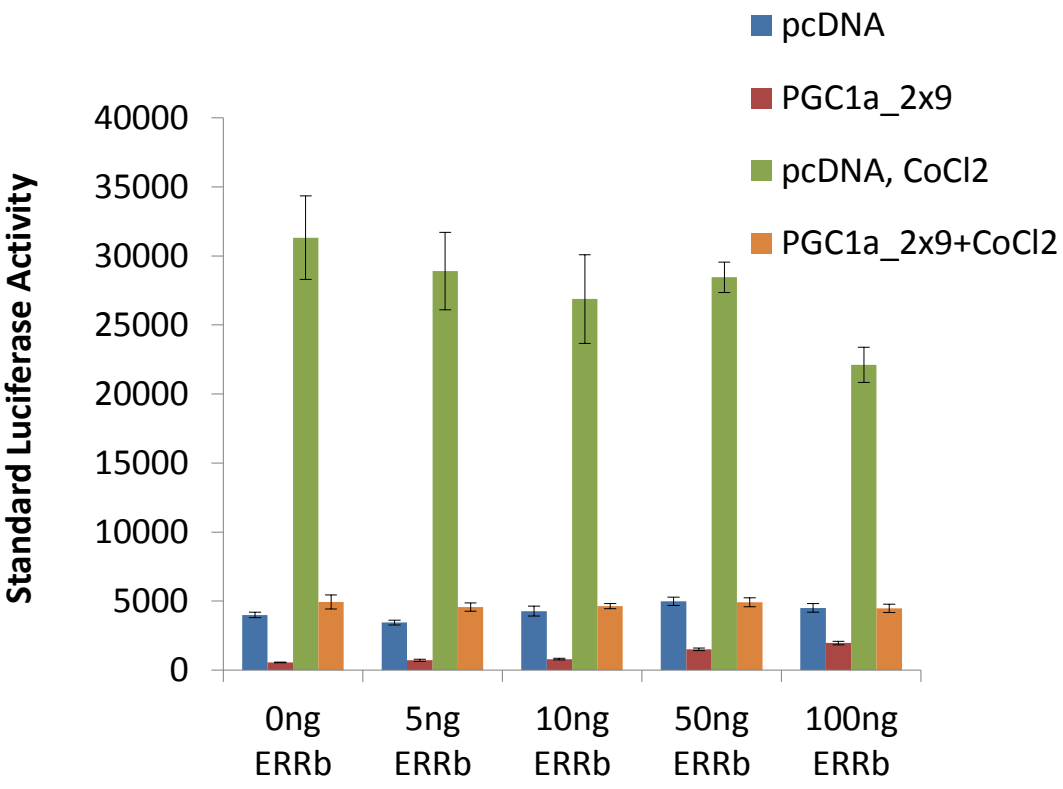
pcDNA
PGC1a_2x9
pcDNA, CoCl2
PGC1a_2x9+CoCl2
Standard Luciferase Activity
40000
35000
30000
25000
20000
15000
10000
5000
0
0ng ERRb
5ng ERRb
10ng ERRb
50ng ERRb
100ng ERRb

Figure 3.7 PGC-1α decreases HIF-1 transcriptional activity on HRE_luc reporter

Hela cells were seeded in wells of 96-well plates 24 hours prior to transfection. For triplicate wells, plasmid DNA containing 300 ng HRE_luc, 20 ng pCMV B-GAL, 100 ng pcDNA_PGC1α_2X9 and indicated amount of pcDNA_ERRα or pcDNA_ERRβ was normalized to a total of 600 ng DNA with pBSII. The plasmid DNA was mixed with Lipofectin® in OptiMEM. Cells in each well were transfected with 10 μl DNA-lipofectin mixture. After 2 hours of transfection, cells were treated with 100 μM $CoCl_2$ to stabilize the HIF-1α protein. Non-treated samples were included as negative controls. After 20 hours of treatment, cells were harvested, when luciferase and β-galactosidase (β-gal) activities were measured using a Fusion™ Universal Microplate Analyzer (PerkinElmer). Each experiment was repeated at least three times. Representative results are presented as standard luciferase activity normalized with β-Gal for transfection efficiency, ± standard error of the mean (SEM) per triplicate samples.

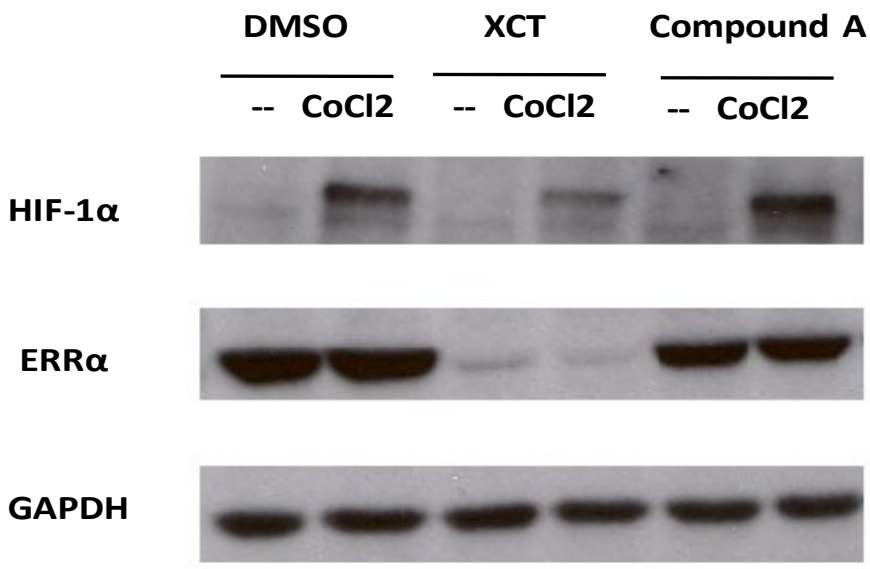

Figure 3.8 Effect of ERRα antagonists on HIF-1α protein level in SKBR3 cells

XCT790, but not compound A, reduces the protein level of HIF-1α stabilized by $CoCl_2$. SKBR3 cells were treated with ERRα antagonists for 8 hours, including 10 μM XCT790, 10 μM Compound A or DMSO vehicle prior to treatment with 100 μM $CoCl_2$ for 16 hours. Western blot analysis of HIF-1α, ERRα and GAPDH loading control was performed to harvested protein samples.

3.3.4 DBD mutants as a tool to study non-canonical role of ERRα

It is clear from studies of our own and others' that part of the ERRα biology is attributable to its crosstalk with other signaling transduction pathways such as Wnt-signaling and the hypoxia response. However, the molecular mechanism(s) by which ERRα interacts with these transcription factors on target gene promoter to activate transcription is still not clear.

Figure 3.9 depicts our proposed model of ERRα canonical and non-canonical transcriptional regulation. Different mechanisms may get involved in the transcriptional activities of ERRα. The canonical pathway is shown on the right, where ERRα directly recognizes ERRE and recruits coactivators like PGC-1α for transcriptional regulation. The non-canonical pathway is shown on the left, where ERRα can physically interact with transcriptional factors such as the hypoxia inducible factor 1 heterodimer (HIF-1α/β), or transcriptional cofactors such as β-catenin (β-cat) to regulate gene transcription. Whether direct binding to DNA is necessary for ERRα non-canonical pathway remains unknown.

The most obvious way to distinguish between direct ERRE binding versus a tethering mechanism is to mutate the ERRα DBD so that it is not able to bind DNA. Although a crystal structure of ERRα DBD is not yet available, the DNA binding domains of other NRs have been characterized extensively. Since ERRα and ERα shared the highest degree of structural and sequence homology in their DNA binding domains,

the DNA binding requirement of ERRα DBD can be inferred from what is known for ERα (Jakacka, Ito et al. 2001). Upon activation by estrogens, ERα dimerizes and binds directly to estrogen response elements (EREs) to regulate gene transcription. In addition, ERα can also regulate the transcription of AP1 target genes through a non-classical mechanism. The effects of ERα DBD mutations were examined in DNA binding assays using reporter constructs containing either EREs (classical) or AP1 (nonclassical) response elements. DBD mutations in the proximal (P-box) of the first zinc finger of the ERα (E207A/G208A and E207G/G208S) eliminated ERE binding. While these mutants were inactive on the ERE reporter, they retained partial or full activity on AP1 reporter, suggesting DNA binding is not required for ERα activity through the non-classical AP1 pathway.

It is possible that ERRα can adopt a similar mode in its transcription regulation. To test the hypothesis that ERRα non-canonical pathway involves ERRα interactions with other proteins rather than direct binding to DNA, we introduced mutations into the DNA binding domain (DBD) of ERRα. Based on the residues on ERα known to be important for the formation of ERα/ERE protein/DNA complex, we chose residues Lysine 104 and Arginine 105 on ERRα for mutation.

To characterize these ERRα mutants, a transcriptional assay was performed. Hela cells were transfected with ERRα reporter gene 3xERE_luc, the transcriptional of which can be induced by ERRα expression. As shown in Figure 3.10, DBD mutation on Lysine

104, Arginine 105, or both sites, indeed abolishes the transcriptional activity of ERRα on 3xERE_luc reporter.

The DNA binding of these mutants was examined by a mammalian one-hybrid assay. As shown in Figure 3.11, the loss of function observed in Figure 3.9 could be largely due to the incapability of the mutants to bind DNA response element. While K104A mutant still retains a weak binding to ERE, the R105A mutant completely loses the binding affinity to ERE.

To evaluate the AF2 coactivator binding ability of these DBD mutants, a mammalian two-hybrid assay was performed to test the interaction between ERRα DBD mutants and PGC1α_L3 peptide, a fragment from the third LXXLL motif of PGC-1α. As shown in Figure 3.12, ERRα wild-type, K104A mutant, R105A mutant and the double site mutant all exhibit similar binding to PGC1α_L3 peptide. Thus, we successfully constructed ERRα DBD mutants that lose ERE-binding but retain ability to interact with coactivators in the AF2 domain.

Initially, these DBD mutants were aimed at separating canonical and non-canonical pathways of ERRα. However, our study found that the DBD is required for both canonical and non-canonical target genes. As shown in Figure 3.13, when cells were transfected with the TOPFlash reporter, the transcription was synergistically upregulated by β-cat and ERRα. However, the upregulation by ERRα was completely abolished by ERRα DBD mutations. In a similar manner, the repression of HRE_luc

reporter gene by ERRα was also demolished by DBD mutations on ERRα (Figure 3.14). To rule out the possibility that the effects seen were due to a variance in expression levels, western blot analysis confirmed that all mutants were expressed at the same level (data not shown). Clearly the intact DBD domain is required for ERRα activity on these reporters.

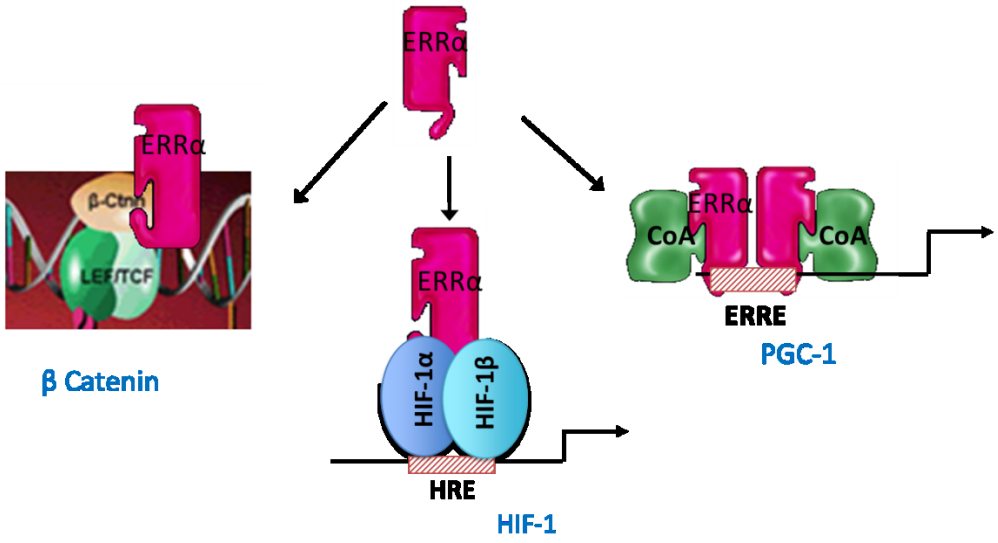

Figure 3.9 Model of ERRα canonical and non-canonical transcriptional activities

Depicted is an updated model showing how different mechanisms may get involved in the transcriptional activities of ERRα. The canonical pathway is shown on the right, where ERRα directly recognizes ERRE and recruits coactivators like PGC-1α for transcriptional regulation. The non-canonical pathway is shown on the left, where ERRα can physically interact with transcriptional factors such as hypoxia inducible factors 1 heterodimer (HIF-1α/β), or transcriptional cofactors such as β-catenin (β-cat) to regulate gene transcription.

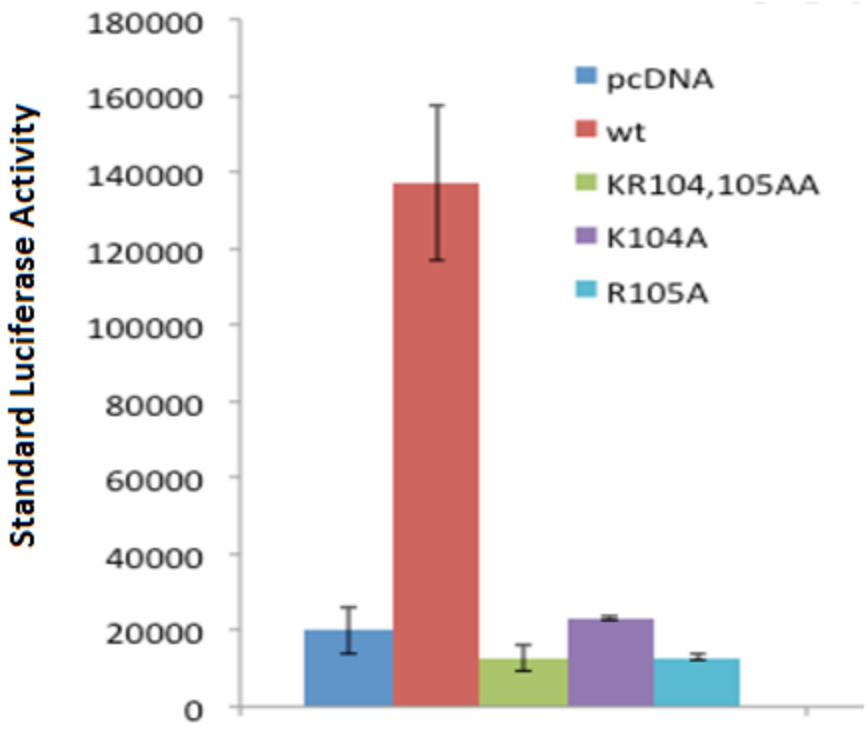

Figure 3.10 ERRα DBD mutants abolish activity on 3xERE reporter

Hela cells were seeded in wells of 96-well plates 24 hours prior to transfection. For triplicate wells, plasmid DNA containing 300 ng 3xERE_luc, 20 ng pCMV B-GAL and 10 ng of pcDNA or pcDNA_ERRα (either wild type or DBD mutants) was normalized to a total of 600 ng DNA with pBSII. The plasmid DNA was mixed with Lipofectin® in OptiMEM. Cells in each well were transfected with 10 µl DNA-lipofectin mixture. After 48 hours of transfection, cells were harvested, when luciferase and β-galactosidase (β-gal) activities were measured using a Fusion™ Universal Microplate Analyzer (PerkinElmer). Each experiment was repeated at least three times. Representative results are presented as standard luciferase activity normalized with β-Gal for transfection efficiency, ± standard error of the mean (SEM) per triplicate samples

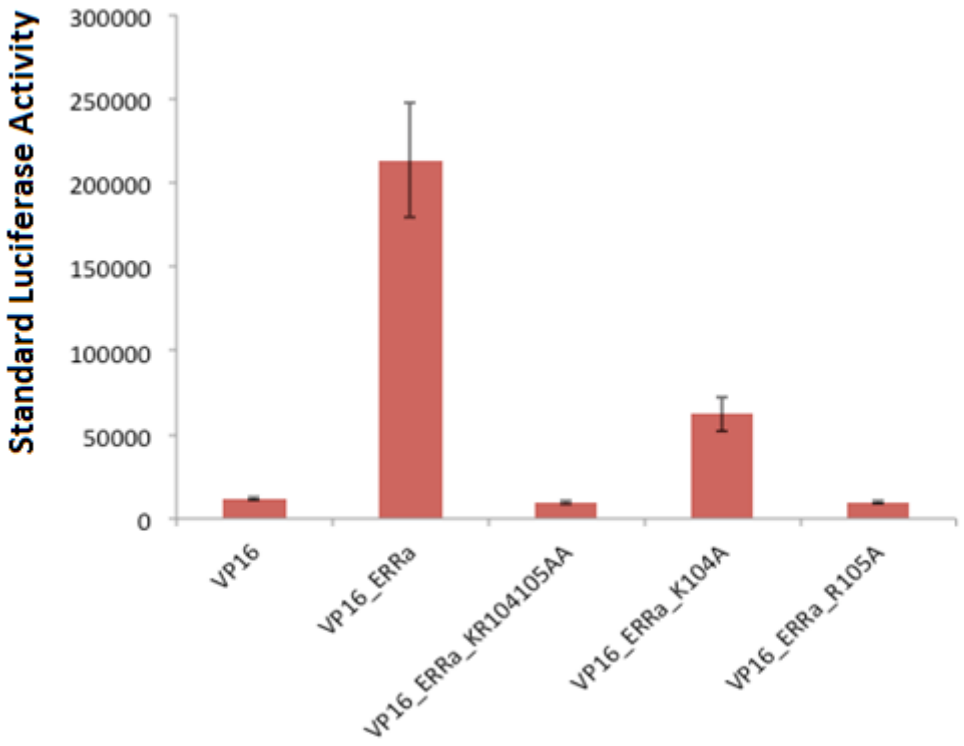

Figure 3.11 ERRα DBD mutants abolish DNA binding activity

To test the DNA binding activity of ERRα DBD mutants, "mammalian one-hybrid" assay was performed. HepG2 cells were seeded in wells of 96-well plates 24 hours prior to transfection. For triplicate wells, plasmid DNA containing 300 ng 3xERE_luc, 20 ng pCMV B-GAL and 100 ng of VP16 or VP16_ERRα (either wild type or DBD mutants) was normalized to a total of 600 ng DNA with pBSII. The plasmid DNA was mixed with Lipofectin® in OptiMEM. Cells in each well were transfected with 10 µl DNA-lipofectin mixture. After 48 hours of transfection, cells were harvested, when luciferase and β-galactosidase (β-gal) activities were measured using a Fusion™ Universal Microplate Analyzer (PerkinElmer). Each experiment was repeated at least three times. Representative results are presented as standard luciferase activity normalized with β-Gal for transfection efficiency, ± standard error of the mean (SEM) per triplicate samples.

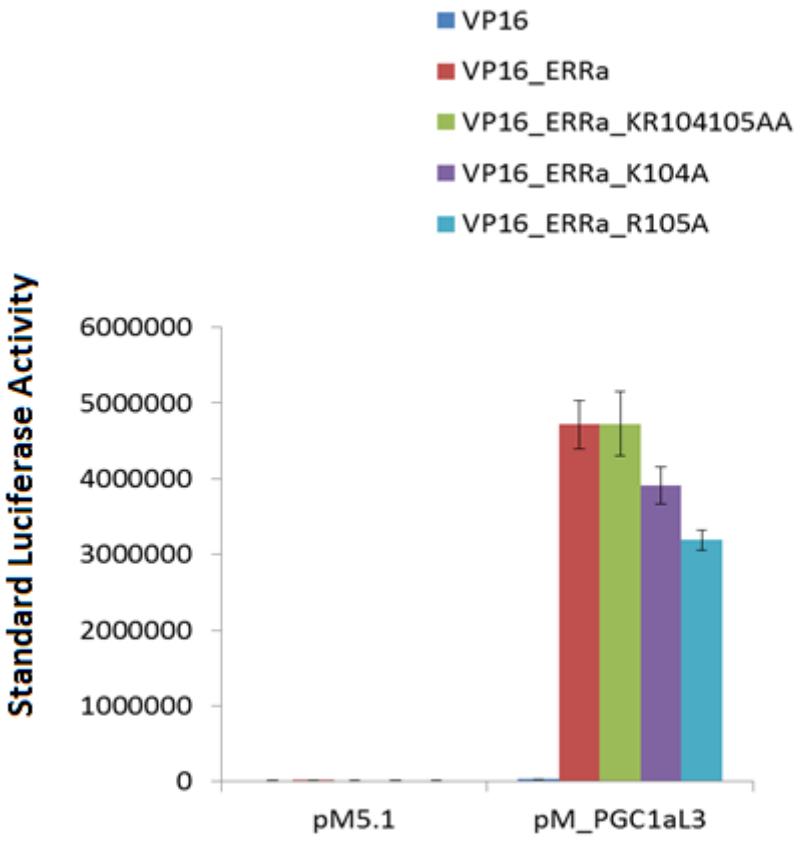

Figure 3.12 ERRα DBD mutants retain ability to interact with PGC-1α fragment

To test ability of ERRα DBD mutants to interact with PGC1α_L3 peptide, a fragment from the third LXXLL motif of PGC-1α, mammalian two-hybrid assay was performed. HepG2 cells were seeded in wells of 96-well plates 24 hours prior to transfection. For triplicate wells, plasmid DNA containing 180 ng 5xGal4-luciferase, 20 ng pCMV B-GAL, 200 ng of pM or pM_PGC1aL3, 200 ng of VP16 or VP16_ERRα (either wild type or DBD mutants) was normalized to a total of 600 ng DNA with pBSII. The plasmid DNA was mixed with Lipofectin® in OptiMEM. Cells in each well were transfected with 10 µl DNA-lipofectin mixture. After 48 hours of transfection, cells were harvested, when luciferase and β-galactosidase (β-gal) activities were measured using a Fusion™ Universal Microplate Analyzer (PerkinElmer). Each experiment was repeated at least three times. Representative results are presented as standard luciferase activity normalized with β-Gal for transfection efficiency, ± standard error of the mean (SEM) per triplicate samples.

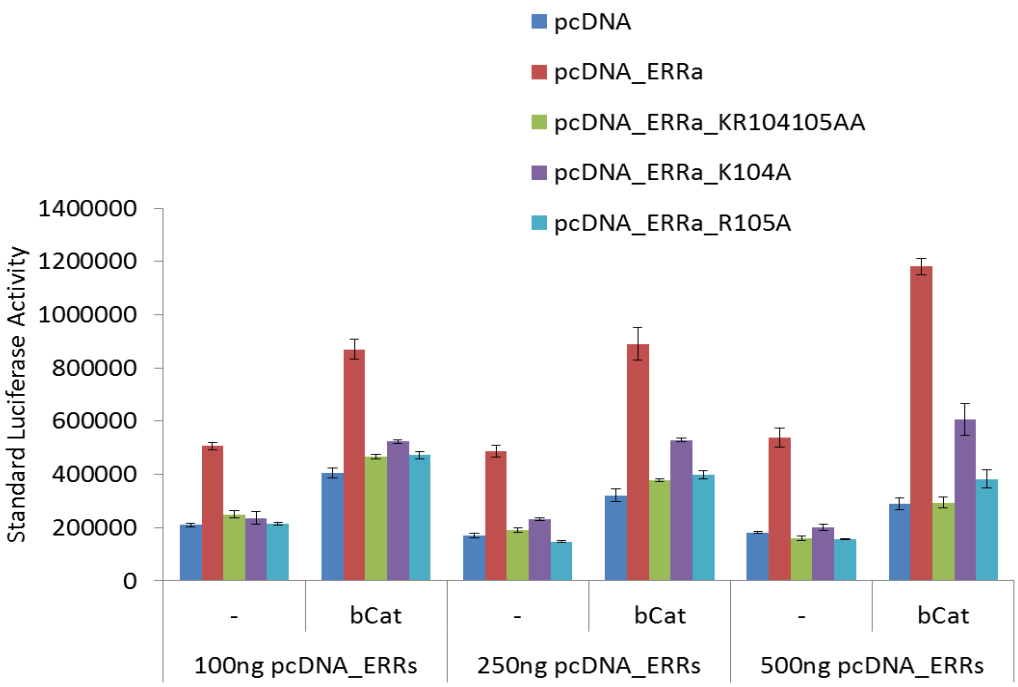

Figure 3.13 ERRα DBD mutants lose transactivation on TOPFlash reporter

Hela or HepG2 cells were seeded in wells of 96-well plates 24 hours prior to transfection. For triplicate wells, plasmid DNA containing 300 ng TOPFlash reporter, 20 ng pCMV B-GAL, 12 ng pCAN_deleN_Bcat (or pcDNA control) and indicated amount of pcDNA or pcDNA_ERRα (either wild type or DBD mutants) was normalized to a total of 600 ng DNA with pBSII. The plasmid DNA was mixed with Lipofectin® in OptiMEM. Cells in each well were transfected with 10 μl DNA-lipofectin mixture. After 48 hours of transfection, cells were harvested, when luciferase and β-galactosidase (β-gal) activities were measured using a Fusion™ Universal Microplate Analyzer (PerkinElmer). Each experiment was repeated at least three times. Representative results are presented as standard luciferase activity normalized with β-Gal for transfection efficiency, ± standard error of the mean (SEM) per triplicate samples.

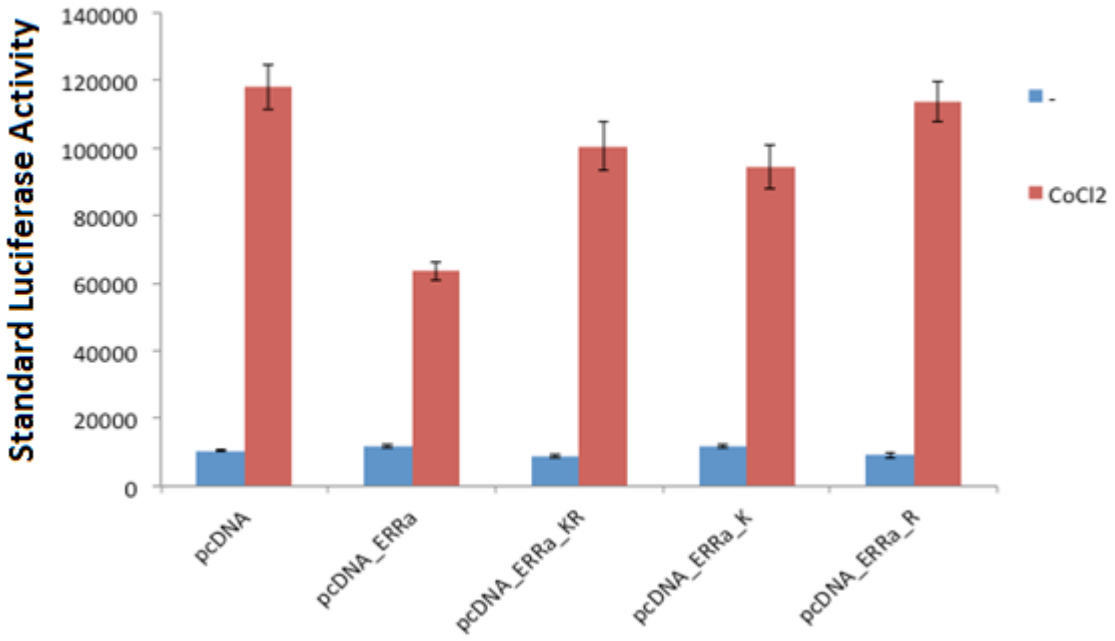

Figure 3.14 ERRα DBD mutants lose suppressive activity on HRE_luc reporter

Hela cells were seeded in wells of 96-well plates 24 hours prior to transfection. For triplicate wells, plasmid DNA containing 300 ng HRE_luc reporter, 10 ng pCMV B-GAL, 100 ng of pcDNA or pcDNA_ERRα (either wild type or DBD mutants) was normalized to a total of 600 ng DNA with pBSII. The plasmid DNA was mixed with Lipofectin® in OptiMEM. Cells in each well were transfected with 10 µl DNA-lipofectin mixture. After 2 hours of transfection, cells were treated with 100 µM $CoCl_2$ to stabilize the HIF-1α protein. Non-treated samples were included as negative controls. After 20 hours of treatment, cells were harvested, when luciferase and β-galactosidase (β-gal) activities were measured using a Fusion™ Universal Microplate Analyzer (PerkinElmer). Each experiment was repeated at least three times. Representative results are presented as standard luciferase activity normalized with β-Gal for transfection efficiency, ± standard error of the mean (SEM) per triplicate samples.

3.4 Discussion

One of the primary issues we sought to address in this study was how ERRα modulates its non-canonical pathways, which mainly focused on understanding the mechanism(s) of ERRα/HIF-1cross talk. It's known that NRs collaborate with various other signaling pathways to regulate target gene transcription. For example, the wnt/β-cat signaling pathway has been shown to cross talk with a variety of NRs, such as androgen receptor (AR), retinoid X receptor (RXR), Liver receptor homolog-1 (LRH-1) (Mulholland, Dedhar et al. 2005). β-cat serves as an AR coactivator in regulating endogenous AR target genes such as PSA (Taplin, Rajeshkumar et al. 2003). Cross talk between the Wnt pathway and LRH-1 induces cell proliferation through the concomitant induction of cyclin D1 and E1 One of the primary issues we sought to address in this study was to determine how ERRα modulates its non-canonical pathways, which mainly focused on understanding the mechanism(s) of ERRα/HIF-1cross talk. It is known that NRs collaborate with various other signaling pathways to regulate target gene transcription. For example, the Wnt/β-cat signaling pathway has been shown to cross talk with a variety of NRs, such as androgen receptor (AR), retinoid X receptor (RXR), Liver receptor homolog-1 (LRH-1) (Mulholland, Dedhar et al. 2005). β-cat serves as an AR coactivator in regulating endogenous AR target genes such as PSA (Taplin, Rajeshkumar et al. 2003). Cross talk between the Wnt pathway and LRH-1 induces cell proliferation through the concomitant induction of cyclin D1 and E1

(Botrugno, Fayard et al. 2004). It is therefore not surprising that we and others have found that ERRα is also able to interact and crosstalk with other signaling pathways. We have previously reported the crosstalk between ERRα and Wnt-signaling pathways, which cooperate in the regulation of cell migration. ERRα has also been shown to be involved in the hypoxia response through direct interaction with HIF-1. We are particularly interested in these two pathways because of their relevance to cancer. Previous studies used a candidate gene approach to characterize the crosstalk. In this study, we used a bioinformatics analysis with the goal of identifying additional target genes/pathways that are the results of ERRα/HIF-1 crosstalk. In this manner, we identified 54 putative ERRα/HIF-1 coregulated genes (Table 3.2). However, qPCR analysis failed to confirm most of the genes identified to be HIF-1/ERRα coregulated. The reason could be that the genes regulated by PGC-1α/ERRα may not have ERRα involved when regulated by HIF-1.

As an alternative to the bioinformatics analysis, we also used a candidate gene approach and identified CA9 as a gene that is coregulated by ERRα and HIF. CA9 is an interesting target gene in signaling, given its role in maintaining the intracellular / extracellular pH balance and its association with cancer. The regulation of CA9 suggests ERRα may be involved in coping with the acidic environment of tumor. Importantly, we identified that CA9 is regulated by ERRα/HIF in a PGC-1α independent manner.

It is clear that ERRα can crosstalk with other signaling pathways. However, the mechanism(s) and molecular basis behind these pathways are still unclear. To address the first model (direct DNA binding of ERRα), we asked whether the genes coregulated by ERRα and HIF-1 or βcat contain any ERRE for potential ERRα binding. Our lab had previously performed a preliminary examination of available ChIP-ChIP and ChIP-seq datasets. A small but significant overlap were found between genes with enriched ERRα binding in MCF7 or SKBR3 breast cancer cells and genes with enriched β-catenin binding in HCT116 colon cancer cells. Also, bioinformatics analyses using Patser revealed that out of the 988 β-catenin target genes identified in the HCT116, approximately 17% of the genes also contain at least one putative ERRα binding site within 600-bp region of DNA enriched for β-catenin binding (Dwyer, Joseph et al. 2010). This suggests that it is possible for direct ERE binding to be involved in the ERRα/β-cat signaling. However, for the ERRα/HIF signaling, no dataset for ERRα under hypoxia or hypoxia mimic condition is available. Instead, we compared the genes identified with the HIF stabilizer DMOG and genes regulated by ERRα coactivator PGC-1α overexpression in MCF7 cells. Using this method, we found some HIF target genes that can also be regulated by PGC-1α. Surprisingly, most of these genes are down-regulated by PGC-1α under normoxia. However, with a few genes tested by qPCR analysis, we were unable to validate if they are co-regulated by PGC-1 and HIF-1. The opposing roles of HIF and PGC-1α may be explained by their physiological stimuli: while HIF is an

oxygen stress sensor, PGC-1α is a metabolic stress sensor. Thus, it is possible that PGC-1α copes with the need to meet high-energy demand, such as upregulating mitochondria function, while HIF copes with low oxidation and suppresses mitochondria function.

In addition to mechanisms described in the first model, ERRα can also regulate target gene transcription by tethering to other transcription factors (Model 2). Because it has been previously shown that ERRα and HIF-1 can physically interact to enhance HIF-1 mediated target gene transcription, we wanted to confirm this observation using a simple reporter gene assay. Surprisingly, our transcriptional assay revealed that both ERRα and PGC-1α expression decreased the transcription of HRE_luc reporter, a widely-used reporter for HIF activity. This reporter contains three hypoxia response elements (24-mers) from the Pgk-1 gene upstream of firefly luciferase. It is possible that the presence of ERRE sites is also necessary for ERRα to be recruited in an "active" state for ERRα/HIF signaling. Without binding sites for ERRα on the promoter, the interaction between ERRα and HIF may block HIF and cofactor recruitment, thus dampen the transcription.

In an attempt to further probe the tethering mechanism, ERRα DBD mutants were used as a tool to define the molecular mechanism for ERRα/β-cat and ERRα/HIF signaling. Our finding suggests that ERRα DBD is important for the receptor to influence β-cat and HIF transcriptional activity. It is likely that the DNA binding of

ERRα on potential ERRE sites of the promoters is necessary for the receptor to potentiate the transcription. However, our results do not preclude the possibility that the mutated residues in DBD are involved in the protein- protein interaction of ERRα/β-cat or ERRα/HIF, thus the mutants abolished the effect of ERRα on these pathways. In the future, a CoIP assay could be used to test whether these ERRα DBD mutants can still interact with β-cat and HIF-1.

For future work, whole genome studies, such as ChIP-chip and CHIP-seq, will enable an evaluation of the extent to which HIF and ERRα binding sequences overlap in endogenous genes under hypoxia conditions and the relative importance of this mechanism of receptor crosstalk.

Chapter 4 Probing structure of ERRα using M13 phage display

4.1 Introduction

Estrogen-related receptors (ERRs) are orphan members of the nuclear receptor superfamily, which include ERRα, ERRβ and ERRγ. So far, no known natural ligand has been identified that could bind ERRs. The folding of α-helices and β-sheets of the C-terminus of a nuclear receptor forms a ligand binding cavity, its volume and the amino acid residues lining the pocket determine the ligand recognition. Unlike some steroid receptors with large volume of ligand binding pocket (ERα ~450 Å^3, GR ~600 Å^3), (Brzozowski, Pike et al. 1997, Bledsoe, Montana et al. 2002), the cavities of ERRs are very small. The volume of ERRγ ligand binding pocket is 220 Å^3 (Greschik, Wurtz et al. 2002), while that of ERRα is even smaller, only 100 Å^3. While the sequences of ERRα and ERRγ in ligand binding domain (LBD) are very similar, ERRα LBD contains a phenylalanine (Phe 232), whose side chain largely fills the cavity and blocks potential binding of a natural ligand (Kallen, Schlaeppi et al. 2004). That said, several synthetic ligands have been identified for the ERRs and their binding to the ligand binding pockets of ERRα and ERRγ have been confirmed by crystallography studies (Greschik, Flaig et al. 2004, Kallen, Lattmann et al. 2007).

Although no natural ligand has been identified for ERRα, several classes of synthetic ERRα antagonists have been developed. For example, XCT790 (or XCT for short) is an ERRα antagonist that blocks its transcriptional activity of ERRα and also

causes degradation of the receptor (Busch, Stevens et al. 2004). Compound A, on the other hand, only interferes with the transcriptional activity of ERRα but is without an effect on the receptor protein level (Chisamore, Mosley et al. 2008). Besides the differences on ERRα stability, these two antagonists also exert different effects on cancer cells. Previously our lab has shown that although both compounds inhibited cell proliferation, only the ERRα degrader XCT790 reduced cell migration, while compound A was without an effect in this assay.

It has been well established that NRs depend on interactions with specific transcriptional coregulators to regulate distinct biological processes. In general, recruitment of coactivators facilitates the assembly of a large protein complex, which acetylates chromatin and engages general transcription machinery to enhance transcription initiation and elongation of target genes. Recruitment of co-repressor proteins, on the other hand, deacetylates chromatin and shuts down transcription. Furthermore, it has been demonstrated that different ligands can induce distinct receptor conformations and thereby facilitate the differential recruitment of functionally distinct coregulators. Therefore, NRs could manifest different biological activity depending on their conformational states induced by ligands and relative expression levels of cellular cofactors. This type of activity is exemplified by the selective estrogen receptor modulators (SERMs), such as tamoxifen. Tamoxifen is widely used in the treatment of ER positive breast cancer for its ER antagonist activity in the breast;

however it functions as an ER agonist in the uterus and bone. Much of the resistance observed in the clinic to tamoxifen endocrine therapy was attributable to its partial agonist activity and, therefore, pure antagonists, such as fulvestrant, which degrade the receptor are highly desirable for oncological use. By extrapolation, we propose that ERRα degraders such as XCT790 will antagonize all aspects of ERRα function, while non-degrading antagonists like compound A may actually function in a selective manner, much as the SERMs do on ERα. The balance between complete and partial antagonism depends on the spectrum of biological functions the receptor is involved in and the proposed indications of the ligands. Therefore, a better understanding of the molecular basis of the antagonism of ERRα ligands would facilitate the development of compounds that exhibit favorable biological activities.

At the onset of this study, no structural information was available for antagonists that bind to ERRs. Whether XCT and Compound A manipulate the receptor in similar manners or not was unknown. Given the relatively small ligand binding pocket in the Apo-ERRα, it is possible that binding of an antagonist would force the receptor to undergo global conformational changes. It is also possible that some ERRα antagonists may bind regions other than the canonical ligand-binding pocket, as is currently being investigated for ligands of the androgen receptor. Understanding how antagonists alter ERRα structure is important. Not only because such information could help explain the

functional differences between different classes of antagonists, it will be instructive in the development of novel ERRα inhibitors.

In the current study, we screened for small peptides that can interact with ERRα in Apo, XCT-bound, and Compound A-bound forms using M13 phage display. These peptides served as surface probes for ERRα structures. This chapter details the purification of full-length ERRα as well as the validation and characterization of the small peptides identified.

4.2 Materials and Methods

4.2.1 Plasmids

The construction of pcDNA3-ERRα, VP16-ERRα and 5xGal4-luciferase plasmids was described previously (Chang, Norris et al. 1999, Stein, Gaillard et al. 2009). All the pM5.1_peptide plasmids to express Gal4DBD-peptide fusions were constructed as follows: DNA sequences coding for the peptides were PCR amplified from the M13 phage, digested with Xba I and Xho I and subcloned into the pM5.1 vector (modified from pM, Clontech) (Mettu, Stanley et al. 2007) . All PCR products were sequenced to ensure the fidelity of the resulting constructs.

4.2.2 Production and purification of recombinant ERRα

The construction of baculovirus for ERRα production has been previously described in the lab (Gaillard, Grasfeder et al. 2006). Briefly, the full-length ERRα cDNA was subcloned into a modified baculovirus shuttle vector pDW464-rTEV (Chang, Norris et al. 1999) to generate a fusion of ERRα with a biotin acceptor peptide (BAP) linked by a recombinant tobacco etch virus (rTEV) protease cleavage site. The recombination of this plasmid with the baculovirus genome resulted in recombinant baculoviral DNA, which could be transfected into Spodoptera frugiperda (Sf9) cells to produce baculovirus.

Sf9 cells were maintained in serum-free SFX media (Hyclone) in a 27°C incubator shaking at 245 rpm. Sf9 cell culture density was maintained between 0.5~8x10^6 cells /ml for best cell growth. (The doubling time of Sf9 was measured to be around 20 hours.) At

the log-phase (cell density around $2x10^6$ cells /ml), Sf9 cells were centrifuged at 900rpm, re-suspended in fresh SFX media to reach $2x10^6$ cells /ml, and infected with 1-5 MOI of ERRα baculovirus. After 48-hour infection, Sf9 cells were harvested. Cell culture supernatant was collected as new baculovirus stock and kept at 4°C. Cell pellets were washed once with ice-cold PBS, frozen in liquid nitrogen and stored at -80°C.

To extract the biotinylated full-length ERRα protein, cell pellets of 600 ml culture were lysed in 100 ml lysis buffer (50 mM Tris-HCl, pH 8.0, 10 mM β-mercaptoethanol, 100 mM KCl, 1% NP-40, 1:200 protease inhibitor cocktail III (Calbiochem, EMD Biosciences, Inc., San Diego, CA), 50 mM sodium fluoride, and 50 mM β-glycerophosphate). The lysate was incubated at 4°C with gentle rocking for 1 hour, followed by centrifugation at 20,000 rpm for 30 min. 20% glycerol was added to the soluble fraction of the lysates for storage at -80°C.

Before protein purification, the sample lysates was first run on a reducing SDS-PAGE gel, transferred to a nitrocellulose membrane followed by detection with an anti-ERRα (1148) antibody to confirm the production of biotinylated ERRα. Then, recombinant biotin-tagged-ERRα was purified from the soluble lysate using Streptavidin Mutein Matrix resin (Roche, Indianapolis, IN). The beads were packed in a 5ml column and washed with water using "AKTA" FPLC (GE Healthcare Life Sciences). Cell lysate was filtered through a 0.45 μm filter and loaded onto the column at a flow rate of 5 ml/minute. The column was first equilibrated with 20 column volume (100 ml)

of Equilibration buffer (10 mM Tris-HCl, pH=8.0, 300 mM NaCl), then washed with 20 column volume (100 ml) of Washing buffer (20 mM Tris-HCl, pH=8.0, 150 mM NaCl, 10 mM β-mercaptoethanol, 10% glycerol), and finally eluted with 5 column volume (25 ml) of Elution buffer (50 mM Tris-HCl, pH 8.0, 200 mM NaCl, 4 mM DTT, 5 mM D-Biotin, 10% glycerol) and collected into 6 separate fractions. To determine protein sample concentration, Bradford assay was used. To assess protein purity, protein samples were run on an SDS-PAGE gel followed by Coomassie staining. To determine the expression of biotin-tagged-ERRα, western blots were performed by transferring the proteins to a nitrocellulose membrane followed by detection with an anti-ERRα (1148) antibody.

4.2.3 Functional Testing of Recombinant ERRα

The functionality of the purified ERRα protein was assessed by two criteria (1) its DNA binding ability and (2) its ability to bind coactivators. The latter was determined using an M13 phage (D30), which was shown previously to bind ERRα and expresses a short peptide, HPTHSSRLWELLMEATPTM, containing the coactivator:receptor interacting LXXLL motif.

96-well plates were coated with 10 μg neutravidin (Pierce Biotechnology, Rockford, IL) in 100 μl of 100 mM $NaHCO_3$ (pH 8.5) overnight at 4°C, blocked with 150 μl of 2% milk in $NaHCO_3$ for 1 hour at RT, washed five times with 300 μl PBST (Phosphate Buffered Saline with 1% Tween) and incubated for 1 hour with 100 μl of 2 pmoles of biotinylated dsDNA containing an estrogen response element (ERE) sequence

(Forward: biotin- GATCTAGGTCACAGTGACCTGCG; Reverse: biotin-GATCCGCAGGTCACTGTGACCTA). Extra biotin binding sites were blocked with 150 μl of 5 mM biotin in PBS for 1 hour, and washed five times with 300 μl PBST. As a negative control, wells were coated with 10 μg milk instead of neutravidin and the incubation with biotinylated dsDNA and biotin was also replaced with PBS.

0, 2, 5, 10 pmoles of purified biotinylated ERRα in PBST were added to the coated wells and incubated overnight at 4°C. Each well was blocked with 150 μl of 2% milk in PBST at RT for 1 hour, and then washed five times with PBST to remove unbound ERRα and milk. Meanwhile, M13-D30 phage was blocked with 2% milk in PBST on ice for 1 hour. Next, each well coated was incubated with $5x10^9$ phage in 100 μl of 2% milk/PBST at RT for 1 hour, and washed five times with PBST to remove unbound phage.

To detect the binding of M13-D30 phage to ERRα, each well was incubated with 100 μl of the diluted horseradish peroxidase-conjugated anti-M13 antibody (1:5000 in PBST) (Pharmacia, catalog # 27-9402-01) at RT for 1 hour, washed ten times with PBST, and incubated with 100 μl of ABTS (29,29-azino-bis-3-ethylbenzthiazoline-6-sulfonic acid) reagent containing 0.05% H_2O_2. The reaction was quantified by measuring the absorbance at 405 nm with a microtiter plate reader after 10 minutes.

4.2.4 M13 Phage Display

To detect the conformations of ERRα with and without DNA binding, two different coating conditions were used. i) For DNA-bound ERRα detection, the coating of wells was similar to the method described above. In brief, 96-well plates (Costar, Corning, Acton, MA) were coated at RT with 10 μg neutravidin in 100 mM $NaHCO_3$ (pH 8.5) for 2 hours, blocked with 2% milk in $NaHCO_3$ for 1 hour, washed five times with PBST, incubated with 10 pmoles of biotinylated dsDNA containing ERE for 1 hour, blocked with 5 mM biotin in PBS for 1 hour, and washed five times with PBST. Each well was incubated overnight at 4°C with 10 pmoles (520 ng) of biotinylated full-length ERRα diluted in 100 μl PBST. To detect the conformations of ERRα in apo and ligand-bound form, each well was supplemented with 0.1 μl DMSO, 0.1 μl of 10mM XCT-790, or 0.1 μl of 10 mM Compound A. ii) For non-DNA-bound ERRα detection, 96-well plates were directly coated with 10 pmoles ERRα in 100 μl of 100 mM $NaHCO_3$ (pH 8.5) supplemented with 0.1 μl DMSO, 0.1 μl of 10 mM XCT-790, or 0.1 μl of 10 mM Compound A and incubated overnight at 4°C.

The construction of the M13 phage library displaying LXXLL peptides was previously described (Chang, Norris et al. 1999). To pre-clear the phage library, 10^8 pfu phage from phage library were diluted with 150 μl of 2% milk in PBS and incubated on ice for 1 hour. Meanwhile, coated wells were blocked with 150 μl of 2% milk in PBS at RT for 1 hour, and washed five times with PBST. Pre-cleared phage were transferred to

the washed wells and incubated at RT for 3 hours (Panning). Wells were washed ten times with PBST to remove unbound phage. Finally, phage were eluted by adding 100 μl of 0.1 M HCl and incubated at RT for 10 minutes. Eluents were neutralized with 50 μl of 1 M Tris-HCl (pH=7.4). Eluted phage were stored at 4°C until proceeded to amplification.

To amplify the eluted phage, phage were mixed with *E. coli* DH5αF′ cells (Invitrogen, Carlsbad, CA) and incubated in 37°C shaker for 5 hours. Cells were spun down at 4000 g for 10 minutes, and the supernatant containing amplified phage was collected and stored at 4°C for subsequent rounds of panning. A total of five rounds of panning were conducted.

4.2.5 Phage ELISA

To confirm the enrichment of ERRα-binding phage, a phage ELISA assay similar to the M13-D30 phage ELISA was used. The plates coating was as described above in the M13 Phage Display, with the addition of negative control wells, which were incubated with 520 ng powdered milk instead of ERRα protein in 100 μl of 100 mM $NaHCO_3$ at 4°C overnight. Wells were blocked with 150 μl of 2% milk in PBS at RT for 1 hour. Wells were washed five times with PBST followed by the addition of 5 $x10^9$ pfu pre-cleared phage (amplified from each panning) in 100 μl PBST and incubated at RT for 1 hour. Wells were washed five times with PBST to remove unbound phage.

To detect the binding of phage to ERRα, each well was incubated with 100 μl of the diluted horseradish peroxidase-conjugated anti-M13 antibody (1:5000 in PBST) at RT for 1 hour, washed ten times with PBST, and incubated with 100 μl of ABTS reagent containing 0.05% H_2O_2. Reaction was quantified by measuring the absorbance at 405 nm with a microtiter plate reader after 10 minutes of reaction.

PCR amplification of the peptides was performed using amplified phage from bacterial supernatants that showed significant enrichment of phage binding in ELISA. The PCR products were purified using Qiagen PCR clean-up kit, digested with Xba I and Xho I and ligated into pM5.1 vector. The peptide sequences were deduced by DNA sequencing. The recombinant pM5.1_peptide constructs were used for mammalian two-hybrid analysis.

4.2.6 Mammalian Two-Hybrid Assay

Mammalian two-hybrid analyses were performed in HepG2 cells and Hela cells, both of which were obtained from American Type Culture Collection (Manassas, VA) and maintained in a humidified 37°C incubator with 5% CO_2. Cells were cultured in Minimal Essential Medium (MEM) (Invitrogen) supplemented with 10% fetal bovine serum (HyClone, Logan, UT), 0.1 mM non-essential amino acids and 1 mM sodium pyruvate (Invitrogen). For cell transfection and mammalian two-hybrid assay, cells were switched to Basal Medium Eagle (BME) supplemented with 10% fetal bovine serum

(HyClone, Logan, UT), 2 mM L-Glutamine, 0.1 mM non-essential amino acids and 1 mM sodium pyruvate (Invitrogen).

For transient transfections, HepG2 cells were seeded in wells of 96-well plates 24 hours prior to transfection. On the day of transfection, the media was aspirated and cells were washed once with PBS. 600 ng of total plasmids (containing 200 ng pM5.1_peptide, 200 ng VP16_ERRα, 180 ng 5xGal4-luciferase and 20 ng pCMV B-GAL) per triplicate samples in 96-well were mixed with Lipofectin® in OptiMEM according to manufacturer's protocol (Invitrogen). Cells in each well were transfected with 10 μl DNA-lipofectin mixture.

All ligand stocks were dissolved in DMSO before use in cell culture, and cells were treated with 10 μM XCT-790, 10 μM Compound A, or equivalent amount of DMSO vehicle 1-2 hours post-transfection. Cells were lysed 42-48 hours after transfection and assayed for luciferase and β-galactosidase activities as described (Norris, Paige et al. 1999) using a Fusion™ Universal Microplate Analyzer (PerkinElmer). Results were presented as luciferase activity normalized with β-Gal for transfection efficiency ± standard error of the mean (SEM) per triplicate samples. Results presented were representative of three independent transfection experiments.

4.3 Results

4.3.1 Purification of biologically active full-length ERRα

To study the conformation of ERRα, we purified biologically active full-length protein of this receptor. ERRα was selected because of our interest in its role in breast cancer. It's been described previously for other NRs that binding of ligands to the LBD can influence the orientation and/or activity of other domains of the same receptor. . Therefore, by using full-length ERRα for the peptide screen, it stands a better chance to identify global conformational differences between ERRα apo form and antagonist-bound form.

The expression system to produce full-length biologically active nuclear receptors in insect cells was previously described (Duffy, Tsao et al. 1998)). The ERRα cDNA with a canonical biotinylation sequence at the amino-terminus for the *E. coli* biotin holoenzyme synthetase (BirA) was cloned into a baculovirus expression vector and introduced into insect cells together with an expression vector for the BirA enzyme (Gaillard, Dwyer et al. 2007). The recombinant receptor was purified to homogeneity using Streptavidin Mutein Matrix resin column. Figure 4.1 shows a coomassie-stained SDS-PAGE gel of the steps of ERRα purification. A protein band between 50 kD and 75 kD, which was the correct size for biotinylated ERRα was purified. It is shown by the coomassie stained gel that Elution 2 and Elution 3 appear to have highest protein level, and the purified protein has greater than 90% purity. Using Bradford protein assay, it

was determined that the protein concentration of Elution 2 and Elution 3 combined is about 480 ng/μl.

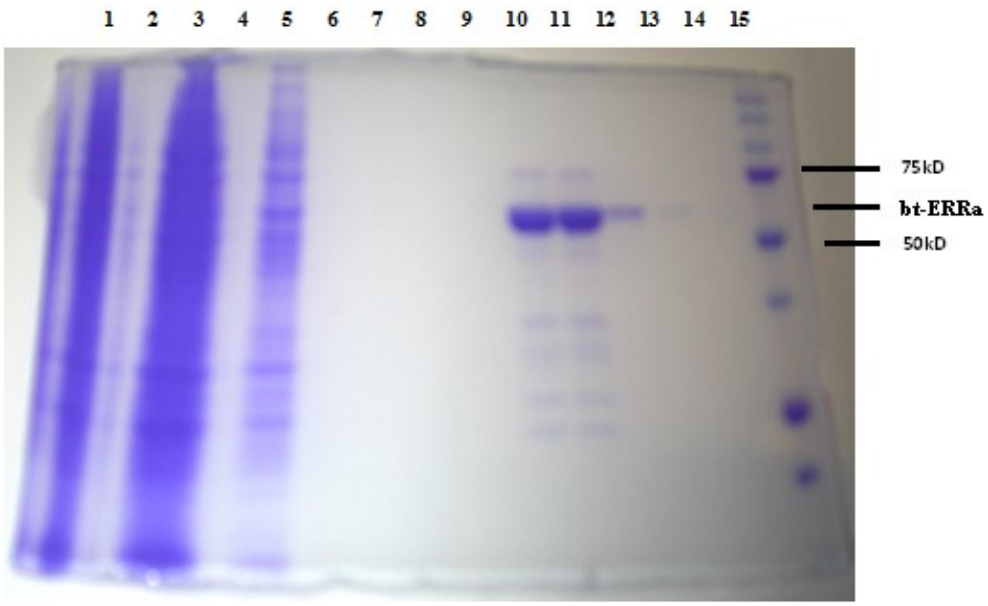

Figure 4.1 Purification of biotin-tagged full-length ERRα.

Biotin-tagged full-length human ERRα was purified using a baculoviral expression system in Sf9 cells. Sf9 cells infected with baculovirus to express biotin-tagged ERRα were lysed and samples were collected during multiple stages of the purification process and loaded into each well of a 10 % SDS-PAGE gel Coomassie staining. (1, Input; 2, blank lane; 3, flow through; 4, blank lane; 5, Wash 1; 6, Wash 2; 7, Wash 3; 8, Wash 4; 9, Elute 1; 10, Elute 2; 11, Elute 3; 12, Elute 4; 13, Elute 5; 14, Elute 6; 15, Protein molecular Ladder)

4.3.2 Functional Verification of Recombinant ERRα

To confirm the purified ERRα protein is folded correctly, its ability to bind coactivators was used as the main criterion to assess its biological activity. Peptide D30 is a peptide (HPTHSSRLWELLMEATPTM) that contains a leucine-rich motif (LXXLL) frequently found within NR-interaction domains of coactivators and is known to bind ERRα (Gaillard, Dwyer et al. 2007). Thus, using a phage ELISA assay, we directly assessed the ability of the purified ERRα protein to bind M13-D30 peptide phage as a proxy of the biological activity of the purified ERRα protein.

Figure 4.2 depicts the components of the phage ELISA assay. The neutravidin-coated wells were first incubated with biotinylated double-stranded DNA that contains an estrogen response element (ERE) sequence, which is known to bind ERRα. Then, ERRα protein was incubated with the ERE. Following binding of the protein, M13-D30 phage was added to the wells, and binding of the phage to the purified receptor was detected with an anti-M13-HRP antibody.

Figure 4.3 shows the results of a representative ELISA assay, demonstrating that the purified ERRα was able to (1) bind ERE-containing DNA and (2) the D30 peptide. The ability of the purified ERRα to bind to the LXXLL motif of a coactivator confirms that the purified receptor is biologically active with respect to DNA binding and its ability to recruit coactivator proteins.

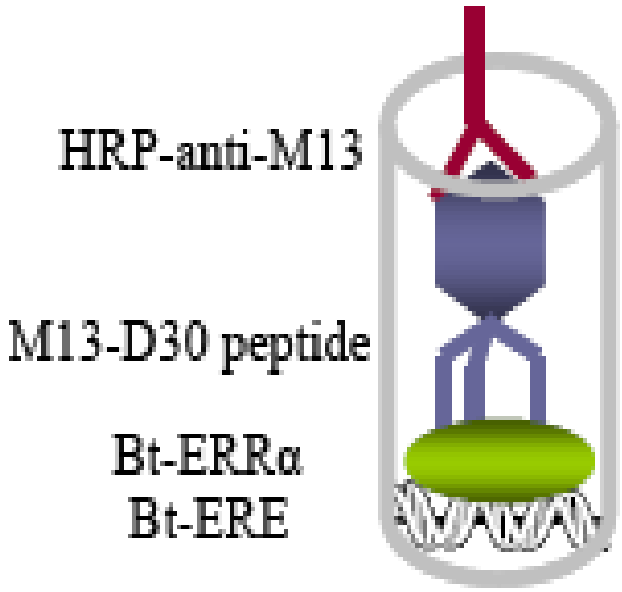

Figure 4.2 Diagram of the phage ELISA assay

Phage ELISA assay was used to assess coactivator-binding capacity of the purified full-length recombinant ERRα. HRP: horseradish peroxidase; Bt-ERRα: biotinylated ERRα protein; Bt-ERE: biotinylated double-stranded DNA containing an estrogen response element (ERE).

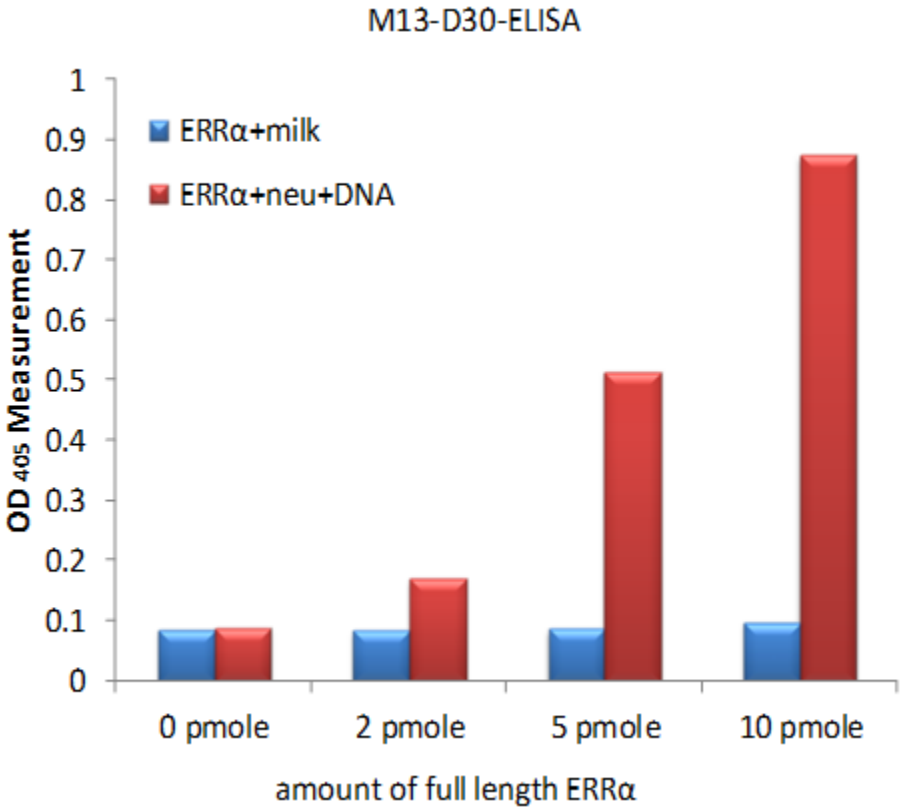

Figure 4.3 Purified human ERR*α* is biologically active.

The phage ELISA assay demonstrated that the purified ERR*α* is capable of binding to DNA and subsequently interacting with an LXXLL motif-containing peptide *in vitro*. Neutravidin-coated wells on 96-well plates were blocked with milk and incubated with biotinylated dsDNA containing ERE for 1 hour. Extra biotin binding sites were blocked with biotin for 1 hour. As a negative control, instead of neutravidin coating, biotinylated dsDNA incubation and biotin blocking, wells were coated with powdered milk. Next, 0, 2, 5, 10 pmoles of purified biotinylated ERR*α* were added to the coated wells and incubated overnight at 4°C. The wells were incubated with pre-cleared M13-D30 phage on ice for 1 hour, washed with PBST to remove unbound phage, and treated with horseradish peroxidase-conjugated anti-M13 antibody. The quantification of the bound antibody was performed by incubating wells with ABTS reagent and measuring the absorbance at 405 nm.

4.3.3 Identification of ERRα interacting peptides by M13 phage display

Various methods have been used to probe the conformational changes induced upon ligand biding to NR. One of the approaches that has been optimized by our lab is the M13 phage display, which has been used successfully in the past to search for peptide sequences that mimic endogenous protein-protein interactions. To screen for small peptides that can interact with ERRα and serve as probes for the conformational changes of the receptor, an M13 phage library expressing 19 amino acid peptides $(X)_7LXXLL(X)_7$ on phage capsids were incubated with purified ERRα protein as apo, XCT-bound or Compound A-bound forms. The screen was conducted in two formats with ERRα either bound directly to the plastic or ERRα bound to an ERE because it is possible that the DNA binding of ERRα could influence its conformation. Therefore, combining screens performed under both conditions should increase the likelihood of detecting subtle conformational changes within receptor. After incubating phage library with ERRα in coated wells, unbound phage were washed off, while the phage bound to the receptor were eluted and amplified. The amplified phage was carried on to more rounds of binding, washing, elution, and amplification. This process known as "biopanning" is depicted in Figure 4.4. A total of five rounds of panning were conducted.

In order to confirm the enrichment of ERRα-binding phage, a phage ELISA assay similar to that described earlier in the chapter was performed. Instead of a single

isolated phage, coated wells were incubated with amplified pools of phage from each pan. In our phage ELISA assay, six different conditions were tested to probe ERRα conformations with or without DNA binding, and in the presence of vehicle (DMSO), XCT, or Compound A. For conditions 1-3, the wells were first coated with neutravidin and biotinylated DNA containing ERE for ERRα binding, while conditions 4-6 used wells with ERRα bound directly to the plastic. For each condition, negative control wells incubated with milk instead of ERRα protein were used to indicate indicate whether the binding of phage was specific to the ERRα protein.

Figure 4.5 is a representative phage ELISA showing the enrichment of phage for ERRα binding. For DNA-bound ERRα in the presence of Compound A (Condition 3), the phage binding was enriched from pan three through pan five, which is much slower than Apo-form ERRα (Condition 1). Comparing ERRα bound to DNA versus ERRα bound directly to plastic, the latter was enriched much slower, especially in the presence of Compound A (condition 6), where the phage binding was non-specific.

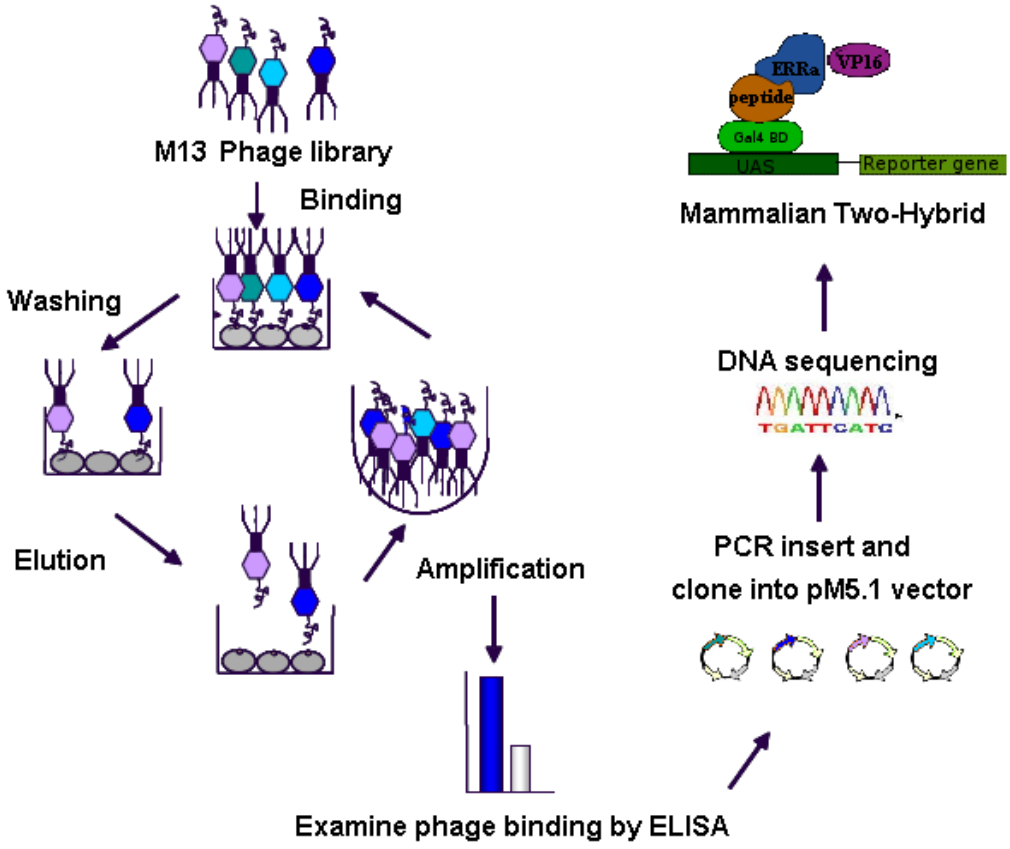

Figure 4.4 Workflow of peptide screen using M13 Phage Display.

In the M13 phage display screen, a pool of M13 phage expressing 19-amino acid peptides containing LXXLL on their capsids are incubated in 96-well plate with the purified ERRα protein. Unbound phage clones are washed away, while phage bound to ERRα are eluted and amplified. During these rounds of "biopanning", phage clones compete for ERRα binding and phage that bind with high affinity will be enriched. The enrichment of ERRα-binding phage is tested using phage ELISA assay. DNA sequencing is used to identify the sequence of each phage-expressed, and the binding of each individual phage peptide to ERRα can be confirmed in cells using a mammalian two hybrid assay.

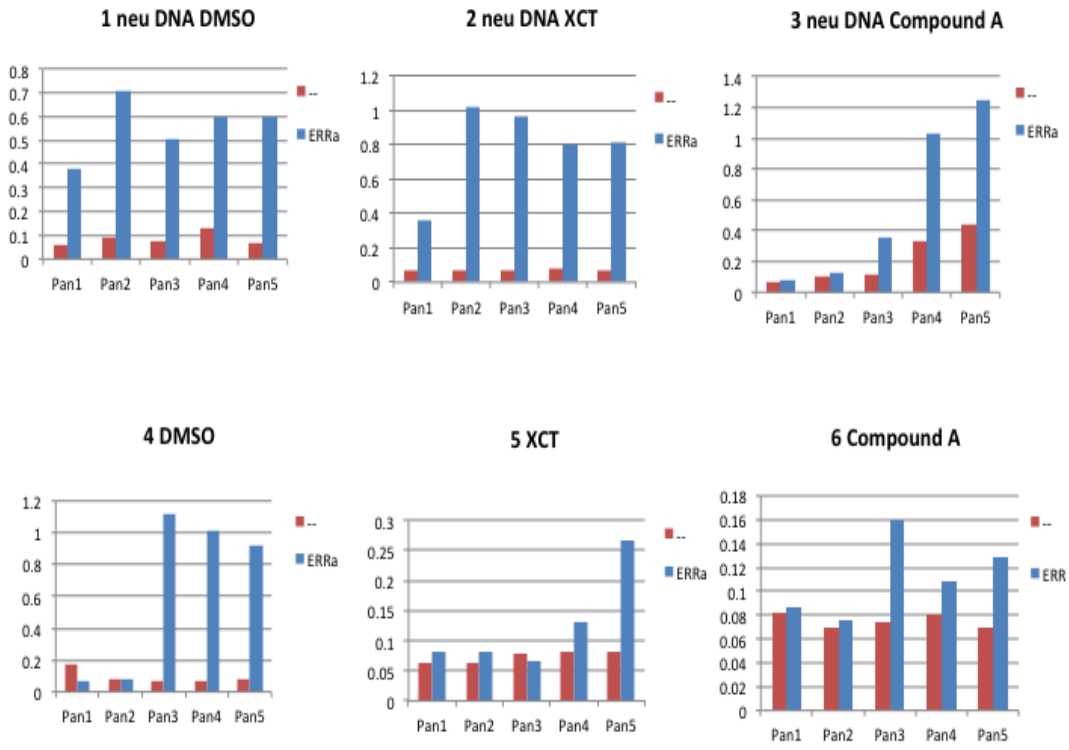

Figure 4.5 Enrichment of ERRα - interacting phage

A phage ELISA assay was performed to determine whether the biopanning enriched for phage that expressed peptides that bound to ERRα. Condition 1, 2, 3: wells were coated with neutravidin and biotinylated double-stranded DNA oligomers containing a canonical ERE. Throughout the process of plate coating, ERRα incubation, and phage binding, each of the three conditions was supplemented with vehicle (DMSO), XCT and Compound A, respectively. Condition 4, 5, 6: wells were coated directly with ERRα protein and the panning was performed in the presence of vehicle (DMSO), XCT and Compound A, respectively. To test the selectivity of phage binding to ERRα protein, negative control wells incubated with milk instead of ERRα protein were included for all the six coating conditions. The presence of phage was detected using an anti-M13-HRP-conjugated antibody and quantified by measuring the absorbance at 405 nm upon the addition of a colorimetric HRP substrate ABTS.

4.3.4 Characterization of ERRα interacting peptides

To confirm the ability of individual peptides to bind ERRα, their coding DNA fragments were subcloned into a pM5.1 vector creating a Gal4 DNA binding domain (Gal4DBD)-fusion protein for mammalian-two-hybrid assays (M2H). Interaction between the Gal4DBD-peptide fusion and the VP16- ERRα fusion activates the transcription of a luciferase reporter gene under the control of the Gal4-response element. After transformation of pM5.1_peptide plasmids into DH5α, 95 isolated clones were picked for DNA sequencing, which resulted in the identification of 24 unique peptide sequences. Further characterization by cell-based mammalian two-hybrid assays confirmed the interaction between ERRα and 22 of the 24 peptides. The list of these confirmed peptides is shown in Table 4.1. A representative mammalian-two hybrid result is shown in Figure 4.6. PGC1α_L3 is a peptide from the third LXXLL motif of PGC-1α, and was included as a positive control in this assay. VP16 vector instead of VP16-ERRα plasmid was used as a negative control, which demonstrated none of these peptides had intrinsic transcriptional capacity in the absence of ERRα receptor.

As shown in Figure 4.6, peptides found to bind to ERRα fall into two categories based on the peptide-receptor interaction patterns. Some peptides interact with ERRα with decreased binding affinity in the presence of ERRα antagonist XCT or Compound A, while other peptides interact with ERRα and are not affected by ERRα antagonists. Surprisingly, none of the peptides selectively bind only one form of ERRα.

To pinpoint the ERRα surfaces available and important for peptide/protein interaction, peptides that interact with wild type ERRα were tested for binding to various ERRα mutants using a mammalian-two hybrid assay (Figure 4.7). The deletion mutants deleN, deleLBD and deleH12 are ERRα mutant with deletions of the N-terminus, the ligand binding domain (LBD) and the Helix 12 of the LBD, respectively. K244A/3x is a mutant with the following mutations K244A, K412N, E416Q and E419Q, and has been shown to abolish ERRα/PGC-1α interaction (Gaillard, Dwyer et al. 2007). Strikingly, all these mutations we tested can cause changes to the binding affinity of the peptide to the receptor.

Since these peptides can interact with ERRα, overexpression of these peptides may interfere with receptor activity by competing with cofactors for ERRα binding. To test the potential utility of these peptides, a transactivation assay was used. HeLa cells were transfected with 3xERE-TATA-luciferase reporter, pcDNA_ERRα and pM5.1_peptide plasmid. pM5.1 empty vector was used as a negative control for the effect of the peptides to be tested. pM_PGC1αL3 and pM_L3_09 express two peptides known to interrupt ERRα/PGC-1α interaction and served as positive controls. As shown in Figure 4.8, several peptides (such as JL11, JL16 and JL20) decrease the transcriptional activity of ERRα, suggesting these small peptides can compete with endogenous ERRα cofactor, most likely PGC-1α in this case. However, other peptides (such as JL1 and JL8) did not affect the transcriptional activity of ERRα. One possible explanation is that these

peptides do not have high enough binding affinity to compete with endogenous ERRα cofactor(s). It is also possible that these peptides are binding to regions of the receptor not required for cofactor interaction.

Table 4.3: List of ERRα-interacting peptides identified by M13 phage display screen.

JL1 - JL22 are 22 unique peptides that were identified by M13 phage display screen of ERRα, with the receptor either binding DNA or directly on the plastic. The interaction between these peptides and ERRα was confirmed in cell-based assays.

Peptide	Sequence
JL1	DLTRYPVLWELLTQGSGAE
JL2	TCVNYPLLCGLLNDRPIIT
JL3	DVTQYPELLRLLLSMEQTD
JL4	NCWEFPWLCGLLTQDRKTT
JL5	DIARYPELMGLLLSNRPVV
JL6	ELSDSWLLRQLLGQHPVNQ
JL7	PPEKFPMLRGLLTDGVGNQ
JL8	PAEGSWLLRCLLGQCEGGY
JL9	SVDRWPELLRLLQPTEFSM
JL10	GLTRYPVLWELLTQGSGAE
JL11	MASDWPLLAALLNGGSPQM
JL12	LPSGFPELFRLLTEPELQV
JL13	HPEDFPLLRSLLSCESFEC
JL14	PLENFPLLLSLLTSEGPEV
JL15	GPSDFPILWNLLTTSVSGD
JL16	NLDEWPILAALLQSPEGEL
JL17	HSQDYPLLFSLLTKEHLAD
JL18	PLTQGSWLERLLSTGVADA
JL19	GVDDYPLLRALLLGQQQRG
JL20	VPEAYPYLLELLSRDDLRL
JL21	DMTGYPLLRGLLLQGMEPA
JL22	DIARYPVLWELLTQGSGAE

A

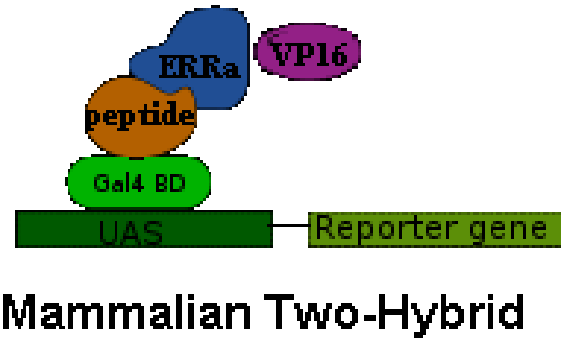

Mammalian Two-Hybrid

B

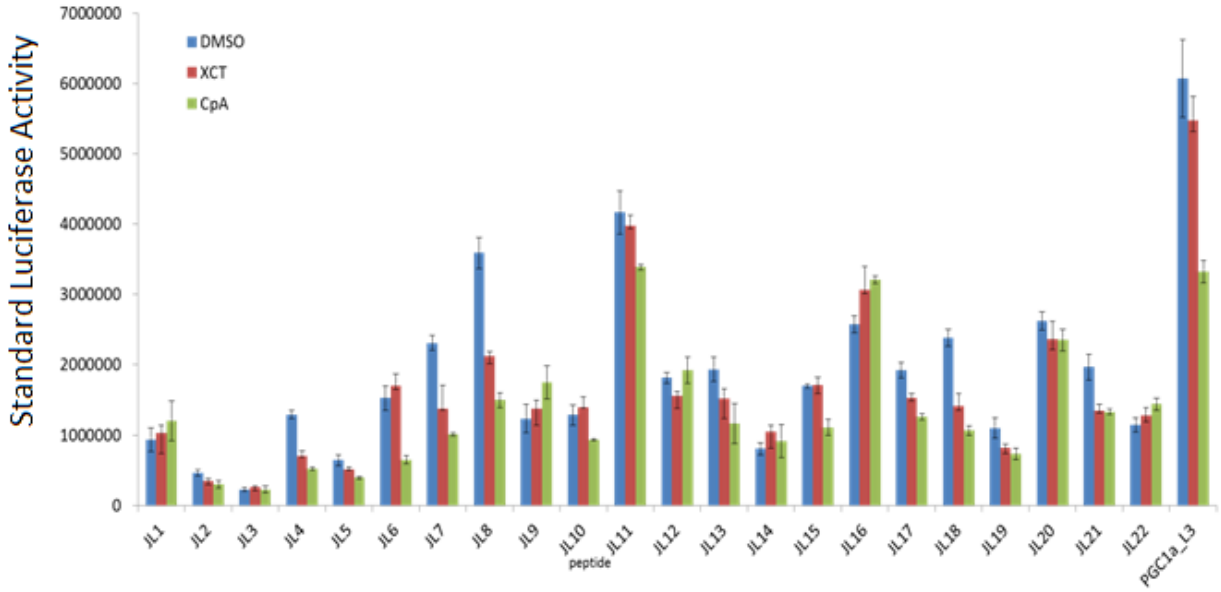

Figure 4.6 Selected peptides interact with ERRα in a mammalian-two-hybrid assay

A. Diagram of mammalian-two-hybrid assay used in (B). Interaction between a small peptide fused to a Gal4-DNA binding domain (Gal4DBD) and ERRα fused to VP16 activates the transcription of a luciferase reporter construct under the control of Gal4-response element. B. Mammalian two-hybrid assay assessing the ability of the indicated peptides to interact with ERRα. HepG2 cells in 96-well plates were transfected with 600 ng of total plasmids containing 180 ng 5xGal4-luciferase, 20 ng pCMV B-GAL, 200 ng VP16_ERRα and 200 ng of indicated pM5.1_peptide per triplicate samples. PGC1α_L3 is a positive control peptide that contains the third LXXLL motif from PGC-1α and is known to interact with ERRα. Cells were treated with 10 μM XCT-790, 10 μM Compound A, or equivalent amount of DMSO vehicle for 8 hours before harvest. Cells were lysed 24 or 48 hours after transfection and assayed for luciferase and β-galactosidase activities. Results are expressed as luciferase activity normalized with β-Gal for transfection efficiency +/- standard error of the mean (SEM) per triplicate samples.

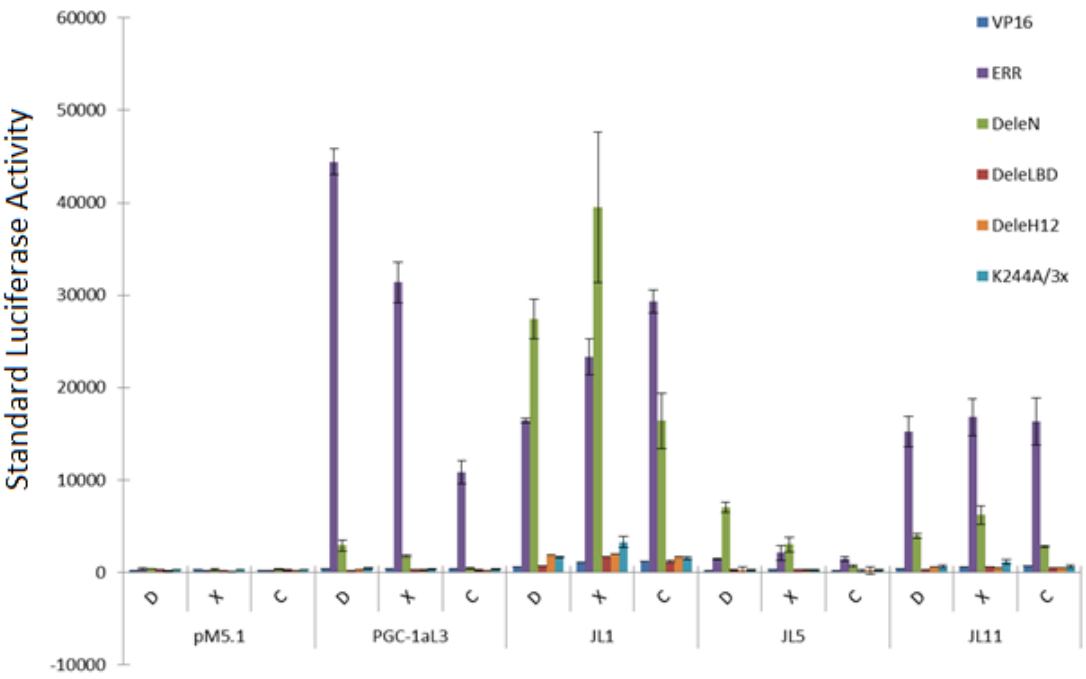

Figure 4.7 Interaction between selected peptides and ERR*α* mutants

Interactions between small peptides fused to Gal4DBD and ERR*α* mutants fused to VP16 were assessed by mammalian-two-hybrid assay. HepG2 cells in 96-well plates were transfected with 600 ng of total plasmids containing 180 ng 5xGal4-luciferase, 20 ng pCMV B-GAL, 200 ng VP16_ERR*α* (or mutants) and 200 ng of indicated pM5.1_peptide per triplicate samples. Cells were treated with 10 μM XCT-790 (labeled as X), 10 μM Compound A (labeled as C), or equivalent amount of DMSO (labeled as D) vehicle for 8 hours before harvest. Cells were lysed 48 hours after transfection and assayed for luciferase and β-galactosidase activities. Results are expressed as luciferase activity normalized with β-Gal for transfection efficiency +/- standard error of the mean (SEM) per triplicate samples.

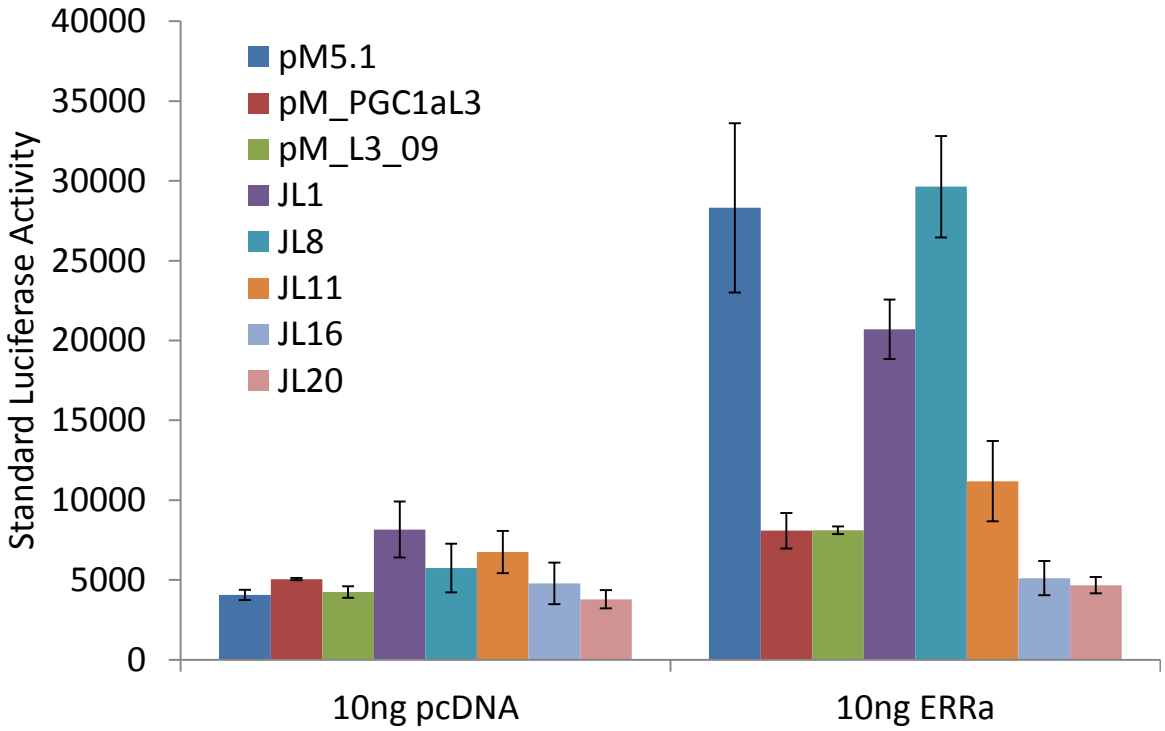

Figure 4.8 Selected peptides interfere with ERRα transcriptional activity

The identified peptides were tested for their potential to disrupt ERRα activity in a transactivation assay. HeLa cells were transfected with 1000 ng 3xERE-TATA-luciferase, 50 ng CMV β-Gal, either 10 ng ERRα or 10 ng pcDNA empty vector, and 1000 ng of the indicated pM5.1_peptide plasmid. The total amount of plasmid DNA was normalized to a total of 3000 ng with pBSII. Results are expressed as luciferase activity normalized with β-Gal for transfection efficiency) +/- standard error of the mean (SEM) per triplicate sample of cells.

4.4 Discussion

To our knowledge, this is the first time that ERRα antagonists have been used to probe for conformational differences in the full-length ERRα protein. So far, crystallography studies have explored the structures of the ligand binding domains (LBD) of ERRα and ERRγ. Several available LBD crystal structures include ERRα LBD in complex with a PGC-1α peptide (PDB accession code 1XB7 and 3D24), ERRα LBD in complex with an inverse agonist cyclohexylmethyl-(1-p-tolyl-1H-indol-3-ylmethyl)-amine (also known as compound 1a ; PDB accession code 2PJL), ERRγ LBD in complex with a SRC1 peptide (PDB accession code 1KV6 and 1TFC), and ERRγ LBD in complex with diethylstilbestrol or 4-hydroxytamoxifen (PDB accession code 1S9P and 1S9Q) (Greschik, Wurtz et al. 2002, Greschik, Flaig et al. 2004, Kallen, Schlaeppi et al. 2004, Kallen, Lattmann et al. 2007, Greschik, Althage et al. 2008). However, no structural information is available for full-length ERRα in either apo or antagonist-bound form. Here we utilized this phage display strategy to survey conformation of the full-length ERRα protein in Apo, XCT-bound and Compound A-bound states.

The affinity of a given peptide for ERRα may be indicated by the number of times the clone is pulled out of the screen. The appearance frequency of a peptide in a screen can largely depend on its binding affinity, although phage with considerably higher amplification rate may also affect the screen result. Many peptide clones such as JL1 and JL8 were each pulled out of the screen multiple times. Our cell-based assays

confirmed that 22 out of the 24 peptides can interact with ERRα in cells, suggesting the effectiveness of our phage screen to identify ERRα-interacting peptides.

The peptides identified in our screen include those which bind with higher affinity to apo ERRα than to antagonist bound ERRα, although the majority of the peptides are those that are unaffected by the presence of an ERRα antagonist. In fact, several peptides were each identified in multiple screen conditions. For example, peptide JL1 was recovered from ERRα + ERE + XCT, ERRα + ERE + Compound A, and ERRα + Compound A conditions. Furthermore, mammalian two-hybrid assay (Figure 4.6) demonstrated that the interactions between ERRα and many peptides including JL1 were not affected by XCT or Compound A treatment indicating that these peptides bind to regions of ERRα that are available in apo ERRα and antagonist-bound forms.

Given the LXXLL motif contained in the peptides, and the fact that ERRα deleLBD and K244A/3X mutants both abolished the binding of these peptides, it is highly likely that these peptides bind the AF2 coactivator binding pocket or nearby region of ERRα LBD. Using a random peptide library instead of the LXXLL peptide library for a future phage screen may have a better chance of identifying new regions on ERRα that can distinguish differently conformed receptor. Sequence alignment reveals that the peptides we identified have a consensus sequence with residues such as Tyrosine (Y) on position 5 and Phenylalanine (F) on position 6 of the small peptide. To understand how these peptides could bind ERRα, we modeled the binding of these

peptides using the crystal structure of the SRC1 peptide in complex with ERRγ as a scaffold. We found that, if the peptides bind ERRα on the same coactivator interaction surface as the SRC1 peptide, the Tyrosine on position 5 could form a hydrogen bond with a Glutamine in Helix 4 of ERRα, while the Leucine or Valine residue on position 7 could pack nicely with a Leucine on Helix 12 of ERRα.

One thing worth noticing is that some peptides showed different binding affinities to wild-type ERRα and deleN mutant. This suggests that the NH2-terminal of the receptor is also involved in the interaction. The interdomain interaction between the NH2-terminal and carboxyl-terminal (N/C interaction) has been reported for Androgen (Langley, Zhou et al. 1995, He and Wilson 2002), Estrogen (Kraus, McInerney et al. 1995), Progesterone (Tetel, Giangrande et al. 1999) and Mineralocorticoid receptors (Pippal, Yao et al. 2009). Although the NH2-terminal of ERRα receptor is much shorter compared to these other nuclear receptors, it is possible that these domains form a similar interaction in the ERRα protein.

Not only could the peptides identified in these studies serve as conformational probes to assess how an antagonist modulates ERRα, the fact that some peptides can block the ERRα/PGC-1α interaction suggests that these peptides have the potential to selectively modulate ERRα activity.

Conclusions and Implications

Our study of ERRα covers both the functional definition and the molecular dissection of this receptor. In this chapter, our findings will be summarized in the context of literature reports and discuss their implications for future research in this area.

Functional definition of ERRα in breast cancer

Over the past few years, a number of papers were published that examined the role of ERRα in breast cancer. The correlation between ERRα expression/activity and poor prognosis was established in breast cancer patients (Suzuki, Miki et al. 2004, Chang, Kazmin et al. 2011). Targeting ERRα also exhibited an inhibitory effect in breast tumor xenograft growth (Stein, Chang et al. 2008, Bianco, Lanvin et al. 2009, Chisamore, Cunningham et al. 2009). These findings inspired our exploration of ERRα function in breast cancer. Here, we sought to address the question of how ERRα promotes breast cancer growth and progression, the answer to which may potentially lead to the development of novel therapeutic targets.

At the outset of this project, it was reported that breast cancer cells with ERRα knock-down did not show a difference in proliferative rate *in vitro*, while significantly retarded growth was observed when these cells were implanted as xenograft tumors (Stein, Chang et al. 2008). This finding forced us to consider the differences between *in vitro* culture versus a xenograft model. One striking difference is an increased metabolic

requirement and hypoxic stress of the tumor environment, both of which induce angiogenesis. In fact, several groups have shown that VEGF is a direct target gene of ERRα (Ao, Wang et al. 2008, Arany, Foo et al. 2008, Stein, Gaillard et al. 2009, Klimcakova, Chenard et al. 2012). Thus, we hypothesized that ERRα may be involved in breast cancer angiogenesis by induction of pro-angiogenic factors.

A previous microarray study using the ERRα-selective PGC-1α coactivator surveyed the ERRα transcriptome in breast cancer cells. In this study, we observed a dramatic induction of ECM1. Given its prospective role in angiogenesis, we focused on ECM1 as a potential target to understand the implication of ERRα regulation in angiogenesis. Our data clearly shows that (1) ECM1 is a target gene of ERRα; (2) ECM1 has pro-angiogenic activity; and (3) ECM1 knockdown retarded tumor xenograft growth. These findings support our hypothesis that ERRα regulates pro-angiogenic genes to promote breast cancer growth. However, several questions remain to be determined to link the regulation of ECM1 by ERRα and the role of ERRα in tumor angiogenesis.

One major question is: how is ECM1 regulated by ERRα in tumor setting? The massive induction of ECM1 in our study was achieved using exogenous overexpression of PGC-1α to activate ERRα, yet the role of PGC-1α in cancer remains controversial. Our assumption is that, although not highly expressed in breast cancer cells, PGC-1α can be upregulated as a metabolic sensor in the tumor environment, and thus induces ECM1

expression. How robust this induction is as compared to our overexpression of PGC-1α remains to be examined. While this study used PGC-1α to activate ERRα, it has recently been shown that PGC-1β can be upregulated in breast cancer cells by activation of the Her2/IGF-1R signaling pathways and subsequent C-MYC stabilization (Chang, Kazmin et al. 2011). Thus, using PGC-1α alone to study the role of ERRα function in cancer may introduce bias in target gene searching. In fact, our preliminary studies suggested a similar induction of ECM1 by exogenous overexpression of PGC-1β. However, it is unclear whether this induction is biologically relevant. In our available cell models for breast cancer, MDA-MB-231 and MDA-MB-436 cells, there is high expression of ECM1, but these cells lack Her2 and thus cannot activate the Her2/IGF-1R signaling pathway. While MCF7 and SKBR3 cells are Her2 positive cells, they have very low basal expression of ECM1, and we did not observe ECM1 induction by of Her2/IGF-1R signaling activation in these cells.

Another important question is to what extent does the pro-angiogenic effect of ECM1 account for the role of ERRα in breast tumor growth and angiogenesis. As we mentioned, VEGF expression can also be upregulated by ERRα, both through ERRα/PGC-1α and ERRα/HIF signaling. While we observed ECM1 induction by ERRα/PGC-1α, we did not see the effect of HIF stabilization on ECM1 expression. The relative contribution of ECM1 and VEGF in tumor angiogenesis remains to be tested.

Our preliminary *in vitro* studies suggested no synergistic effect from co-treatment with recombinant VEGF and ECM1 on endothelial cell tube formation. This leads to another interesting question: what is the molecular mechanism of ECM1 stimulated angiogenesis? We tested some known angiogenesis pathways that VEGF is involved in, such as Erk, Akt and p38. However, treating endothelial cells *in vitro* with recombinant ECM1 did not turn on these pathways. It has been reported that ECM1 interacts with many extracellular matrix proteins, including perlecan, fibulin-1C/D, MMP-9, collagen type IV and laminin 332 (Mongiat, Fu et al. 2003, Fujimoto, Terlizzi et al. 2005, Fujimoto, Terlizzi et al. 2006, Sercu, Zhang et al. 2008, Sercu, Lambeir et al. 2009). Thus, it is possible that the effect of ECM1 on endothelial cell tube formation is through its interacting components in the Matrigel, and the effect of knocking down ECM1 on tumor xenograft is through the alteration of extracellular matrix remodeling in the tumor microenvironment. This proposed mechanism remains to be tested.

Molecular dissection of ERRα

Dissecting the molecular mechanisms of ERRα function is another aspect of this research. Given the newly recognized ERRα activity on β-catenin and hypoxia-inducible factor-1 transcription, we focused on the mechanism of these non-canonical pathways regulated by ERRα. Unlike traditional transcriptional cofactors such as PGC-1, ERRα possesses a DNA Binding Domain that recognizes ERRE response element. Thus, we asked the question whether (1) DNA recognition is still required for ERRα activity, or (2)

ERRα is tethered to other transcriptional components via protein-protein interactions. Our preliminary data using ERRα DBD mutants in transcriptional reporter assays suggests the importance of an intact DNA binding domain for these non-canonical activities. However, our results do not definitively exclude (1) or (2), since the interactions between ERRα DBD mutants and β-cat or HIF-1 have not been tested. Nevertheless, the hypothesis that DNA recognition is still required for ERRα activity is currently preferred. Genomic bioinformatics studies suggested the existence of ERREs near TCF/LEF binding sites. Our transcriptional assay on a HIF reporter gene (HRE_luc) suggested a dampen effect of ERRα, which is contradictory to a previous report (Ao, Wang et al. 2008). This discrepancy may be due to the difference in reporter genes used, which suggests the minimum HRE element may be insufficient for ERRα activation.

It has been recently shown that PGC-1α expression is induced under hypoxia conditions (Zhu, Wang et al. 2010). Thus, we asked the question of what is the role of PGC-1α on these HIF target genes under hypoxia conditions. When comparing the genes with enrichment of HIF binding sites and those regulated by ERRα coactivator PGC-1α overexpression in MCF-7 cells, we found many HIF target genes were downregulated by PGC-1α under normoxia. Future work to examine how ERRα coordinates between its canonical ERRα/ PGC-1α pathway and its non-canonical ERRα / HIF pathway will help in answering this question.

Despite the seemingly opposing effects of PGC-1α/ERRα and HIF-1 on some target genes, several target genes were identified to be regulated in the same direction by these two transcription factors. VEGF has been shown to be upregulated by both PGC-1α and HIF, and transient overexpression of PGC-1α under hypoxia has a synergistic effect with HIF activity. Similarly, we found that CA9, another HIF target gene, is downregulated by ERRα inhibition. Interestingly, overexpression of PGC-1α either under normoxia or hypoxia cannot upregulate CA9 expression. It is possible that in this context, the HIF-dependent and PGC-1α-independent effect of ERRα is mediated through its tethering to HIF. It is also possible that ERRα is acting through indirect mechanism on CA9. This question remains to be addressed.

Finally, we surveyed the structure of full-length ERRα in Apo, XCT-bound and Compound A-bound forms using phage display and identified several peptides that interact with ERRα under these three conditions. Using ERRα mutants we concluded that the identified peptides bind in or near the AF2 coactivator binding pocket. However, some but not all peptides are discriminative in their binding of antagonist-occupied ERRα. For future studies, using a random peptide library rather than the LXXLL peptide library for the phage screen may help in identify peptides that bind to other regions on ERRα. Not only could these peptides serve as conformational probes in assessing how antagonists impact the structure of ERRα, the discovery of small peptides

that block specific protein-protein interactions involving ERRα may have the potential to selectively modulate ERRα activity.

In conclusion, we have explored various aspects of ERRα biology in this work. We identified a novel PGC-1α /ERRα target gene, ECM1, which is involved in breast tumor growth and angiogenesis. We proposed the potential mechanisms of ERRα non-canonical pathways. Finally, we examined the effects ERRα antagonists have on ERRα structure. Our findings provide more insight into our understanding of ERRα function. However, these findings also leave many important questions unanswered and bring up new and unexplored aspects of ERRα biology. Future research to address these questions will further elucidate the role of ERRα in breast cancer, and thus lead to the development of novel therapeutic options for breast cancer patients.

References

Ao, A., H. Wang, S. Kamarajugadda and J. Lu (2008). "Involvement of estrogen-related receptors in transcriptional response to hypoxia and growth of solid tumors." Proc Natl Acad Sci U S A 105(22): 7821-7826.

Arany, Z., S. Y. Foo, Y. Ma, J. L. Ruas, A. Bommi-Reddy, G. Girnun, M. Cooper, D. Laznik, J. Chinsomboon, S. M. Rangwala, K. H. Baek, A. Rosenzweig and B. M. Spiegelman (2008). "HIF-independent regulation of VEGF and angiogenesis by the transcriptional coactivator PGC-1alpha." Nature 451(7181): 1008-1012.

Ariazi, E. A., G. M. Clark and J. E. Mertz (2002). "Estrogen-related receptor alpha and estrogen-related receptor gamma associate with unfavorable and favorable biomarkers, respectively, in human breast cancer." Cancer Res 62(22): 6510-6518.

Bapat, A. R. and D. E. Frail (2003). "Full-length estrogen receptor alpha and its ligand-binding domain adopt different conformations upon binding ligand." J Steroid Biochem Mol Biol 86(2): 143-149.

Bhalla, K., B. J. Hwang, R. E. Dewi, L. H. Ou, W. Twaddel, H. B. Fang, S. B. Vafai, F. Vazquez, P. Puigserver, L. Boros and G. D. Girnun (2011). "PGC1 alpha Promotes Tumor Growth by Inducing Gene Expression Programs Supporting Lipogenesis." Cancer Research 71(21): 6888-6898.

Bianco, S., O. Lanvin, V. Tribollet, C. Macari, S. North and J. M. Vanacker (2009). "Modulating estrogen receptor-related receptor-alpha activity inhibits cell proliferation." J Biol Chem 284(35): 23286-23292.

Bledsoe, R. K., V. G. Montana, T. B. Stanley, C. J. Delves, C. J. Apolito, D. D. McKee, T. G. Consler, D. J. Parks, E. L. Stewart, T. M. Willson, M. H. Lambert, J. T. Moore, K. H. Pearce and H. E. Xu (2002). "Crystal structure of the glucocorticoid receptor ligand binding domain reveals a novel mode of receptor dimerization and coactivator recognition." Cell 110(1): 93-105.

Botrugno, O. A., E. Fayard, J. S. Annicotte, C. Haby, T. Brennan, O. Wendling, T. Tanaka, T. Kodama, W. Thomas, J. Auwerx and K. Schoonjans (2004). "Synergy between LRH-1 and beta-catenin induces G1 cyclin-mediated cell proliferation." Mol Cell 15(4): 499-509.

Boylan, K. L., J. D. Andersen, L. B. Anderson, L. Higgins and A. P. Skubitz (2010). "Quantitative proteomic analysis by iTRAQ(R) for the identification of candidate biomarkers in ovarian cancer serum." Proteome Sci 8: 31.

Brzozowski, A. M., A. C. Pike, Z. Dauter, R. E. Hubbard, T. Bonn, O. Engstrom, L. Ohman, G. L. Greene, J. A. Gustafsson and M. Carlquist (1997). "Molecular basis of agonism and antagonism in the oestrogen receptor." Nature 389(6652): 753-758.

Busch, B. B., W. C. Stevens, Jr., R. Martin, P. Ordentlich, S. Zhou, D. W. Sapp, R. A. Horlick and R. Mohan (2004). "Identification of a selective inverse agonist for the orphan nuclear receptor estrogen-related receptor alpha." J Med Chem 47(23): 5593-5596.

Carpentier, G. (2012). "ImageJ contribution: Angiogenesis Analyzer." ImageJ News.

Chang, C., J. D. Norris, H. Gron, L. A. Paige, P. T. Hamilton, D. J. Kenan, D. Fowlkes and D. P. McDonnell (1999). "Dissection of the LXXLL nuclear receptor-coactivator interaction motif using combinatorial peptide libraries: discovery of peptide antagonists of estrogen receptors alpha and beta." Mol Cell Biol 19(12): 8226-8239.

Chang, C. Y., D. Kazmin, J. S. Jasper, R. Kunder, W. J. Zuercher and D. P. McDonnell (2011). "The metabolic regulator ERRalpha, a downstream target of HER2/IGF-1R, as a therapeutic target in breast cancer." Cancer Cell 20(4): 500-510.

Chegwidden, W. R. and N. D. Carter (2000). "Introduction to the carbonic anhydrases." EXS(90): 14-28.

Chen, E. I., J. Hewel, J. S. Krueger, C. Tiraby, M. R. Weber, A. Kralli, K. Becker, J. R. Yates and B. Felding-Habermann (2007). "Adaptation of energy metabolism in breast cancer brain metastases." Cancer Research 67(4): 1472-1486.

Chen, F., Q. Zhang, T. McDonald, M. J. Davidoff, W. Bailey, C. Bai, Q. Liu and C. T. Caskey (1999). "Identification of two hERR2-related novel nuclear receptors utilizing bioinformatics and inverse PCR." Gene 228(1-2): 101-109.

Chen, H., W. D. Jia, J. S. Li, W. Wang, G. L. Xu, J. L. Ma, W. H. Ren, Y. S. Ge, J. H. Yu, W. B. Liu, C. H. Zhang and Y. C. Wang (2011). "Extracellular matrix protein 1, a novel prognostic factor, is associated with metastatic potential of hepatocellular carcinoma." Medical Oncology 28: S318-S325.

Chia, S. K., C. C. Wykoff, P. H. Watson, C. Han, R. D. Leek, J. Pastorek, K. C. Gatter, P. Ratcliffe and A. L. Harris (2001). "Prognostic significance of a novel hypoxia-regulated marker, carbonic anhydrase IX, in invasive breast carcinoma." J Clin Oncol 19(16): 3660-3668.

Chisamore, M. J., R. T. Mosley, S. J. Cai, E. T. Birzin, G. O'Donnell, P. Zuck, O. Flores, J. Schaeffer, S. P. Rohrer, J. D. Chen and H. A. Wilkinson (2008). "Identification of small molecule estrogen-related receptor alpha-specific antagonists and homology modeling to predict the molecular determinants as the basis for selectivity over ERR beta and ERR gamma." Drug Development Research 69(4): 203-218.

Chisamore, M. J., H. A. Wilkinson, O. Flores and J. D. Chen (2009). "Estrogen-related receptor-alpha antagonist inhibits both estrogen receptor-positive and estrogen receptor-negative breast tumor growth in mouse xenografts." Mol Cancer Ther 8(3): 672-681.

Cormio, A., F. Guerra, G. Cormio, V. Pesce, F. Fracasso, V. Loizzi, P. Cantatore, L. Selvaggi and M. N. Gadaleta (2009). "The PGC-1 alpha-dependent pathway of mitochondrial biogenesis is upregulated in type I endometrial cancer." Biochemical and Biophysical Research Communications 390(4): 1182-1185.

Coward, P., D. Lee, M. V. Hull and J. M. Lehmann (2001). "4-Hydroxytamoxifen binds to and deactivates the estrogen-related receptor gamma." Proc Natl Acad Sci U S A 98(15): 8880-8884.

Curtis, V. F., H. Wang, P. Y. Yang, R. E. McLendon, X. H. Li, Q. Y. Zhou and X. F. Wang (2013). "A PK2/Bv8/PROK2 Antagonist Suppresses Tumorigenic Processes by Inhibiting Angiogenesis in Glioma and Blocking Myeloid Cell Infiltration in Pancreatic Cancer." Plos One 8(1).

Deblois, G., J. A. Hall, M. C. Perry, J. Laganiere, M. Ghahremani, M. Park, M. Hallett and V. Giguere (2009). "Genome-wide identification of direct target genes implicates estrogen-related receptor alpha as a determinant of breast cancer heterogeneity." Cancer Res 69(15): 6149-6157.

Duffy, S., K. L. Tsao and D. S. Waugh (1998). "Site-specific, enzymatic biotinylation of recombinant proteins in Spodoptera frugiperda cells using biotin acceptor peptides." Anal Biochem 262(2): 122-128.

Dwyer, M. A., J. D. Joseph, H. E. Wade, M. L. Eaton, R. S. Kunder, D. Kazmin, C. Y. Chang and D. P. McDonnell (2010). "WNT11 expression is induced by estrogen-

related receptor alpha and beta-catenin and acts in an autocrine manner to increase cancer cell migration." Cancer Res 70(22): 9298-9308.

Eudy, J. D., S. Yao, M. D. Weston, M. Ma-Edmonds, C. B. Talmadge, J. J. Cheng, W. J. Kimberling and J. Sumegi (1998). "Isolation of a gene encoding a novel member of the nuclear receptor superfamily from the critical region of Usher syndrome type IIa at 1q41." Genomics 50(3): 382-384.

Feilchenfeldt, J., M. A. Brundler, C. Soravia, M. Totsch and C. A. Meier (2004). "Peroxisome proliferator-activated receptors (PPARs) and associated transcription factors in colon cancer: reduced expression of PPAR gamma-coactivator 1 (PGC-1)." Cancer Letters 203(1): 25-33.

Fujimoto, N., J. Terlizzi, S. Aho, R. Brittingham, A. Fertala, N. Oyama, J. A. McGrath and J. Uitto (2006). "Extracellular matrix protein 1 inhibits the activity of matrix metalloproteinase 9 through high-affinity protein/protein interactions." Exp Dermatol 15(4): 300-307.

Fujimoto, N., J. Terlizzi, R. Brittingham, A. Fertala, J. A. McGrath and J. Uitto (2005). "Extracellular matrix protein 1 interacts with the domain III of fibulin-1C and 1D variants through its central tandem repeat 2." Biochemical and Biophysical Research Communications 333(4): 1327-1333.

Gaillard, S., M. A. Dwyer and D. P. McDonnell (2007). "Definition of the molecular basis for estrogen receptor-related receptor-alpha-cofactor interactions." Mol Endocrinol 21(1): 62-76.

Gaillard, S., L. L. Grasfeder, C. L. Haeffele, E. K. Lobenhofer, T. M. Chu, R. Wolfinger, D. Kazmin, T. R. Koves, D. M. Muoio, C. Y. Chang and D. P. McDonnell (2006). "Receptor-selective coactivators as tools to define the biology of specific receptor-coactivator pairs." Molecular Cell 24(5): 797-803.

Generali, D., S. B. Fox, A. Berruti, M. P. Brizzi, L. Campo, S. Bonardi, S. M. Wigfield, P. Bruzzi, A. Bersiga, G. Allevi, M. Milani, S. Aguggini, L. Dogliotti, A. Bottini and A. L. Harris (2006). "Role of carbonic anhydrase IX expression in prediction of the efficacy and outcome of primary epirubicin/tamoxifen therapy for breast cancer." Endocr Relat Cancer 13(3): 921-930.

Giatromanolaki, A., M. I. Koukourakis, E. Sivridis, J. Pastorek, C. C. Wykoff, K. C. Gatter and A. L. Harris (2001). "Expression of hypoxia-inducible carbonic anhydrase-9 relates to angiogenic pathways and independently to poor outcome in non-small cell lung cancer." Cancer Res 61(21): 7992-7998.

Giguere, V., N. Yang, P. Segui and R. M. Evans (1988). "Identification of a new class of steroid hormone receptors." Nature 331(6151): 91-94.

Glass, C. K. (1994). "Differential recognition of target genes by nuclear receptor monomers, dimers, and heterodimers." Endocr Rev 15(3): 391-407.

Greschik, H., M. Althage, R. Flaig, Y. Sato, V. Chavant, C. Peluso-Iltis, L. Choulier, P. Cronet, N. Rochel, R. Schule, P. E. Stromstedt and D. Moras (2008). "Communication between the ERRalpha homodimer interface and the PGC-1alpha binding surface via the helix 8-9 loop." J Biol Chem 283(29): 20220-20230.

Greschik, H., R. Flaig, J. P. Renaud and D. Moras (2004). "Structural basis for the deactivation of the estrogen-related receptor gamma by diethylstilbestrol or 4-hydroxytamoxifen and determinants of selectivity." J Biol Chem 279(32): 33639-33646.

Greschik, H., J. M. Wurtz, S. Sanglier, W. Bourguet, A. van Dorsselaer, D. Moras and J. P. Renaud (2002). "Structural and functional evidence for ligand-independent transcriptional activation by the estrogen-related receptor 3." Mol Cell 9(2): 303-313.

Hamada, T., W. H. I. McLean, M. Ramsay, G. H. S. Ashton, A. Nanda, T. Jenkins, I. Edelstein, A. P. South, O. Bleck, V. Wessagowit, R. Mallipeddi, G. E. Orchard, H. Wan, P. J. C. Dopping-Hepenstal, J. E. Mellerio, N. V. Whittock, C. S. Munro, M. A. M. van Steensel, P. M. Steijlen, J. Ni, L. R. Zhang, T. Hashimoto, R. A. J. Eady and J. A. McGrath (2002). "Lipoid proteinosis maps to 1q21 and is caused by mutations in the extracellular matrix protein 1 gene (ECM1)." Human Molecular Genetics 11(7): 833-840.

Han, Z., J. Ni, P. Smits, C. B. Underhill, B. Xie, Y. Chen, N. Liu, P. Tylzanowski, D. Parmelee, P. Feng, I. Ding, F. Gao, R. Gentz, D. Huylebroeck, J. Merregaert and L. Zhang (2001). "Extracellular matrix protein 1 (ECM1) has angiogenic properties and is expressed by breast tumor cells." FASEB J 15(6): 988-994.

Harris, A. L. (2002). "Hypoxia--a key regulatory factor in tumour growth." Nat Rev Cancer 2(1): 38-47.

He, B. and E. M. Wilson (2002). "The NH(2)-terminal and carboxyl-terminal interaction in the human androgen receptor." Mol Genet Metab 75(4): 293-298.

Heard, D. J., P. L. Norby, J. Holloway and H. Vissing (2000). "Human ERRgamma, a third member of the estrogen receptor-related receptor (ERR) subfamily of

orphan nuclear receptors: tissue-specific isoforms are expressed during development and in the adult." Mol Endocrinol 14(3): 382-392.

Hlubek, F., T. Brabletz, J. Budczies, S. Pfeiffer, A. Jung and T. Kirchner (2007). "Heterogeneous expression of Wnt/beta-catenin target genes within colorectal cancer." Int J Cancer 121(9): 1941-1948.

Huss, J. M., K. Imahashi, C. R. Dufour, C. J. Weinheimer, M. Courtois, A. Kovacs, V. Giguere, E. Murphy and D. P. Kelly (2007). "The nuclear receptor ERRalpha is required for the bioenergetic and functional adaptation to cardiac pressure overload." Cell Metab 6(1): 25-37.

Huss, J. M., I. P. Torra, B. Staels, V. Giguere and D. P. Kelly (2004). "Estrogen-related receptor alpha directs peroxisome proliferator-activated receptor alpha signaling in the transcriptional control of energy metabolism in cardiac and skeletal muscle." Mol Cell Biol 24(20): 9079-9091.

Jakacka, M., M. Ito, J. Weiss, P. Y. Chien, B. D. Gehm and J. L. Jameson (2001). "Estrogen receptor binding to DNA is not required for its activity through the nonclassical AP1 pathway." J Biol Chem 276(17): 13615-13621.

Kallen, J., R. Lattmann, R. Beerli, A. Blechschmidt, M. J. Blommers, M. Geiser, J. Ottl, J. M. Schlaeppi, A. Strauss and B. Fournier (2007). "Crystal structure of human estrogen-related receptor alpha in complex with a synthetic inverse agonist reveals its novel molecular mechanism." J Biol Chem 282(32): 23231-23239.

Kallen, J., J. M. Schlaeppi, F. Bitsch, I. Filipuzzi, A. Schilb, V. Riou, A. Graham, A. Strauss, M. Geiser and B. Fournier (2004). "Evidence for ligand-independent transcriptional activation of the human estrogen-related receptor alpha (ERRalpha): crystal structure of ERRalpha ligand binding domain in complex with peroxisome proliferator-activated receptor coactivator-1alpha." J Biol Chem 279(47): 49330-49337.

Kamei, Y., H. Ohizumi, Y. Fujitani, T. Nemoto, T. Tanaka, N. Takahashi, T. Kawada, M. Miyoshi, O. Ezaki and A. Kakizuka (2003). "PPARgamma coactivator 1beta/ERR ligand 1 is an ERR protein ligand, whose expression induces a high-energy expenditure and antagonizes obesity." Proc Natl Acad Sci U S A 100(21): 12378-12383.

Klimcakova, E., V. Chenard, S. McGuirk, D. Germain, D. Avizonis, W. J. Muller and J. St-Pierre (2012). "PGC-1 alpha Promotes the Growth of ErbB2/Neu-Induced

Mammary Tumors by Regulating Nutrient Supply." Cancer Research 72(6): 1538-1546.

Kraus, W. L., E. M. McInerney and B. S. Katzenellenbogen (1995). "Ligand-dependent, transcriptionally productive association of the amino- and carboxyl-terminal regions of a steroid hormone nuclear receptor." Proc Natl Acad Sci U S A 92(26): 12314-12318.

Lal, G., S. Hashimi, B. J. Smith, C. F. Lynch, L. Zhang, R. A. Robinson and R. J. Weigel (2009). "Extracellular matrix 1 (ECM1) expression is a novel prognostic marker for poor long-term survival in breast cancer: a Hospital-based Cohort Study in Iowa." Ann Surg Oncol 16(8): 2280-2287.

Langley, E., Z. X. Zhou and E. M. Wilson (1995). "Evidence for an anti-parallel orientation of the ligand-activated human androgen receptor dimer." J Biol Chem 270(50): 29983-29990.

Lanvin, O., S. Bianco, N. Kersual, D. Chalbos and J. M. Vanacker (2007). "Potentiation of ICI182,780 (Fulvestrant)-induced estrogen receptor-alpha degradation by the estrogen receptor-related receptor-alpha inverse agonist XCT790." J Biol Chem 282(39): 28328-28334.

Laudet, V. (1997). "Evolution of the nuclear receptor superfamily: early diversification from an ancestral orphan receptor." J Mol Endocrinol 19(3): 207-226.

Livak, K. J. and T. D. Schmittgen (2001). "Analysis of relative gene expression data using real-time quantitative PCR and the 2(T)(-Delta Delta C) method." Methods 25(4): 402-408.

Mettu, N. B., T. B. Stanley, M. A. Dwyer, M. S. Jansen, J. E. Allen, J. M. Hall and D. P. McDonnell (2007). "The nuclear receptor-coactivator interaction surface as a target for peptide antagonists of the peroxisome proliferator-activated receptors." Mol Endocrinol 21(10): 2361-2377.

Minn, A. J., G. P. Gupta, P. M. Siegel, P. D. Bos, W. P. Shu, D. D. Giri, A. Viale, A. B. Olshen, W. L. Gerald and J. Massague (2005). "Genes that mediate breast cancer metastasis to lung." Nature 436(7050): 518-524.

Mole, D. R., C. Blancher, R. R. Copley, P. J. Pollard, J. M. Gleadle, J. Ragoussis and P. J. Ratcliffe (2009). "Genome-wide association of hypoxia-inducible factor (HIF)-1alpha and HIF-2alpha DNA binding with expression profiling of hypoxia-inducible transcripts." J Biol Chem 284(25): 16767-16775.

Mongiat, M., J. Fu, R. Oldershaw, R. Greenhalgh, A. M. Gown and R. V. Iozzo (2003). "Perlecan protein core interacts with extracellular matrix protein 1 (ECM1), a glycoprotein involved in bone formation and angiogenesis." J Biol Chem 278(19): 17491-17499.

Mootha, V. K., C. Handschin, D. Arlow, X. Xie, J. St Pierre, S. Sihag, W. Yang, D. Altshuler, P. Puigserver, N. Patterson, P. J. Willy, I. G. Schulman, R. A. Heyman, E. S. Lander and B. M. Spiegelman (2004). "Erralpha and Gabpa/b specify PGC-1alpha-dependent oxidative phosphorylation gene expression that is altered in diabetic muscle." Proc Natl Acad Sci U S A 101(17): 6570-6575.

Mulholland, D. J., S. Dedhar, G. A. Coetzee and C. C. Nelson (2005). "Interaction of nuclear receptors with the Wnt/beta-catenin/Tcf signaling axis: Wnt you like to know?" Endocr Rev 26(7): 898-915.

Nguyen, D., M. Bail, G. Pesant, V. N. Dupont, E. Rouault, J. Deschenes, W. Rocha, G. Melancon, S. V. Steinberg and S. Mader (2007). "Rational design of an estrogen receptor mutant with altered DNA-binding specificity." Nucleic Acids Res 35(10): 3465-3477.

Norris, J. D., L. A. Paige, D. J. Christensen, C. Y. Chang, M. R. Huacani, D. Fan, P. T. Hamilton, D. M. Fowlkes and D. P. McDonnell (1999). "Peptide antagonists of the human estrogen receptor." Science 285(5428): 744-746.

Pan, S., L. Cheng, J. T. White, W. Lu, A. G. Utleg, X. Yan, N. D. Urban, C. W. Drescher, L. Hood and B. Lin (2009). "Quantitative proteomics analysis integrated with microarray data reveals that extracellular matrix proteins, catenins, and p53 binding protein 1 are important for chemotherapy response in ovarian cancers." OMICS 13(4): 345-354.

Pedroza-Gonzalez, A., K. L. Xu, T. C. Wu, C. Aspord, S. Tindle, F. Marches, M. Gallegos, E. C. Burton, D. Savino, T. Hori, Y. Tanaka, S. Zurawski, G. Zurawski, L. Bover, Y. J. Liu, J. Banchereau and A. K. Palucka (2011). "Thymic stromal lymphopoietm fosters human breast tumor growth by promoting type 2 inflammation." Journal of Experimental Medicine 208(3): 479-490.

Pippal, J. B., Y. Yao, F. M. Rogerson and P. J. Fuller (2009). "Structural and functional characterization of the interdomain interaction in the mineralocorticoid receptor." Mol Endocrinol 23(9): 1360-1370.

Sahin, E., S. Colla, M. Liesa, J. Moslehi, F. L. Muller, M. Guo, M. Cooper, D. Kotton, A. J. Fabian, C. Walkey, R. S. Maser, G. Tonon, F. Foerster, R. Xiong, Y. A. Wang, S. A.

Shukla, M. Jaskelioff, E. S. Martin, T. P. Heffernan, A. Protopopov, E. Ivanova, J. E. Mahoney, M. Kost-Alimova, S. R. Perry, R. Bronson, R. Liao, R. Mulligan, O. S. Shirihai, L. Chin and R. A. DePinho (2011). "Telomere dysfunction induces metabolic and mitochondrial compromise." Nature 470(7334): 359-365.

Schreiber, S. N., R. Emter, M. B. Hock, D. Knutti, J. Cardenas, M. Podvinec, E. J. Oakeley and A. Kralli (2004). "The estrogen-related receptor alpha (ERR alpha) functions in PPAR gamma coactivator 1 alpha (PGC-1 alpha)-induced mitochondrial biogenesis." Proceedings of the National Academy of Sciences of the United States of America 101(17): 6472-6477.

Schreiber, S. N., R. Emter, M. B. Hock, D. Knutti, J. Cardenas, M. Podvinec, E. J. Oakeley and A. Kralli (2004). "The estrogen-related receptor alpha (ERRalpha) functions in PPARgamma coactivator 1alpha (PGC-1alpha)-induced mitochondrial biogenesis." Proc Natl Acad Sci U S A 101(17): 6472-6477.

Schreiber, S. N., D. Knutti, K. Brogli, T. Uhlmann and A. Kralli (2003). "The transcriptional coactivator PGC-1 regulates the expression and activity of the orphan nuclear receptor estrogen-related receptor alpha (ERR alpha)." Journal Of Biological Chemistry 278(11): 9013-9018.

Schreiber, S. N., D. Knutti, K. Brogli, T. Uhlmann and A. Kralli (2003). "The transcriptional coactivator PGC-1 regulates the expression and activity of the orphan nuclear receptor estrogen-related receptor alpha (ERRalpha)." J Biol Chem 278(11): 9013-9018.

Schwabe, J. W., L. Chapman, J. T. Finch and D. Rhodes (1993). "The crystal structure of the estrogen receptor DNA-binding domain bound to DNA: how receptors discriminate between their response elements." Cell 75(3): 567-578.

Sercu, S., A. M. Lambeir, E. Steenackers, A. El Ghalbzouri, K. Geentjens, T. Sasaki, N. Oyama and J. Merregaert (2009). "ECM1 interacts with fibulin-3 and the beta 3 chain of laminin 332 through its serum albumin subdomain-like 2 domain." Matrix Biology 28(3): 160-169.

Sercu, S., M. Zhang, N. Oyama, U. Hansen, A. E. Ghalbzouri, G. Jun, K. Geentjens, L. Zhang and J. H. Merregaert (2008). "Interaction of extracellular matrix protein 1 with extracellular matrix components: ECM1 is a basement membrane protein of the skin." J Invest Dermatol 128(6): 1397-1408.

Shiota, M., A. Yokomizo, Y. Tada, J. Inokuchi, K. Tatsugami, K. Kuroiwa, T. Uchiumi, N. Fujimoto, N. Seki and S. Naito (2010). "Peroxisome Proliferator-Activated

Receptor gamma Coactivator-1 alpha Interacts with the Androgen Receptor (AR) and Promotes Prostate Cancer Cell Growth by Activating the AR." Molecular Endocrinology 24(1): 114-127.

Sladek, R., J. A. Bader and V. Giguere (1997). "The orphan nuclear receptor estrogen-related receptor alpha is a transcriptional regulator of the human medium-chain acyl coenzyme A dehydrogenase gene." Mol Cell Biol 17(9): 5400-5409.

Stein, R. A., C. Y. Chang, D. A. Kazmin, J. Way, T. Schroeder, M. Wergin, M. W. Dewhirst and D. P. McDonnell (2008). "Estrogen-related receptor alpha is critical for the growth of estrogen receptor-negative breast cancer." Cancer Res 68(21): 8805-8812.

Stein, R. A., S. Gaillard and D. P. McDonnell (2009). "Estrogen-related receptor alpha induces the expression of vascular endothelial growth factor in breast cancer cells." J Steroid Biochem Mol Biol 114(1-2): 106-112.

Supuran, C. T. (2008). "Carbonic anhydrases--an overview." Curr Pharm Des 14(7): 603-614.

Suzuki, M. and N. Yagi (1994). "DNA recognition code of transcription factors in the helix-turn-helix, probe helix, hormone receptor, and zinc finger families." Proc Natl Acad Sci U S A 91(26): 12357-12361.

Suzuki, T., Y. Miki, T. Moriya, N. Shimada, T. Ishida, H. Hirakawa, N. Ohuchi and H. Sasano (2004). "Estrogen-related receptor alpha in human breast carcinoma as a potent prognostic factor." Cancer Res 64(13): 4670-4676.

Taplin, M. E., B. Rajeshkumar, S. Halabi, C. P. Werner, B. A. Woda, J. Picus, W. Stadler, D. F. Hayes, P. W. Kantoff, N. J. Vogelzang, E. J. Small, Cancer and B. S. Leukemia Group (2003). "Androgen receptor mutations in androgen-independent prostate cancer: Cancer and Leukemia Group B Study 9663." J Clin Oncol 21(14): 2673-2678.

Tetel, M. J., P. H. Giangrande, S. A. Leonhardt, D. P. McDonnell and D. P. Edwards (1999). "Hormone-dependent interaction between the amino- and carboxyl-terminal domains of progesterone receptor in vitro and in vivo." Mol Endocrinol 13(6): 910-924.

Tian, H. Y., K. Mythreye, C. Golzio, N. Katsanis and G. C. Blobe (2012). "Endoglin mediates fibronectin/alpha 5 beta 1 integrin and TGF-beta pathway crosstalk in endothelial cells." Embo Journal 31(19): 3885-3900.

Tremblay, G. B., D. Bergeron and V. Giguere (2001). "4-Hydroxytamoxifen is an isoform-specific inhibitor of orphan estrogen-receptor-related (ERR) nuclear receptors beta and gamma." Endocrinology 142(10): 4572-4575.

Tremblay, G. B., T. Kunath, D. Bergeron, L. Lapointe, C. Champigny, J. A. Bader, J. Rossant and V. Giguere (2001). "Diethylstilbestrol regulates trophoblast stem cell differentiation as a ligand of orphan nuclear receptor ERR beta." Genes Dev 15(7): 833-838.

Vanacker, J. M., E. Bonnelye, S. Chopin-Delannoy, C. Delmarre, V. Cavailles and V. Laudet (1999). "Transcriptional activities of the orphan nuclear receptor ERR alpha (estrogen receptor-related receptor-alpha)." Mol Endocrinol 13(5): 764-773.

Wang, L., J. Yu, J. Ni, X. M. Xu, J. Wang, H. Ning, X. F. Pei, J. Chen, S. Yang, C. B. Underhill, L. Liu, J. Liekens, J. Merregaert and L. Zhang (2003). "Extracellular matrix protein 1 (ECM1) is over-expressed in malignant epithelial tumors." Cancer Lett 200(1): 57-67.

Watkins, G., A. Douglas-Jones, R. E. Mansel and W. G. Jiang (2004). "The localisation and reduction of nuclear staining of PPAR gamma and PGC-1 in human breast cancer." Oncology Reports 12(2): 483-488.

Watkins, G., A. G. Douglas-Jones, R. E. Mansel and W. G. Jiang (2003). "Reduction of nuclear peroxisome proliferator activated receptor (PPAR)-gamma coactivator, PGC-1, in human breast cancer." Breast Cancer Research and Treatment 82: S68-S68.

Wenger, R. H., D. P. Stiehl and G. Camenisch (2005). "Integration of oxygen signaling at the consensus HRE." Sci STKE 2005(306): re12.

Willy, P. J., I. R. Murray, J. Qian, B. B. Busch, W. C. Stevens, Jr., R. Martin, R. Mohan, S. Zhou, P. Ordentlich, P. Wei, D. W. Sapp, R. A. Horlick, R. A. Heyman and I. G. Schulman (2004). "Regulation of PPARgamma coactivator 1alpha (PGC-1alpha) signaling by an estrogen-related receptor alpha (ERRalpha) ligand." Proc Natl Acad Sci U S A 101(24): 8912-8917.

Xiong, G. P., J. X. Zhang, S. P. Gu, Y. B. Wu and J. F. Liu (2012). "Overexpression of ECM1 Contributes to Migration and Invasion in Cholangiocarcinoma Cell." Neoplasma 59(4): 409-415.

Zhang, H., P. Gao, R. Fukuda, G. Kumar, B. Krishnamachary, K. I. Zeller, C. V. Dang and G. L. Semenza (2007). "HIF-1 inhibits mitochondrial biogenesis and cellular

respiration in VHL-deficient renal cell carcinoma by repression of C-MYC activity." Cancer Cell 11(5): 407-420.

Zhang, Y., Y. Ba, C. Liu, G. X. Sun, L. Ding, S. Y. Gao, J. H. Hao, Z. T. Yu, J. F. Zhang, K. Zen, Z. S. Tong, X. A. Yang and C. Y. Zhang (2007). "PGC-1 alpha induces apoptosis in human epithelial ovarian cancer cells through a PPAR gamma-dependent pathway." Cell Research 17(4): 363-373.

Zhu, L., Q. Wang, L. Zhang, Z. Fang, F. Zhao, Z. Lv, Z. Gu, J. Zhang, J. Wang, K. Zen, Y. Xiang, D. Wang and C. Y. Zhang (2010). "Hypoxia induces PGC-1alpha expression and mitochondrial biogenesis in the myocardium of TOF patients." Cell Res 20(6): 676-687..

Biography

Junfei Liu

Education:

2009-current: Graduate Research Assistant in Laboratory of Donald P. McDonnell, Ph.D

Department of Pharmacology and Cancer Biology, Duke University

2008-current: Doctoral Program in Department of Biochemistry, Duke University

2004-2008: Bachelors of Science (Biological Science), Fudan University